DEVELOPMENT OF NEUROPATHOLOGY IN MURINE MPS IIIA AND MPS VII AND THE EFFECT OF *N*-BUTYLDEOXYNOJIRIMYCIN TREATMENT ON MPS IIIA MICE

Xenia Kaidonis

BSc (Biomed), BSc (Hons)

Matrix Biology Unit
SA Pathology

Thesis submitted for the degree of
Doctor of Philosophy

in

Discipline of Genetics

School of Molecular and Biomedical Sciences
Faculty of Science
The University of Adelaide

February 2014

Table of Contents

Abstract

The mucopolysaccharidoses (MPSs) are a family of heritable diseases caused by deficiencies in glycosaminoglycan (GAG) degrading lysosomal enzymes. GAGs accumulate in a range of tissues, resulting in diverse pathology that includes brain degeneration. The secondary accumulation of glycosphingolipids, specifically G_{M2} and G_{M3} gangliosides, occurs in the MPS brain. In MPS IIIA and MPS VII mouse models GAGs and gangliosides began to accumulate prior to the onset of behavioural changes. G_{M2} levels began to rise early, following the trend of GAG accumulation, and increased to 548% and 219% of normal levels in MPS IIIA and MPS VII respectively. G_{M3} levels began to rise later, reaching a peak of 484% and 313% of normal in MPS IIIA and MPS VII respectively.

Given that brain G_{M2} and G_{M3} accumulation precedes behavioural deficits, it is possible that these gangliosides contribute to brain degeneration. Thus, gangliosides may be a target for the treatment of MPS brain disease. *N*-butyldeoxynojirimycin (*N*B-DNJ) is an iminosugar capable of crossing the blood brain barrier and reducing brain ganglioside synthesis, consequently deceasing overall brain G_{M2} and G_{M3} levels. *N*B-DNJ treatment of MPS IIIA mice decreased brain G_{M2} and G_{M3} levels in the short but not in the long term. Despite this, the innate fear response was restored and learning ability was equivalent to normal with both lengths of treatment.

MPS IIIA mice treated with *N*B-DNJ also had a reduction in cytokine gene expression, astroglial activation and oxidation of inflammatory lipids. Whether MPS IIIA behavioural improvements were due to a delay in ganglioside accumulation with *N*B-DNJ treatment, or due to an anti-inflammatory function of *N*B-DNJ is not known. However, this thesis

demonstrates that *N*B-DNJ can improve MPS brain dysfunction in the MPS IIIA mouse model and may be a potential therapy for CNS disease for children with MPS.

Declaration

This work contains no material which has been accepted for the award of any other degree or diploma in any university or other tertiary institution to Xenia Kaidonis and, to the best of my knowledge and belief, contains no material previously published or written by another person, except where due reference has been made in the text.

I give consent to this copy of my thesis, when deposited in the University Library, being made available for loan and photocopying, subject to the provisions of the Copyright Act 1968.

I also give permission for the digital version of my thesis to be made available on the web, via the University's digital research depository, the Library catalogue, the Australian Digital Thesis Program (ADTP) and also through web search engines, unless permission has been granted by the University to restrict access for a period of time.

Xenia Kaidonis

.../.../……

Acknowledgements

Over the course of my PhD, many people have shared their support and expertise. First and foremost, I'd like to thank my supervisors Dr Sharon Byers and Dr Janice Fletcher for their guidance, support and patience. Their knowledge in the field of mucopolysaccharidosis research is extraordinary and I was fortunate to have had the opportunity to learn from them.

Thank you to the members of the Matrix Biology Unit, past and present: Ainslie, Matilda, Nathan, Elle, Carmen, Wan Chin, Krystyna, Kavita, Mardiah, Chun Hong, Xiao Dan, Zarpana, Marleesa, Chun Hao, Wesley and Sharvin. Their friendship, support and good humour made the lab a truly enjoyable place to come to every day. I would especially like to thank Ainslie for her help over the years, particularly with the behaviour testing of MPS IIIA mice and *N*B-DNJ injections.

Special thanks must go to Enzo Ranieri, who taught me mass spectrometry, and to Peter Sharp, who passed on some of his vast knowledge of lipid biochemistry. Both were always happy to lend their equipment and to give their time for me and for this I am very grateful. Thank you also to Dr Craig Freeman for helping me with methods for the hydrolysis of heparan sulphate and the separation of glucuronic acid and iduronic acid residues.

Thank you to Dr Tomas Rozek for allowing me to use the mass spectrometer at the University of South Australia when our machine at the Women's and Children's hospital was finally decommissioned. Thank you to the Women's and Children's hospital animal house staff for their excellent care of the mice used in this study. Thank you also to the SA Pathology histology department (WCH site) for use of their cryostat.

To the University of Adelaide department of genetics and post-graduate coordinators Dr Michael Lardelli and Dr Frank Grutzner, thank you for your support throughout my candidature and for providing such a well organised programme.

I would like to acknowledge funding for this work by the NH&MRC and the kind donation of *N*B-DNJ used for the oral treatment of mice by Actelion.

Finally, I would like to thank those most important to me: Tom, my parents and sisters, for their constant love, encouragement and support throughout this journey.

Abbreviations

12(s)-HETE	12(s)-hydroxyeicosatetraenoic acid
13(s)-HODE	13(s)-hydroxyoctadecadienoic acid
15(s)-HETE	15(s)-hydroxyeicosatetraenoic acid
6-keto-PGF1α	6-keto-prostogmandin F1 alpha
α Syn	alpha-synuclein
AA	arachidonic acid
AAV	adeno-associated virus
BBB	blood brain barrier
BLAST	basic local alignment search tool
BMT	bone marrow transplant
CB	cerebellum
Ccl3	chemokine (C-C motif) ligand 3
Cer	ceramide
CH	cerebral hemisphere
CL	cardiolipin
CNS	central nervous system
CS	chondroitin sulphate
CSF	cerebrospinal fluid
Ctsb	cathepsin B
Cypa	cyclophilin A
d_3-G_{M1}	N-octadecanoyl-d_3-monosialoganglioside 1
DAPI	4',6-diamidino-2-phenylindole
DHA	docosahexaenoic acid
DEAE	diethylaminoethyl

DS	dermatan sulphate
EDTA	sodium ethylenediaminetetraacetic acid
EPA	eicosapentaenoic acid
ERT	enzyme replacement therapy
FITC	fluorescein isothiocyanate
GAG	glycosaminoglycan
Gal	galactose
GalNAc	*N*-acetylgalactosamine
GalNAc T	*N*-acetylgalactosamine transferase
GalT I	galactosyltransferase I
GalT II	galactosyltransferase II
GFAP/ *Gfap*	glial fibrillary acidic protein
Glc	glucose
GlcA	glucuronic acid
GlcT	glucosyltransferase
G_M	monosialoganglioside
G_{M2}-AP	monosialoganglioside 2 activator protein
GSL	glycosphingolipid
GT	gene therapy
GUSB	β-glucuronidase
HA	hyaluronan
Hex A/B	hexosaminidase A/B
HIV	human immunodeficiency virus
HS	heparan sulphate
HSD	highly significant difference
IdoA	iduronic acid
Ifnγ	interferon gamma

Il1β	interleukin 1 beta
iso-PGF2α	iso-prostoglandin F2 alpha
KS	keratan sulphate
LC-ESI MS/MS	liquid chromatography- electrospray ionisation tandem mass spectrometry
LSD	lysosomal storage disorder
MCB	membranous cytoplasmic bodies
Mip1a	chemokine (C-C motif) ligand 3
MPA/B	mobile phases A/B
MPS	mucopolysaccharidosis
MRM	multiple reaction monitoring
MS/MS	tandem mass spectrometry
*N*B-DGJ	*N*-butyldeoxygalactonojirimycin
*N*B-DNJ	*N*-butyldeoxynojirimycin
NEB	New England Biolabs
NPC	Niemann Pick C
NSAID	non-steroidal anti-inflammatory drug
OCT	optimal cutting temperature
PA	phosphatidic acid
PBS	phosphate buffered saline
PC	phosphatidylcholine
PCR	polymerase chain reaction
PE	phosphatidylethanolamine
PGD2	prostoglandin D2
PGE2	prostoglandin E2
PGF2α	prostoglandin F2 alpha
PI	phosphatidylinositol

PUFA	polyunsaturated fatty acid
RAPC	repeated acquisition and performance chamber
ROS	reactive oxygen species
RVD1α	resolvin D1 alpha
SA	sialic acid
SAT I	sialotransferase I
SDS	sodium dodecyl sulphate
SDT	substrate deprivation therapy
SHIRPA	SmithKline Beecham, Harwell, Imperial College, Royal London Hospital, phenotype assessment
SM	sphingomyelin
SOD	superoxide dismutase
TAE	tris-acetate/ sodium ethylenediaminetetraacetic acid
TFA	trifluoroacetic acid
Tgfβ1	transforming growth factor beta 1
TLC	thin layer chromatography
Tnfα	tumor necrosis factor alpha
Tnfrs1α	tumor necrosis factor family receptor superfamily member 1a
TXB2	thromboxane B2
UA	uronic acid
UDP	uridine diphosphate

Chapter One: Introduction

1.1 Overview

Lysosomal storage disorders (LSDs) are hereditary deficiencies in lysosomal enzymes required for the degradation of macromolecules. They lead to increased levels of enzyme substrate within the lysosomes and a range of phenotypes. The mucopolysaccharidoses (MPSs) are a subset of LSDs that store one or more of the complex carbohydrate extracellular matrix, cell associated or intracellular components known as glycosaminoglycans (GAGs). Eleven different enzyme deficiencies can impact on GAG degradation and each results in a different MPS. Disease symptoms may include skeletal deformities, hepatosplenomegaly, corneal clouding and progressive central nervous system (CNS) degeneration (Neufield and Muenzer 2001).

The accumulation of the GAG heparan sulphate is associated with the secondary storage of glycosphingolipids (GSLs), specifically G_{M2} and G_{M3} gangliosides, in the CNS (Constantopoulos and Dekaban 1978; Constantopoulos *et al.* 1980; McGlynn *et al.* 2004). While no LSDs have been attributed to G_{M3} storage, G_{M2} is a primary storage product in the G_{M2} gangliosidoses and is associated with progressive CNS degeneration (Svennerholm 1962; Sandhoff *et al.* 1971; Rosengren *et al.* 1987). Thus, it has been suggested that CNS pathology present in many of the MPSs may be due to the secondary accumulation of ganglioside rather than the primary accumulation of GAG. This thesis is the first undertaking to separate the role of GAG and ganglioside in the progression of MPS CNS degeneration.

Current therapies that replace the dysfunctional enzyme have limited efficacy in treating CNS pathology in the MPS disorders due to the inability of functional enzyme to cross the blood brain barrier (BBB). Substrate deprivation therapy (SDT) is an alternative that aims to reduce synthesis of the storage product such that residual enzyme activity is sufficient for its degradation (Inokuchi and Radin 1987). SDT utilises small chemical inhibitors that are able to cross the BBB to treat the brain. One of these agents is the iminosugar *N*-

butyldeoxynojirimycin (*N*B-DNJ), which inhibits ganglioside synthesis and has shown some promise treating brain pathology associated with both primary and secondary ganglioside accumulation (Cox *et al.* 2000; Patterson *et al.* 2007). This suggests that *N*B-DNJ has the potential to treat brain disease in the MPSs. The investigation of the effect of *N*B-DNJ treatment on murine MPS IIIA CNS degeneration is another important component of this thesis.

1.2 Lysosomal storage disorders

Lysosomes are membranous sac-like organelles responsible for the degradation of macromolecules derived from either the intracellular or extracellular environment (de Duve 1983). They contain a range of acid hydrolases including phosphatases, sulphatases, glycosidases, proteases and lipases, which are active at the lysosomal pH of approximately 4.7 (Ohkuma and Poole 1978; de Duve 1983). These enzymes sequentially cleave molecules into their basic components, which are then expelled from the lysosome and recycled.

Genetic mutation can result in the loss of function of a lysosomal enzyme or structural protein. This results in the accumulation of enzyme substrate within the organelle and pathology that characterises one of the LSDs. There are currently 46 known LSDs with a collective Australian incidence of one in 7700 live births (Meikle *et al.* 1999). Each of these is due to a deficiency in a different lysosomal component, but can be grouped into an LSD family according to the type of storage material and the mechanism of accumulation. These families include the sphingolipidoses, mucopolysaccharidoses, oligosaccharidoses, glycogenoses, cholesterol lipidoses, membrane transport disorders, enzyme transport disorders, peptide storage disorders and protein storage disorders (Table 1.1).

Table 1.1: Families of lysosomal storage disorders (LSDs) and their Australian prevalence.

LSD family	LSD family examples	Australian incidence
Sphingolipidoses (n=12)	Gaucher disease	1 in 57 000
	Tay-Sachs disease	1 in 201 000
	Sandhoff disease	1 in 384 000
	G_{M1} gangliosidosis	1 in 384 000
	Niemann-Pick type A and B	1 in 248 000
	Fabry	1 in 117 000
	Krabbe	1 in 141 000
Mucopolysaccharidoses (n=11)	MPS IH/IS (Hurler/Scheie)	1 in 88 000
	MPS II (Hunter)	1 in 136 000
	MPS IIIA (Sanfilippo A)	1 in 114 000
	MPS IIIB (Sanfilippo B)	1 in 211 000
	MPS IIIC (Sanfilippo C)	1 in 1 407 000
	MPS IIID (Sanfilippo D)	1 in 1 056 000
	MPS IIIE (Sanfilipo E)	unknown
	MPS IVA (Morquio A)	1 in 169 000
	MPS VI (Maroteaux-Lamy)	1 in 235 000
	MPS VII (Sly)	1 in 2 111 000
Glycogenoses (n=2)	Pompe	1 in 146 000
Oligosaccharidoses (n=6)	Mannosidosis	1 in 1 056 000
Cholesterol lipidoses (n=3)	Niemann-Pick type C	1 in 211 000
Membrane transport disorders (n=3)	Cystinosis	1 in 192 000
Enzyme transport disorders (n=3)	Mucolipidosis type II/III	1 in 325 000
Peptide storage disorders (n=1)	Pycnodysostosis	unknown
Protein storage disorders (n=5)	Batten disease	unknown

Adapted from Meikle *et al*. (1999) and Kowalewski *et al*. (2012).

1.2.1 The Mucopolysaccharidoses

The MPSs are a family of related LSDs. With a combined Australian incidence of one in 22 500, they make up 35% of all LSD cases in Australia (Meikle *et al.* 1999). The MPSs result from deficiencies in the GAG complex carbohydrate degradative pathway. The five different types of GAG are heparan sulphate (HS), chondroitin sulphate (CS), dermatan sulphate (DS), keratan sulphate (KS) and hyaluronan (HA), which each have different tissue profiles and rates of turnover according to their functions (Neufield and Muenzer 2001). Each of the 12 MPS disorders result from a loss of function in a different degradative enzyme responsible for the cleavage of monomers from the non-reducing terminus of one or more type of GAG (Table 1.2) (Neufield and Muenzer 2001; Kowalewski *et al.* 2012). Thus, GAGs accumulate within the lysosomes and their increase is observed in multiple tissues, as well as in the urine, serum, and cerebrospinal fluid (CSF) of patients (Constantopoulos *et al.* 1976; Dekaban and Constantopoulos 1977; Neufield and Muenzer 2001).

MPS pathology can include organomegaly, bone and joint deformities including extreme short stature, cardiomyopathy and valvular defects, restrictive lung disease and upper airway obstruction, hearing impairment, corneal clouding, hydrocephalus and CNS degeneration. A range in severity and age of onset also exists within each MPS due to varying levels of residual enzyme activity, which is generally dependent on the underlying genetic mutation (Ruijter *et al.* 2008; Valstar *et al.* 2010a; Valstar *et al.* 2010b; Valstar *et al.* 2010c). However, in some cases the same mutation in different patients (often siblings) can present with different severities demonstrating the effect of other factors, one of which is probably differing rates of GAG internalisation for degradation. As can be expected, a greater rate of GAG accumulation within the lysosome is associated with earlier presentation of disease symptoms and increased severity (Dekaban and Constantopoulos 1977; van de Kamp *et al.* 1981; Gabrielli *et al.* 1992; McDowell *et al.* 1993; Bunge *et al.* 1998; Meikle *et al.* 1999;

Neufield and Muenzer 2001; Ruijter *et al.* 2008; Piotrowska *et al.* 2009; Valstar *et al.* 2010b; Valstar *et al.* 2010c).

Of the 12 MPS disorders, CNS pathology is present with varying severity in eight subtypes. These are MPS I, II, IIIA-E, and VII (Table 1.2) (Neufield and Muenzer 2001; Kowalewski *et al.* 2012). CNS pathology has a significant impact on both life span and quality of life, but thus far treatments have had only limited success on this component of MPS disease, as the mature BBB isolates the CNS from most systemic therapies (treatments described further in Chapter 1.5) (Constantopoulos *et al.* 1976; Neufield and Muenzer 2001). An understanding of MPS brain pathology is important for the development of a treatment for this hard-to-reach organ and this thesis aims to further the current knowledge of the CNS component of disease.

1.2.1.1 CNS pathology in MPS patients

Patients with MPS brain disease display significant clinical manifestations. Behavioural problems of differing severities are observed, which can include extreme restlessness, tantrums, aggression, hyperactivity, poor attention span and anxious and compulsive behaviour. These, along with developmental delays (including speech and motor delays), intellectual disability, disturbed sleep patterns, hydrocephalus and epilepsy can contribute to the CNS component of MPS diseases (Young and Harper 1983; Colville *et al.* 1996; Neufield and Muenzer 2001; Valstar *et al.* 2010b; Valstar *et al.* 2010c; Wooten *et al.* 2013). Due to progressive CNS degeneration, patients at the severe end of the disease spectrum eventually lose motor coordination by six to ten years of age, becoming wheelchair bound with limited responsiveness. Palliative care is the mainstay of treatment (Young and Harper 1983; Neufield and Muenzer 2001; Valstar *et al.* 2010b; Valstar *et al.* 2010c).

Many anatomical changes occur during the progression of MPS CNS disease, which are expected to contribute to the clinical manifestations observed. Autopsied brains of patients

with MPS I, II and IIIA are larger and distorted in shape. In addition, cerebral ventricles are dilated and the leptomeninges are thickened (Dekaban and Constantopoulos 1977; Hamano *et al.* 2008). This results in severe white matter atrophy and severely reduced brain weight despite the increased overall size of the brain (Hamano *et al.* 2008). Histological analysis of the brain tissue has demonstrated thickening of blood vessel walls and a greater amount of surrounding periadventitial space. Within this space, many large cells full of GAG storing cytoplasmic vesicles have been observed. It is believed that these cells are largely responsible for the increased neuronal tissue GAG levels in the brains of patients with MPS I, II and IIIA, which are three to six times greater than those found in the brains of normal control patients. These enlarged regions of the MPS I, II and IIIA brains also contribute to the overall increase in size and distortion of the brain (Constantopoulos *et al.* 1976; Dekaban and Constantopoulos 1977; Constantopoulos and Dekaban 1978; Constantopoulos *et al.* 1980; Werth *et al.* 2001; Kurihara 2006; Kara *et al.* 2008).

In addition to GAG storage, degenerating neurons are observed with meganeurites (expansions at the axon hillock) containing large amounts of lipid-staining material and an associated gliosis (Purpura and Suzuki 1976; Dekaban and Constantopoulos 1977; Hamano *et al.* 2008). The lipid-staining material has been identified as a secondary storage of a combination of G_{M2} and G_{M3} gangliosides and cholesterol (Constantopoulos and Dekaban 1978; Constantopoulos *et al.* 1980). The relationship between neuronal storage of lipid species and resulting CNS degeneration is of interest both to advance our understanding of MPS brain disease and for the development of CNS targeted therapies. Secondary lipid storage in the LSDs is described further in Chapter 1.3.

1.2.2 The G_{M2} gangliosidoses

While no LSDs have been attributed to primary G_{M3} storage, G_{M2} accumulation is associated with CNS degeneration in another group of LSDs, known as the G_{M2} gangliosidoses. These belong to the GSL storing family of LSDs (Table 1.1).

G_{M2} ganglioside is a member of the ganglio-series of glycosphingolipid plasma membrane components (Figure 1.1) (Gravel *et al.* 2001). From its location in the plasma membrane, it is involved in various roles requiring cell-cell and cell-matrix interactions. All three monosialogangliosides, G_{M1}, G_{M2} and G_{M3}, are found primarily in the CNS during neuronal development, after which expression of G_{M2} and G_{M3} decreases to very low levels (Rosenberg and Stern 1966; Kracun *et al.* 1984; Hogan *et al.* 1988; Kotani *et al.* 1993; Kotani *et al.* 1994; Kotani *et al.* 1995).

The G_{M2} gangliosidoses occur when the activity of the enzyme (Hex A) or activator protein (G_{M2}-AP) necessary for the degradation of G_{M2} to G_{M3} is reduced or lost (Figure 1.2) (Bartholomew and Rattazzi 1974; Srivastava and Beutler 1974; Kytzia and Sandhoff 1985; Meier *et al.* 1991; Werth *et al.* 2001). Tay-Sachs and Sandhoff diseases result from a deficiency in Hex A and Hex A/B respectively (Kolodny *et al.* 1969; Sandhoff 1969; Sandhoff *et al.* 1971; Srivastava and Beutler 1974; Rosengren *et al.* 1987). Loss of function of the G_{M2} activator protein affects the ability of Hex A to act upon G_{M2}, and hence, is the third mechanism for obstruction of G_{M2} degradation (Sandhoff *et al.* 1971; Conzelmann and Sandhoff 1978).

In all three disorders, G_{M2} ganglioside accumulates within the lysosomes, particularly in neuronal cells where monosialogangliosides are highly expressed during development (Svennerholm 1962; Sandhoff *et al.* 1971; Rosengren *et al.* 1987). Compared to normal brain, 60-90% of all gangliosides in the Tay-Sachs and Sandhoff brain are G_{M2} and are associated

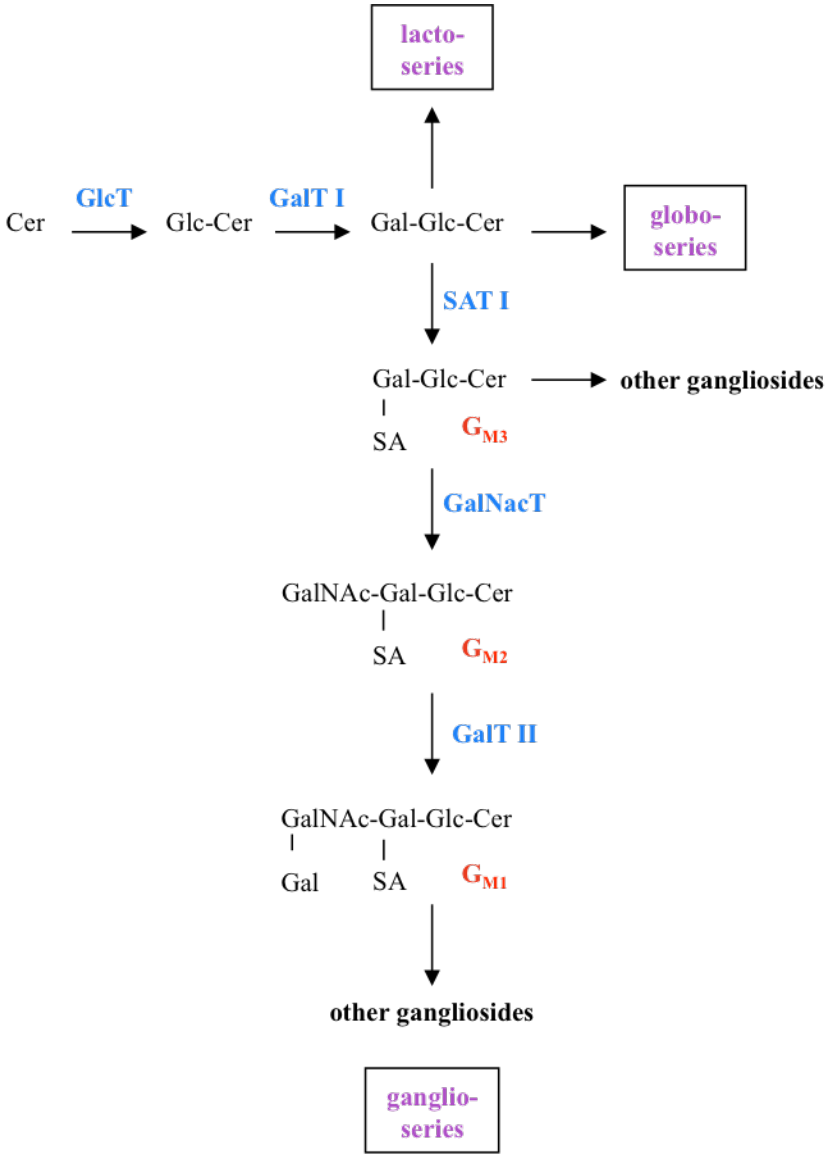

Figure 1.1: GSL synthesis.
The synthesis of GSLs from ceramide (Cer) is a step-wise process catalysed by a series of enzymes (labeled in blue). The addition of glucose (Glc) is catalysed by glucosyltransferase (GlcT) and galactose (Gal) by galactosyltransferase I (GalT I). This forms the base for the lacto-, globo- and ganglio-series GSLs. Monosialoganglioside synthesis begins with G_{M3} through the addition of a sialic acid (SA) residue by sialotransferase I (SAT I), G_{M2} with the addition of N-acetylgalactosamine (GalNAc) by N-acetylgalacyose transferase (GalNAcT) and then G_{M1} with the addition of galactose by galactosyltransferase II (GalT II).

Adapted from Kolter *et al.* (2002).

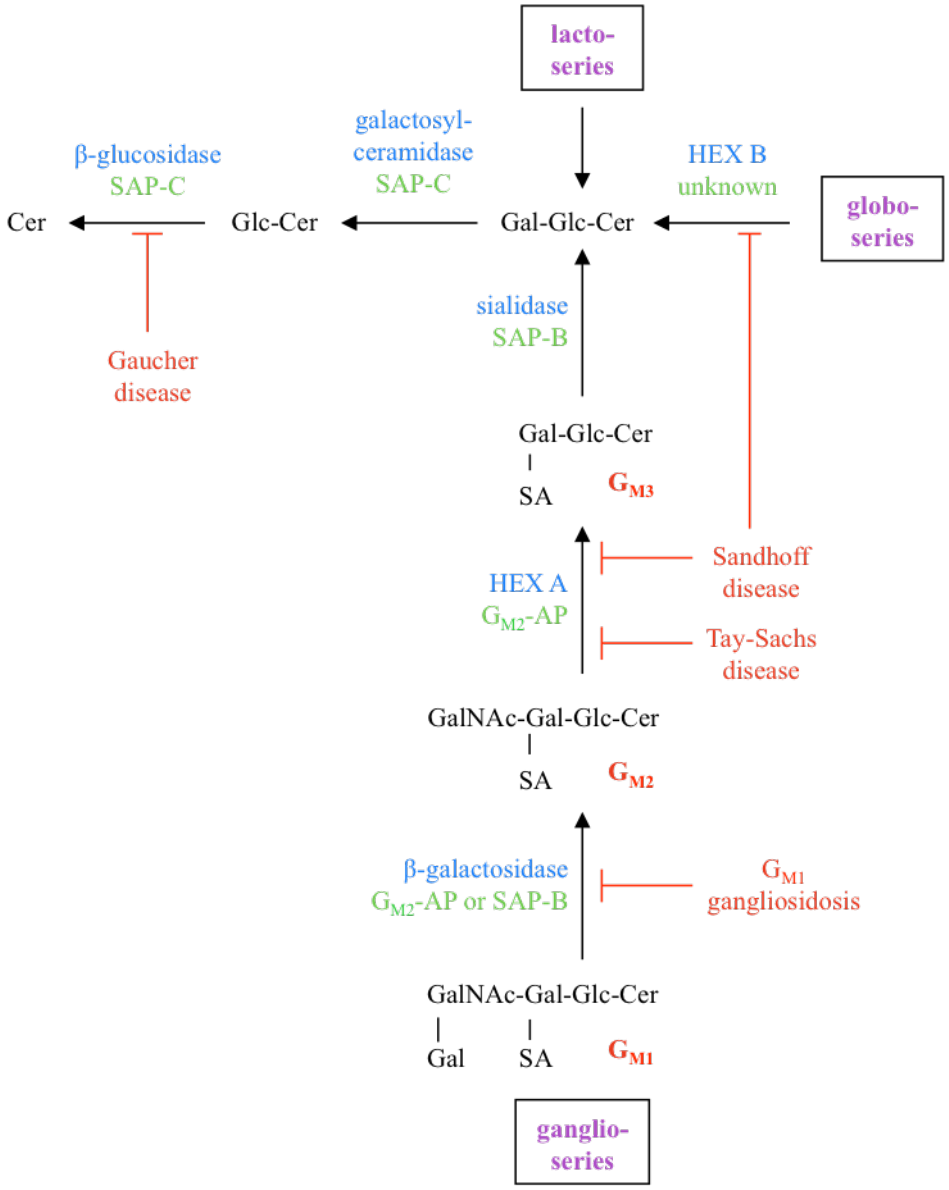

Figure 1.2: The degradation of simple gangliosides.
Simple ganglio- and globo-side degradation is catalysed by specific enzymes (blue) and assisted by activator proteins (green). Enzyme deficiencies result in the lysosomal accumulation of substrate. The lysosomal disorders Gaucher, Tay-Sachs, Sandhoff and G_{M1} gangliosidosis result from a deficiency in β-glucosidase, HEX A, HEX A/B and β-galactosidase respectively.

Adapted from Bartholomew and Rattazzi (1974), Kytzia and Sandhoff (1985), Meier *et al*. (1991), Srivastava and Beutler (1974) and Werth *et al*. (2001).

with CNS pathology (Svennerholm 1962; Kornguth *et al.* 1974; Rosengren *et al.* 1987; Gravel *et al.* 2001). These disorders highlight a potential role for G_{M2} in MPS brain disease.

1.2.2.1 CNS pathology in the G_{M2} gangliosidoses

Studies in both human and murine G_{M2} gangliosidoses have demonstrated a range of neuronal changes. Lysosomes storing G_{M2} are observed as membranous cytoplasmic bodies (MCB; zebra bodies) within neurons, which cause changes in the perikarya, dendrites and axons (Samuels *et al.* 1963; Purpura and Suzuki 1976). Perikaryal enlargement occurs in some neurons and leads to the formation of expansions of axon hillocks (known as meganeurites). The cell membrane develops new dendrite-like spines at the meganeurites resulting in random synapse formation. Ectopic dendrites expand into a secondary basilar dendritic system, while normal apical and basilar dendrites of many neurons are lost (Purpura and Suzuki 1976; Walkley *et al.* 2000). In addition to this, organelles congregate within the axons and produce focal swellings (Walkley *et al.* 1991). This results in the blocking of transport between the perikarya and axons, which can inhibit the release of neurotransmitters and prevent synapse formation (Walkley *et al.* 1991).

CNS pathology in the G_{M2} gangliosidoses most likely occurs through multiple mechanisms. Ectopic dendritogenesis may result directly from G_{M2}, as its normal role is to promote dendritic growth during brain development (Walkley *et al.* 2000). However, G_{M2} storage also leads to many other processes including inflammation, oxidative stress, disrupted autophagy and apoptosis, which can themselves contribute to neuronal pathology (described further in Chapter 1.4) (Huang *et al.* 1997; Jeyakumar *et al.* 2004; Kiselyov *et al.* 2007; Wei *et al.* 2008). An understanding of these processes and the mechanisms that lead to them is important for the development of therapies, not only the G_{M2} gangliosidoses, but also other LSDs with brain G_{M2} storage and subsequent CNS involvement, such as the MPSs.

1.3 Secondary storage in the LSDs

In the G_{M2} gangliosidoses, G_{M2} ganglioside accumulates as a direct result of enzyme loss of function, which causes progressive CNS degeneration. However, in many other LSDs G_{M2} ganglioside accumulates secondary to a primary storage product, which may be another GSL or an unrelated macromolecule. One example of secondary storage is in the cholesterol lipidosis Niemann-Pick type C (NPC), which also displays CNS pathology (Table 1.1). The primary storage product in this disorder is cholesterol, however, widespread storage of both G_{M2} and G_{M3} has been described. In addition, neuronal pathology is reminiscent of the G_{M2} gangliosidoses, with ectopic dendrites and axonal focal swellings occurring in murine, feline and human NPC (Zervas *et al.* 2001a).

MPSs in which HS GAG accumulates, namely MPS I, II, IIIA-E and MPS VII, display CNS pathology and have secondary storage of G_{M2}, G_{M3} and cholesterol (Constantopoulos *et al.* 1976; Constantopoulos and Dekaban 1978; Constantopoulos *et al.* 1980; McGlynn *et al.* 2004). Studies characterising CNS pathology in murine and feline models of MPS disorders have provided similar observations as those seen in the human disease. Pathology is comparable to the G_{M2} gangliosidoses, with MCBs, meganurite formation and ectopic dendrites (Levy *et al.* 1996; McGlynn *et al.* 2004; Walkley *et al.* 2005). As an increase in ganglioside in the gangliosidoses results in severe CNS degeneration, it may be that the cause of CNS pathology in the MPSs is due to the secondary storage of ganglioside rather than the primary storage of GAG. Thus, one of the aims of this thesis is to elucidate the role of gangliosides in MPS brain disease.

Due to the correlation between GAG levels, ganglioside levels and the severity of CNS degeneration observed, it has been suggested that the highly charged, semi-degraded GAG fragments impact on GSL metabolism (Avila and Convit 1975; Constantopoulos *et al.* 1976; Constantopoulos and Dekaban 1978; Constantopoulos *et al.* 1980; McGlynn *et al.* 2004).

Constantopoulos and Dekaban (1978) demonstrated that the activity of β-galactosidase is reduced in the brains of MPS patients with CNS pathology. A study by Avila and Convit (1975) on the inhibition of various lysosomal enzymes by GAGs in human leukocytes revealed that multiple enzymes were affected by HS and CS. HS was responsible for decreases in the activities of α- and β- galactosidase and sialidase by 54%, 72% and 49% respectively. It is unknown how these observations relate to the specific accumulation of the secondary storage products observed in the MPS brain, or whether the decreases in enzyme activity are sufficient to cause storage. Furthermore, the limited co-localisation of stored substrates demonstrates that the process is complex and that while GAGs can inhibit GSL degradation *in vitro* this may not be occurring *in vivo* (McGlynn *et al.* 2004).

A study in feline MPS VI demonstrated that G_{M2}, G_{M3} and cholesterol also accumulate in this DS storing disorder (Walkley *et al.* 2005). Thus, it is possible that undegraded HS and DS have similar properties, which allow them both to cause secondary ganglioside storage. However, neurodegeneration is not common in MPS VI, perhaps because secondary storage does not reach a critical threshold. It has been demonstrated that HS storage results in increased HS biosynthesis, which may result in more damaging levels of storage in HS storing MPSs (McCarty *et al.* 2011).

Another mechanism for the secondary accumulation of lipid may be that growing numbers of GAG-storing lysosomes disrupt normal intracellular trafficking via the endosomal-lysosomal pathway. G_{M2}, G_{M3} and cholesterol are closely associated in lipid rafts in the cell membrane and are internalised during endocytosis (Glaros *et al.* 2005; Ohmi *et al.* 2009a; Ohmi *et al.* 2009b; Sanchez-Wandelmer *et al.* 2009; Singh *et al.* 2010). Thus, it is possible that G_{M2}, G_{M3} and cholesterol containing endosomes may build up within the cell due to a blockage in this pathway. It is not known whether other raft lipids including phospholipids and other glycolipids are also affected by alterations to raft structures in MPS.

Although the relationship between GAG storage and the secondary storage of ganglioside is still being investigated, it is likely that G_{M2} is responsible for a certain degree of CNS pathology in the MPS disorders and this secondary storage could be a therapeutic target. While G_{M2} may have some direct effect on the development of MPS brain disease, it is likely that G_{M2} accumulation leads to the disruption of other processes which themselves affect the CNS.

1.4 Potential mechanisms behind CNS degeneration in the ganglioside-storing brain

In addition to the lysosomal accumulation of storage material and ectopic dendrites that may be regulated by G_{M2} itself, there are some other features that are common amongst ganglioside-storing brains, the exact cause of which are unknown. These are a series of inter-related responses to cellular damage, including inflammation, oxidative stress, disruptions to autophagy and apoptosis. An understanding of these processes and how they fit into a model of CNS degeneration is important to this thesis, in which the role of gangliosides in the development of MPS brain disease is investigated.

1.4.1 Inflammation of the ganglioside-storing brain

The impact of inflammation on the progression of CNS pathology in ganglioside-storing disorders is significant to both brain function and survival. Treatment of MPS IIIB mice with the immunosuppressive drug Prednisolone results in increased survival and functional improvements in neurological disease (DiRosario *et al.* 2009). Improvement of brain disease has also been demonstrated using non-steroidal anti-inflammatory drugs (NSAIDs) in animal models of Sandhoff disease, NPC and MPS IIIA (Jeyakumar *et al.* 2004; Smith *et al.* 2009; Arfi *et al.* 2011).

Aspirin was the NSAID used in the MPS IIIA study (Arfi *et al.* 2011). It inhibits the production of inflammatory lipid metabolites by preventing the oxidation of a phospholipid derived polyunsaturated fatty acid (PUFA) known as arachidonic acid (AA) (Peterson *et al.* 1998; Duda *et al.* 2009). This may suggest an up-regulation of the inflammatory lipid oxidation pathway in the MPS brain. However, there has not yet been an investigation into AA and its metabolites, or into anti-inflammatory PUFAs such as docosahexaenoic acid (DHA) and eicosapentaenoic acid (EPA) and their metabolites in the MPSs. PUFAs have also been implicated in NPC and Sandhoff disease (Kawashita *et al.* 2011; Nakamura *et al.* 2011).

The inflammatory events observed in LSDs with brain ganglioside storage show many similarities. The infiltration of activated microglia and astroglia has been observed in the MPS I, MPS IIIA, MPS IIIB, MPS VII, Sandhoff, Tay Sachs and NPC brain and begins prior to the onset of functional deficits (Wada *et al.* 2000; Li *et al.* 2002; Myerowitz *et al.* 2002; Baudry *et al.* 2003; Jeyakumar *et al.* 2003; Ohmi *et al.* 2003; Wu and Proia 2004; Ausseil *et al.* 2008; Hamano *et al.* 2008; Richard *et al.* 2008; DiRosario *et al.* 2009; Arfi *et al.* 2011). These similarities suggest a common cause for brain inflammation in these disorders, which likely result from the cellular burden of overall storage. It has been suggested that the accumulation of substrates within microglia prevents the efficient clean up of damaged neurons and leads to the recruitment and activation of further microglia from the periphery (Wada *et al.* 2000; Wu and Proia 2004; Ausseil *et al.* 2008). *In vitro* studies specific to MPS have demonstrated that HS oligosaccharides cause the activation of microglia, hence this may be an additional contributor to brain inflammation in the MPSs (Ausseil *et al.* 2008).

1.4.2 Oxidative stress in the ganglioside-storing brain

In addition to inflammation, oxidative stress is another cell-damaging process that is common to ganglioside-storing brains, in MPS I, MPS IIIA, MPS IIIB, MPS VII, Tay-Sachs, Sandhoff and NPC (Ohmi *et al.* 2003; Di Domenico *et al.* 2005; Villani *et al.* 2007; Richard *et al.* 2008;

Wei *et al.* 2008; Reolon *et al.* 2009; Villani *et al.* 2009; Arfi *et al.* 2011). One of the causes behind oxidative stress is inflammation (Richard *et al.* 2008; Di Domenico *et al.* 2009; Arfi *et al.* 2011). It has also been shown that the disruption of lysosomal homeostasis can cause oxidative stress, a significant potential issue in the LSDs (Wei *et al.* 2008).

Reactive oxygen species (ROS) have been reported in the MPS IIIB mouse brain and contribute to the observed increase in protein and lipid oxidation (Villani *et al.* 2007; Villani *et al.* 2009). In response to ROS, antioxidant expression is also up-regulated. Levels of both superoxide dismutase (SOD) and catalase are increased in the MPS I mouse brain, as well as in Tay-Sachs, Sandhoff and NPC disease cells *in vitro* (Wei *et al.* 2008; Reolon *et al.* 2009; Villani *et al.* 2009). While these may ameliorate oxidative damage, oxidised protein and lipid is still present.

1.4.3 Autophagy dysfunction in the ganglioside-storing brain

Autophagy is a protective response to oxidative stress, with superoxide ions inducing constitutive activity and SOD inhibiting the process. Oxidised molecules are normally taken up by autophagosomes and cleared via the lysosome (Kiffin, Christian et al. 2004; Chen, Azad et al. 2009). However, in the LSDs, autophagosomes are unable to fuse with lysosomes burdened with storage material and therefore accumulate within the cell (Kiselyov *et al.* 2007; Settembre *et al.* 2008a). This has been observed in the MPS IIIA, Sandhoff and NPC mouse brain, as well as NPC fibroblasts *in vitro* (Kiselyov *et al.* 2007; Pacheco *et al.* 2007; Settembre *et al.* 2008a; Ishibashi *et al.* 2009; Boland *et al.* 2010). In addition, a subsequent increase in mitochondria and polyubiquinated proteins has been reported in MPS IIIA (Kiselyov *et al.* 2007; Settembre *et al.* 2008a). The build-up of dysfunctional mitochondria results in increased oxidation, which further exacerbates autophagy dysfunction and can lead to apoptosis (Kiselyov *et al.* 2007; Settembre *et al.* 2008a; de Pablo-Latorre *et al.* 2012).

1.4.4 Apoptosis in the ganglioside-storing brain

Apoptosis is another process often observed in neurodegenerative disorders. Apoptotic cells or an up-regulation of pro-apoptotic genes have been observed in MPS II, MPS IIIB, Tay-Sachs, Sandhoff and NPC brains (Huang *et al.* 1997; Myerowitz *et al.* 2002; Ohmi *et al.* 2003; Wu *et al.* 2005; Villani *et al.* 2007; Hamano *et al.* 2008; Richard *et al.* 2008; Arfi *et al.* 2011).

Another interesting observation is that ganglioside G_{M3}, which accumulates in the MPS, Tay-Sachs, Sandhoff and NPC brain, induces apoptosis of normal, actively proliferating neuronal cells during development (Nakatsuji and Miller 2001; Noll *et al.* 2001; McGlynn *et al.* 2004; Sohn *et al.* 2006; Zhou *et al.* 2011). While neurons in the fully developed brain are not actively proliferating, it is possible that the secondary storage of brain G_{M3} results in apoptosis where it would not normally occur. This is supported by *in vitro* studies demonstrating that the addition of high levels of G_{M3} to normal neurons results in apoptosis (Sohn *et al.* 2006). In addition, G_{M3}-induced apoptosis seems to occur in response to oxidative stress, which is a component of CNS disease in the G_{M2}-storing brain (Chapter 1.4.2).

1.5 Therapies for LSDs

Many replacement enzyme therapies are in clinical use for the treatment of LSDs. These involve the introduction of functional enzyme to fill the role of the dysfunctional enzyme and reduce stored substrate. To accomplish this, a number of treatment methods have been employed, individually or in combination. A bone marrow transplant (BMT) can be performed to introduce cells with functional enzyme, enzyme can be introduced intravenously in enzyme replacement therapy (ERT), or the gene coding for the enzyme can be introduced and incorporated into the genome using gene therapy (GT). Alternatively, SDT acts to reduce synthesis of the storage material in order to direct synthesis and degradation towards equilibrium. All of these therapies have been implemented clinically.

1.5.1 Bone marrow transplantation

BMT is a once-only treatment for the introduction of stem cells capable of producing functional enzyme and the secretion of this enzyme for uptake by, and thus cross-correction of, host cells. It is currently in clinical use or being evaluated for around 20 different LSDs, however, it was first used to treat severe MPS I and continues to be effective in treating both somatic and CNS disease is this disorder (Hobbs *et al.* 1981; Whitley *et al.* 1993; Krivit *et al.* 1995; Peters and Steward 2003).

Despite BMT being the treatment of choice for MPS I patients with CNS degeneration, the same is not true for neurological disease in MPS II and III. The reason for the different responses to treatment between MPSs is unknown. Given the high mortality and morbidity rates associated with BMT, due to either graft failure, graft versus host disease or infection, only patients with an MPS for which significant improvements to quality of life have been demonstrated are considered for this treatment (Hobbs *et al.* 1981; Whitley *et al.* 1993; Peters and Steward 2003; Boelens *et al.* 2013). MPS II patients have had mixed clinical outcomes when treated with BMT. Although somatic disease is improved, due to the poor neurological response, this treatment is not recommended (Shapiro *et al.* 1995; McKinnis *et al.* 1996; Vellodi *et al.* 1999). Nor is BMT recommended to treat MPS III disease, which is characterised by CNS degeneration, and has been relatively unresponsive regardless of age and stage of disease at transplant (Vellodi *et al.* 1992; Shapiro *et al.* 1995; Sivakumur and Wraith 1999). MPS IV children suffer mainly from skeletal complications including restrictive lung disease, and cardiac valvular disease. There are very few cases of BMT in these patients and most have been performed in children over the age of two with little evidence of effectiveness for this therapy (Fletcher, personal communication 2012) (Seto *et al.* 2001; Peters and Steward 2003). However, MPS VI children are sometimes considered for BMT, as case studies demonstrate that this therapy can improve airway and cardiac disease

and reduce joint stiffness (Krivit *et al.* 1984; Alvaro *et al.* 1998; Herskhovitz *et al.* 1999). MPS VII patients have also been responsive to BMT (Yamada *et al.* 1998).

It has been suggested that BMT performed prior to the onset of CNS pathology can result in better clinical outcomes for this component of MPS disease, however some case reports indicate that pathology is not improved even with early treatment (Vellodi *et al.* 1992; Shapiro *et al.* 1995; McKinnis *et al.* 1996; Sivakumur and Wraith 1999). Thus, BMT is not appropriate for the treatment of CNS pathology in MPSs outside of MPS I.

1.5.2 Enzyme replacement therapy

The first ERT for a LSD, now in clinical use, was developed for Gaucher disease type I. This sphingolipidosis results from glucoceramide (GlcCer) storage in the lysosomes due to a failure of glucocerebrosidase to complete the final step of GSL degradation (Figure 1.2) (Brady *et al.* 1966). Human placental glucocerebrosidase with a mannose tag at the terminal end was used to promote uptake by GlcCer storing macrophages. Intravenous delivery resulted in a clinical improvement in all pathology without adverse side effects (Barton *et al.* 1990; Beutler *et al.* 1991; Grabowski *et al.* 1995; Weinreb *et al.* 2002). However, ERT is ineffective at treating CNS disease in the neuronal forms of Gaucher disease; type II and III (Prows *et al.* 1997; Schiffmann *et al.* 1997).

1.5.2.1 Enzyme replacement therapy for the MPSs

ERT has since been developed for the treatment of MPS I, II and VI patients. In 2003, laronidase was approved for clinical use for MPS I after clinical trials demonstrated improved respiratory function, increased joint mobility, reduced urinary GAG and reduced liver volume (Kakkis *et al.* 2001; Grabowski and Hopkin 2003; Wraith *et al.* 2004; Laraway *et al.* 2013). Studies monitoring the effect of long-term treatment showed that improvements in urinary

GAG levels were maintained for all patients. In addition, the majority of patients had a normalisation of liver volume and stabilised or improved visual acuity, joint mobility, respiratory function, endurance, as well as overall quality of life (Sifuentes *et al.* 2007; Clarke *et al.* 2009; Laraway *et al.* 2013). Some improvements in growth have also been reported for patients treated prior to puberty (Kakkis *et al.* 2001; Sifuentes *et al.* 2007; Laraway *et al.* 2013). Idursulfase was approved for the treatment of MPS II patients in 2006. Clinical trials demonstrated decreased urinary GAG, decreased liver and spleen volumes, improved endurance and respiratory improvements (Muenzer *et al.* 2007; Sohn *et al.* 2013). In addition, bone disease was improved in a patient treated long-term, prior to puberty (Papadia *et al.* 2011). Galsulfase was approved in 2005 for the treatment of MPS VI patients. Treatment outcomes included decreased urinary GAG, improved joint pain and mobility, reduced liver and spleen volume, increased visual acuity, improved respiratory function, stabilised or improved endurance and stabilised or improved growth (Harmatz *et al.* 2005; Harmatz *et al.* 2006; Harmatz *et al.* 2008; Koseoglu *et al.* 2009; Harmatz *et al.* 2010; Horovitz *et al.* 2013). ERT in all three of these MPSs has been demonstrated to be most effective when treatment begins prior to the onset of symptoms (Laraway *et al.* 2013; Tajima *et al.* 2013).

Although ERT has been successful in the treatment of somatic disease in many LSDs, it is limited by the inability of functional enzyme to diffuse across the BBB into the CNS, or into avascular tissues such as joints and the cornea (Jones *et al.* 1998; Downs-Kelly *et al.* 2000; Weinreb *et al.* 2002; Kakkis *et al.* 2004; Vogler *et al.* 2005b; Wraith 2006). These limitations can be avoided by increasing the dose of ERT or localising treatment to the affected tissues. Attempts at ERT using high concentrations of enzyme in LSD animal models have in some cases demonstrated improved outcomes for these hard-to-reach tissues, however this is not practical due to the extreme cost of ERT drugs (Jones *et al.* 1998; Kakkis *et al.* 2004; Vogler *et al.* 2005b; Wraith 2006). In addition, delivery of enzyme straight into the joints or CNS, although effective, is invasive and can elicit an immune response (Kakkis *et al.* 2004; Auclair

et al. 2007; Dickson *et al.* 2010; Vera *et al.* 2013). This is not surprising given that even systemic treatment has been reported to cause an antibody response in a number of case studies (Saif *et al.* 2012; Barbier *et al.* 2013; Brands *et al.* 2013; Kim *et al.* 2013; Sohn *et al.* 2013).

As described earlier, disorders such as the G_{M2} gangliosidoses and many of the MPSs have significant CNS degeneration and it is vital that treatments target this pathology. ERT can be an effective treatment, but has significant limitations.

1.5.3 Gene therapy

Gene therapy has been investigated for LSDs as it has the advantage over ERT of providing long-term expression of functional enzyme with a single dose, and thus, at a lower cost. Delivery is most often through an adeno-associated viral (AAV) vector (~4.7 kb), which is maintained long-term episomally in non-dividing cells, or a retroviral vector (5-10 kb), which is able to infect cells and incorporate into the patient genome via transposable elements for stable expression (Ponder and Haskins 2007). Similar to other replacement enzyme therapies, MPS animal trials have demonstrated a clearing of liver, spleen and lung storage with the administration of intravenous or intrahepatic therapeutic virus. A smaller response has been observed in the aorta, bone, cartilage and brain, particularly with treatment initiated at a very early age (Ponder *et al.* 2002; Mango *et al.* 2004; Kobayashi *et al.* 2005; Liu *et al.* 2005b; Cardone *et al.* 2006; Ponder *et al.* 2006; Donsante *et al.* 2007a; Ma *et al.* 2007; Traas *et al.* 2007; McIntyre *et al.* 2008; Bielicki *et al.* 2010; McIntyre *et al.* 2010; Macsai *et al.* 2012; Haurigot *et al.* 2013). Brain disease has also been tackled using localised injections of therapeutic virus into the striatum, lateral ventricles, thalamus, cortex or intrathecal space, which has resulted in both biochemical and functional improvements for this aspect of MPS disease (Frisella *et al.* 2001; Brooks *et al.* 2002; Cressant *et al.* 2004; Liu *et al.* 2005a; Ciron *et al.* 2006; Bielicki *et al.* 2010; McIntyre *et al.* 2010; Baldo *et al.* 2013; Heldermon *et al.* 2013).

In developing gene therapy, it is important that the viral vector is effective in infecting a maximum number of cells, safely, with no host immune response directed towards the vector or the therapeutic enzyme itself. Both cytotoxic T lymphocyte and antibody responses towards the transgene have been observed in gene therapy animal trials and this is often overcome through the use of immunosuppressive agents (Di Domenico *et al.* 2005; Ciron *et al.* 2006; Ponder *et al.* 2006; Ma *et al.* 2007). Therapeutic virus that integrates into chromosomes also carries a risk of disrupting tumour suppressor genes, resulting in tumour growth. This outcome has been observed in a small number of AAV gene therapy animal studies and is of significant concern (Donsante *et al.* 2001; Donsante *et al.* 2007b). Despite the many promising results that have come out of animal trials, controlling the safety risks associated with gene therapy is vital and the greatest limiting factor for the development of this treatment for the MPSs.

1.5.4 Substrate deprivation therapy

SDT, originally proposed by Radin and colleagues (Inokuchi and Radin 1987), focuses on decreasing synthesis of the stored substrate rather than increasing its degradation. Provided there is some residual enzyme activity, this allows for the lysosomal burden of the substrate to be reduced and for equilibrium between synthesis and degradation to return close to normal. In support of SDT, Liu et al. (1999) showed that the therapy could be used to reduce Sandhoff disease outcomes by crossing Sandhoff mice with β1,4-N-acetylgalactosaminyltransferase null mice, thus decreasing G_{M2} synthesis (Figure 1.1) and producing offspring with long-term survival. It is important to note that completely blocking synthesis of an enzyme, as was done in this proof of principle study, has the potential to cause other detrimental physiological changes. However, SDT agents that cause a reduction in synthesis rather than a complete block of the pathway do not cause such complications.

SDT is effective in treating LSDs with CNS degeneration in animal models and human trials, using inhibitory molecules that are able to cross the BBB due to their small size and hydrophobic nature. This is an advantage over replacement enzyme therapies and makes it useful for the treatment of the G_{M2} gangliosidoses and for MPS disorders with CNS disease. One of these chemical inhibitors is the isoflavone genistein, which decreases GAG synthesis. It has been used in human clinical trials to treat MPS IIIA and MPS IIIB, resulting in treatment outcomes that include decreased urinary GAG and improved/stabilised sleep habits, general behaviour, speech performance and comprehension in some patients (Piotrowska *et al.* 2008; Piotrowska *et al.* 2011). Trials in a mouse model of MPS II have demonstrated decreased GAG levels in the urine, liver, spleen and heart, as well as a small reduction in brain storage (Friso *et al.* 2010). Genistein treatment also decreased urinary gag in MPS II patients, however, without clinical improvement. Another chemical inhibitor used *in vivo* to treat MPS IIIA mice is the non-specific inhibitor of gag synthesis, rhodamine B. Roberts et al. (2006; 2007) demonstrated that the drug was effective in reducing MPS IIIA mouse liver size, reducing gag storage in both the liver and brain and improving CNS function.

While genistein and rhodamine B target GAG synthesis, the small chemical inhibitor *N*B-DNJ acts upon GSL synthesis (Figure 1.3) (Platt *et al.* 1994; Platt *et al.* 1997a; Platt *et al.* 1997b). Treatment using this drug is at various stages of development, ranging from human clinical trials in the G_{M2} gangliosidoses to clinical use in Gaucher disease type 1 (non-neuronal) (described in Chapter 1.5.4.1.1). *N*B-DNJ is administered orally, which is an advantage as ease of administration encourages patient compliance.

1.5.4.1 N-*Butyldeoxynojirimycin*

*N*B-DNJ (also known as miglustat, OGT 918 and Zavesca) is a small, water soluble, non-cytotoxic, iminosugar, which inhibits GSL synthesis. It prevents the glucosyltransferase catalysed addition of glucose to ceramide, thus reducing the synthesis of down-stream GSLs

(Figure 1.3) (Platt *et al.* 1994; Platt *et al.* 1997a; Platt *et al.* 1997b). The original study of *N*B-DNJ was conducted with an aim to decrease the viral burden in HIV-1 patients, as reduction in the number of GSLs present on the cell surface decreases sites for HIV attachment (Table 1.3). *N*B-DNJ was not effective in these clinical trials, however, these studies provided a lot of the initial knowledge on *N*B-DNJ pharmacokinetics (Fischl *et al.* 1994; Tierney *et al.* 1995).

1.5.4.1.1 N*B-DNJ for the treatment of Gaucher disease type 1*

*N*B-DNJ has also been investigated as an agent for SDT for a number of GSL storage diseases (Table 1.3). The most developed SDT using *N*B-DNJ has been in Gaucher disease type 1 (non-neuropathic). A number of open labelled, long-term treatment studies have been conducted, demonstrating improvements in systemic disease (Cox *et al.* 2003; Elstein *et al.* 2004; Pastores *et al.* 2005; Elstein *et al.* 2007; Pastores *et al.* 2007; Giraldo *et al.* 2009). Side effects observed with *N*B-DNJ treatment have also been well documented in these studies. Diarrhoea and weight loss are often observed, most likely due to intestinal carbohydrate malabsorption (Amiri and Naim 2012); however most patients recover from these side effects by the end of the first 12 months of treatment (Cox *et al.* 2000; Elstein *et al.* 2004; Pastores *et al.* 2005). Tremor is described in 30% of patients, occurring within the first few months of treatment. If this continues, it can be resolved by the reduction/discontinuation of treatment (Cox *et al.* 2003). Parasthesia has been observed in 15-20% of patients, again resolving once treatment is reduced or stopped (Cox *et al.* 2000; Pastores *et al.* 2005). As a result of trial outcomes, *N*B-DNJ was authorised for clinical use in mild to moderate Gaucher disease type I cases where ERT is not suitable (Cox *et al.* 2003).

A

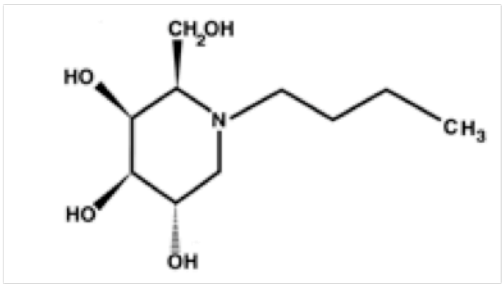

N-butyldeoxynojirimycin

(*N*B-DNJ)

B

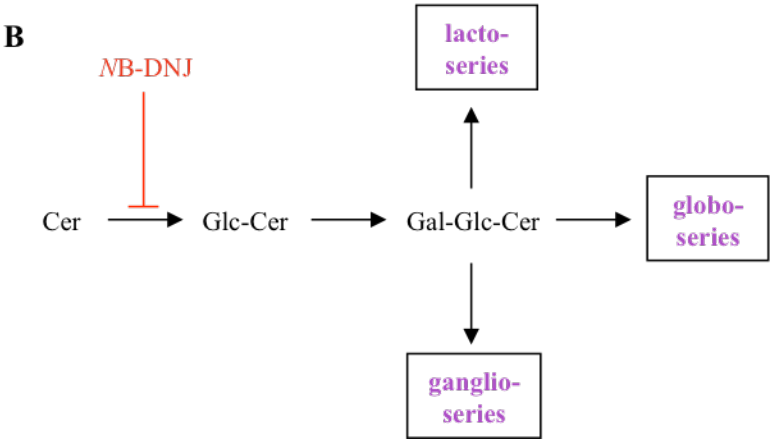

Figure 1.3: Inhibition of ganglioside synthesis by *N*-butyldeoxynojirimycin. *N*-butyldeoxynojirimycin (*N*B-DNJ) is a small imino-sugar that inhibits GSL synthesis **(A)**. It acts by the non-competitive inhibition of the fist step of synthesis, in which a glucose residue is added to ceramide **(B)**. Thus, synthesis of all downstream molecules in the lacto-, globo- and ganglio-series is reduced.

Adapted from Platt *et al*. (1994), Platt *et al.* (1997a) and Platt *et al*. (1997b).

Table 1.3: Therapeutic uses of *N*B-DNJ.

Research area	Application of *N*B-DNJ	Subjects	Status	References
HIV-1	Decrease viral burden in patients	Human	Abandoned	Fischl *et al.* 1994; Tierney *et al.* 1995.
Gaucher disease type 1	SDT for primary GSL storage	in vitro	Progressed to clinical trials	Platt *et al.* 1994.
		Human	Clinical use	Cox *et al.* 2000; Cox *et al.* 2003; Elstein *et al.* 2004; Pastores *et al.* 2005; Elstein *et al.* 2007; Giraldo *et al.* 2009.
Gaucher disease type 3	SDT for primary GSL storage	Human	Ongoing clinical trials	Capablo *et al.* 2007; Schiffmann *et al.* 2008; Accardo *et al.* 2010.
Tay-Sachs disease	SDT for primary GSL storage	Murine	Progressed to clinical trials	Platt *et al.* 1997.
		Human	Ongoing clinical trials	Jacobs *et al.* 2005; Bembi *et al.* 2006; Shapiro *et al.* 2009.
Sandhoff disease	SDT for primary GSL storage	Murine	Progressed to clinical trials	Jeyakumar *et al.* 1999; Jeyakumar *et al.* 2001.
		Human	Ongoing clinical trials	Tallaksen and Berg 2009; Wortmann, Lefeber *et al.* 2009; Maegawa, Banwell *et al.* 2009; Masciullo, Santoro *et al.* 2010.
Niemann-Pick C	SDT for secondary storage	Murine and feline	Progressed to clinical trials	Zervas *et al.* 2001.
		Human	Clinical trials and clinical use	Lachmann *et al.* 2004; Chien *et al.* 2007; Patterson *et al.* 2007; Santos *et al.* 2008; Paciorkowski *et al.* 2008 Galanaud *et al.* 2009; Pineda *et al.* 2009; Wraith and Imrie 2009; Wraith *et al.* 2010; Patterson et al. 2010; Fecarotta, *et al.* 2011; Zarowski *et al.* 2011; Di Rocco *et al.* 2012; Heron *et al.* 2012; Karimzadeh *et al.* 2013; Patterson *et al.* 2012; Skorpen *et al.* 2012; Jesus *et al.* 2013.
MPS IIIA	SDT for secondary storage	Human	First clinical trial	Guffon *et al.* 2011.

1.5.4.1.2 N*B-DNJ for the treatment of LSDs with CNS disease*

Due to the small size of *N*B-DNJ it was suggested that it could cross the BBB to treat neuronal pathology, thus steps have also been taken to develop SDT by *N*B-DNJ for the treatment of LSDs with CNS involvement. This includes both LSDs with primary and secondary GSL storage.

1.5.4.1.2.1 N*B-DNJ for the treatment of primary brain GSL storage*

A *N*B-DNJ therapy has been demonstrated to be effective in the treatment of Sandhoff mice, resulting in decreases in brain and liver ganglioside levels, fewer apoptotic neurons, reduced inflammation, improved behaviour and increased survival (Jeyakumar *et al.* 1999; Jeyakumar *et al.* 2001). *N*B-DNJ has since been trailed in children with Sandhoff disease. Treatment outcomes have varied, with some patients displaying improved or stabilised motor, cognitive and neuromuscular function and MRI brain lesions and other patients displaying little or no change with treatment (Maegawa *et al.* 2009; Tallaksen and Berg 2009; Wortmann *et al.* 2009; Masciullo *et al.* 2010). It is noted that the treatment outcomes from these studies are difficult to assess, given that it is not easy to predict the course of disease, even between patients with a common mutation. Thus, a slowing of disease progression with *N*B-DNJ treatment cannot always be identified (Maegawa *et al.* 2009; Tallaksen and Berg 2009; Masciullo *et al.* 2010).

This is also true for the *N*B-DNJ treatment of the neuronal form of Gaucher disease, Gaucher disease type 3. Some improvements have been observed with treatment, including reduced neuronal storage, reduced seizures and improved CNS function (Capablo *et al.* 2007; Accardo *et al.* 2010). Despite these propounded positive outcomes, patients treated with *N*B-DNJ in combination with ERT in a 24 month, open-label clinical trial have not had any significant

improvements in neurological disease, however, somatic disease has responded to treatment (Schiffmann *et al.* 2008).

The treatment of brain disease using *N*B-DNJ has also been trialled in Tay-Sachs disease. G_{M2} storage has been reduced in non-symptomatic Tay-Sachs disease mice (Platt *et al.* 1997a). In human trials no improvements in neuronal pathology have been observed apart from the prevention of macrocephaly (Jacobs *et al.* 2005; Bembi *et al.* 2006; Shapiro *et al.* 2009). The drug has however been detected in the CSF, demonstrating the ability of *N*B-DNJ to cross the BBB (Bembi *et al.* 2006).

1.5.4.1.2.2 N*B-DNJ for the treatment of secondary brain GSL storage*

SDT by NB-DNJ has also been used to decrease secondary storage in NPC, with more positive outcomes than those observed in human trials in primary brain GSL storing disorders. This has led to its approval for clinical use for NPC patients in 2009 (Wraith and Imrie 2009; Di Rocco *et al.* 2012; Patterson *et al.* 2012).

Initially, *N*B-DNJ was used to treat both murine and feline models of NPC (Zervas *et al.* 2001b). Treatment reduced brain G_{M2} levels, prevented the formation of neuronal axon swellings, delayed tremor and ataxia and extended life span. This supports the theory that secondary storage of ganglioside is responsible for neurological manifestations in NPC.

Trials of *N*B-DNJ in NPC patients have demonstrated that the drug crosses the BBB into the CSF and results in improvement or stabilisation of motor, cognitive and neuromuscular function, as well as a reduction in seizures (Chien *et al.* 2007; Patterson *et al.* 2007; Santos *et al.* 2008; Pineda *et al.* 2009; Patterson *et al.* 2010; Wraith *et al.* 2010; Fecarotta *et al.* 2011; Zarowski *et al.* 2011; Di Rocco *et al.* 2012; Heron *et al.* 2012; Karimzadeh *et al.* 2012; Skorpen *et al.* 2012; Jesus *et al.* 2013; Karimzadeh *et al.* 2013). A decrease in biochemical

markers of brain disease has also been demonstrated in NPC patients after treatment with *N*B-DNJ (Galanaud *et al.* 2009). Contrasting with these promising results, a three-year-old patient in another study had no response to *N*B-DNJ treatment, perhaps due to a severe course of disease suggested by neonatal onset (Paciorkowski *et al.* 2008). It has been demonstrated that therapy is most effective when initiated prior to clinical manifestations (Di Rocco *et al.* 2012).

To date, CSF ganglioside levels have not been measured in NPC patients, however mouse models demonstrate that brain gangliosides are lower in NPC than in Tay-Sachs or Sandhoff disease and may be the reason why altering the rate of ganglioside accumulation using *N*B-DNJ may be more therapeutically effective in the NPC brain (Walkley and Vanier 2009). The MPSs are similar to NPC, in that the accumulation of gangliosides is secondary and is at a lower level than in the gangliosidoses (Guffon *et al.* 2011). This has led to one of the hypotheses tested in this thesis: that MPS neuropathology would respond to SDT using *N*B-DNJ.

1.5.4.1.2.2.1 N*B-DNJ for the treatment of MPS brain disease*

During the course of this thesis, a clinical trial treating MPS III patients with *N*B-DNJ was published. While the drug was detected in the CSF of MPS III patients, no improvements in behavioural pathology were observed (Guffon *et al.* 2011). As described above, the assessment of neurological function in children with degenerative brain disease is problematic given that the patients often do not cooperate and that the course of disease can be difficult to predict (Gabrielli *et al.* 1992; McDowell *et al.* 1993; Bunge *et al.* 1998; Ruijter *et al.* 2008; Valstar *et al.* 2010b; Valstar *et al.* 2010c; Valstar *et al.* 2011). For these reasons, animal models are a valuable resource for the assessment of the effect of treatments. Large numbers can be generated, and neurological function can be characterised following the SHIRPA phenotypic assessment protocol (Chapter 1.7). A number of MPS animal models are available, which could potentially be used for this purpose.

1.6 MPS animal models

Animal models are important for the development and evaluation of disease therapies prior to their use in humans. Canine, feline and a number of murine models exist for the MPS disorders, with varying loss of enzyme function and thus, varying disease severity (Haskins *et al.* 1984; Birkenmeier *et al.* 1989; Fyfe *et al.* 1999; Neufield and Muenzer 2001). The advantages of using murine models of disease are that (i) a large number of animals can be bred over a short period of time to produce less varied results, (ii) they are accurate models of human disease and (iii) tests for rodent behaviour have been well characterised (Neufield and Muenzer 2001).

In this project, two murine models of MPS were characterised to determine the ideal model for a *N*B-DNJ therapeutic trial. MPS III is the only MPS with CNS pathology alone; therefore, this MPS lends itself to a trial focused on brain disease (Bhaumik *et al.* 1999; Bhattacharyya *et al.* 2001; Neufield and Muenzer 2001). The MPS VII mouse also displays CNS pathology and can represent a severe model of disease (Birkenmeier *et al.* 1989; Vogler *et al.* 1990; Sands and Birkenmeier 1993; Vogler *et al.* 2005a). In this study, the brain biochemistry and behaviour of the MPS IIIA and severe MPS VII murine models were examined.

1.6.1 MPS IIIA mouse model

The MPS IIIA mouse model results from a naturally occurring G91A point mutation in the sulphamidase gene, resulting in 3-4% of normal sulphamidase activity (Bhaumik *et al.* 1999; Bhattacharyya *et al.* 2001). Thus, this model represents a more attenuated form of the disease.

Lysosomal storage has been found by both light and electron microscopy to be widespread, being observed in Kupffer cells of the liver, parenchyma of the spleen, epithelial podocytes

and epithelial cells of the kidney, infiltrating fibroblasts and macrophages in the wall of the urinary bladder, fibroblasts and macrophages in the heart, and in a number of cell types in the brain, including neurons, microglia, perineuronal satellite cells, endoneural fibroblasts, endothelial cells and Schwann cells (Bhaumik *et al.* 1999). Many neurons contain floccular inclusions as well as zebra bodies, which stain positive for G_{M2} ganglioside, as is observed in human MPS IIIA autopsied brains (Constantopoulos and Dekaban 1978; Constantopoulos *et al.* 1980; Bhaumik *et al.* 1999).

Consistent with human MPS IIIA, pathology includes increased bodyweight, facial dysmorphism, a hunched posture, hepatosplenomegaly, corneal clouding, bladder distension, and behavioural abnormalities that include learning and memory deficits and aggression (Bhaumik *et al.* 1999).

1.6.2 MPS VII mouse model

The gus^{mps}/gus^{mps} MPS VII mouse model results from a naturally occurring single base pair deletion in exon 10 of the β-glucuronidase (GUSB) gene that produces a premature stop codon and reduces GUSB expression by >200 fold (i.e. less than 0.1% of normal activity) (Birkenmeier *et al.* 1989; Vogler *et al.* 1990; Sands and Birkenmeier 1993). Almost no enzyme activity is detected, resulting in a severe phenotype, which mimics that of severe human MPS VII. Storage has been demonstrated as early as one week prior to birth. By weaning at three weeks of age, MPS VII mice have growth retardation, shorter limbs, a shorter, thicker tail and facial dysmorphism, compared with normal litter-mates. Mice also have splenomegaly and deficits in CNS function, before premature death by eight months of age (Birkenmeier *et al.* 1989; Vogler *et al.* 1990; Sands and Birkenmeier 1993; Vogler *et al.* 2005a). MPS VII male mice are sterile and females are unable to lactate; thus, breeding in the

MPS VII colony must be between heterozygous mice (+/gus^{mps}), which have a wild type phenotype (Birkenmeier *et al.* 1989).

1.7 Behaviour testing in rodents

The challenge in characterising progressive neurological disease in animal models, such as the MPS IIIA and MPS VII mouse models, is maintaining consistency between different mice, ages and groups. A standardised quantitative battery of tests for brain and neuromuscular function, known as SHIRPA, has been developed to minimise inconsistencies and make data comparable. SHIRPA has three components. The first is a scored observation of behaviour, body weight and neuromuscular function (including grip strength and limb tone), while the second and third tiers focus on functional screening and analysis of pathology and neurological assessment respectively (Table 1.4) (Rogers *et al.* 1997; Rogers *et al.* 2001). From each tier, behaviour tests have been chosen to assess known MPS pathologies.

1.7.1 The primary stage of the SHIRPA protocol

In order to satisfy the first stage of the SHIRPA protocol (Table 1.4), mice are weighed frequently and any observational changes in general condition assessed at these times (Rogers *et al.* 1997; Rogers *et al.* 2001). While this stage of the protocol is mainly observational, one behaviour test used to measure neuromuscular strength quantifies some of the first tier elements (Table 1.4). This is the inverted grid test.

1.7.1.1 The inverted grid

In the inverted grid test, a mouse is placed on a wire grid and turned upside-down above a cushioned surface and the amount of time spent holding on is measured. Deficits in neuromuscular strength have been demonstrated using this test in mouse models of

Table 1.4: SHIRPA.

Stage	Observation/ behaviour	Tests
Primary	Observational screen: • Excitability and aggression • Body weight • Visual acuity • Gait and posture • Motor control and coordination • Neuromuscular strength • Defecation • Muscle tone • Temperature	• Observation of undisturbed behaviour • Weight measurement • Tail suspension • Grip strength • Inverted grid • Wire maneuver • Righting reflex
Secondary	Behavioural and pathological screen: • Motor function • Balance • Coordination • Spontaneous locomotor activity • Blood and tissue abnormalities	• Rotarod • Inverted grid • Vertical beam • Open field • Biochemical tests
Tertiary	Specialised neurological screen: • Anxiety • Learning and memory	• Open field • Elevated plus maze • Light-dark box • Morris water maze • Water cross-maze • RAPC

Adapted from Rogers, Perter *et al.* (2001) and Rogers, Fisher *et al.* (1997).

neurodegeneration, including MPS IIIA, IIIB and VII (Rogers *et al.* 1997; Jeyakumar *et al.* 1999; Rogers *et al.* 2001; Hemsley and Hopwood 2005; Langford-Smith *et al.* 2011b; Macsai *et al.* 2012). Thus, the inverted grid could be a useful tool in the current study, to characterise MPS IIIA and MPS VII brain pathology and to assess the effect of treatment.

1.7.2 The secondary stage of the SHIRPA protocol

The second stage of the SHIRPA protocol is a behavioural and pathological screen (Table 1.4). The pathology screen includes a biochemical analysis of GAG, ganglioside and other lipid components of MPS disease and is required for the characterisation of MPS IIIA and MPS VII models, both with and without treatment (McGlynn *et al.* 2004). Behaviour tests in the secondary stage of SHIRPA include the inverted grid (which overlaps with tier one), accelerating rotarod, vertical pole and open field.

1.7.2.1 The rotarod

The rotarod measures motor function, balance, and coordination (Figure 1.4). Mice are placed on a rotating drum and the amount of time that they are able to remain on the apparatus is measured (Dunham and Miya 1957; Jones and Roberts 1968; Rogers *et al.* 1997; Rogers *et al.* 2001). An advantage is that this is an automated test, thus the variation produced by the researcher conducting the test is removed. The rotarod has previously been effective in differentiating between MPS mice and normal age-matched controls in a number of murine MPS models, including MPS II, IIIB and VII, and would therefore be useful in the current study (Garcia-Rivera *et al.* 2007; Heldermon *et al.* 2007; Polito *et al.* 2010; Macsai *et al.* 2012).

1.7.2.2 The vertical pole

The vertical pole is another stage two behaviour test, which can complement data from the rotarod (Figure 1.4). A mouse is placed on a pole over a cushioned surface, and the pole is raised at one end from horizontal to vertical. The angle at which the mouse falls off the pole is recorded. The ability of mice with deficient motor coordination and balance to remain on the pole is reduced as the angle increases (Rogers *et al.* 1997; Rogers *et al.* 2001; Abramow-Newerly *et al.* 2006).

1.7.2.3 The open field

One behaviour test that measures both second and third stage behaviours is the open field animal activity monitor (Figure 1.4) (Rogers *et al.* 1997; Rogers *et al.* 2001). This assesses spontaneous locomotor activity across horizontal and vertical planes (tier two) by measuring infrared sensor beam crosses and converting this data to distance traveled and rearing events. Hyperactivity and an increased fear response can suggest anxiety (tier three), while hypoactivity suggests passive behaviour (Rogers *et al.* 1997; Rogers *et al.* 2001). The open field test is commonly used to assess behaviour in many MPS mouse models, including MPS II, IIIA, IIIB and VII (Hemsley and Hopwood 2005; Reolon *et al.* 2006; Lau *et al.* 2008; Bielicki *et al.* 2010; Malinowska *et al.* 2010; McIntyre *et al.* 2010; Polito *et al.* 2010; Langford-Smith *et al.* 2011a; Langford-Smith *et al.* 2011b; Macsai *et al.* 2012). Furthermore, this test and an effective protocol has been set up and is available for use in this study. It should be noted that other tests such as the elevated plus maze and the light/dark box are also available to measure anxiety in neurological diseases (Figure 1.4). However, these behaviour tests measure anxiety alone, while the open field can measure both anxiety and exploratory activity (Rogers *et al.* 1997; Rogers *et al.* 2001; Reolon *et al.* 2006; Langford-Smith *et al.* 2011a).

1.7.3 The tertiary stage of the SHIRPA protocol

Neuropsychiatric function measured in the third stage of SHIRPA includes an assessment of anxiety and spatial learning and memory (Figure 1.4) (Rogers *et al.* 1997; Rogers *et al.* 2001). The measurement of anxiety via the open field is a part of this tier of the SHIRPA. Learning and memory are measured using a maze. Many mazes have been designed for this purpose and are described below.

1.7.3.1 The repeated acquisition and performance chamber

The repeated acquisition and performance chamber (RAPC) requires mice to learn the sequence of one-way doors that lead through a series of transparent chambers to a saccharin reward (Brooks *et al.* 2000; Brooks *et al.* 2002). The difficulty with this and other dry land mazes is that the positive stimulus often does not encourage mice to perform in and learn the task (Derrick Roberts, unpublished data).

1.7.3.2 The Morris water maze

Water mazes, in which mice are exposed to a water escape scenario, can overcome problems with mouse participation in the task. A number of studies have used the Morris water maze to test special learning and memory in MPS I, IIIA and VII mouse models (Bastedo *et al.* 1994; Sakurai *et al.* 2004; Crawley *et al.* 2006; Pan *et al.* 2008; Wolf *et al.* 2011). In this test rodents use constant visual cues to locate a platform in a circular pool filled with opaque water (Morris 1984). However, the Morris water maze was originally developed for rats and although it has since been adapted for mice, this test still has some shortfalls (Morris 1984; Whishaw and Tomie 1996; Llano Lopez *et al.* 2010). Mice are poorer swimmers than rats and are therefore suited to a smaller pool (Whishaw and Tomie 1996; Llano Lopez *et al.* 2010). A behaviour test that still follows the pool escape scenario, while requiring mice to cover a far smaller area, is the water cross-maze.

1.7.3.3 The water cross-maze

In the water cross-maze, mice use fixed cues to locate a submerged platform within a cross shaped pool filled with opaque water. This is repeated over a number of days to allow mice to learn the task and can then be repeated at monthly intervals to assess memory (Summers *et al.* 2006; Roberts *et al.* 2007; Macsai *et al.* 2012). The water cross-maze has been effective in demonstrating neuropathology in the MPS IIIA and MPS VII mouse models and will now be used to characterise MPS IIIA and MPS VII spatial learning with and without treatment (Roberts *et al.* 2007; Macsai *et al.* 2012).

1.8 Hypothesis and aims

CNS degeneration in many LSDs has been attributed to ganglioside storage. This has been demonstrated in disorders where ganglioside is the primary storage product, as in the G_{M2} gangliosidoses, as well as when it is secondary to storage of another macromolecule, as in NPC (Gravel *et al.* 2001; Zervas *et al.* 2001a). In both cases, ganglioside targeted SDT is being developed to treat CNS pathology, using the general inhibitor of GSL synthesis, *N*B-DNJ (Patterson *et al.* 2007; Santos *et al.* 2008; Galanaud *et al.* 2009; Maegawa *et al.* 2009; Shapiro *et al.* 2009; Fecarotta *et al.* 2011). MPS disorders with CNS involvement also accumulate G_{M2} secondary to the initial storage material, presenting a novel therapeutic target for CNS pathology, which until now has been untreatable (Neufield and Muenzer 2001). This leads to the hypothesis and aim of this project:

HYPOTHESIS: That SDT using *N*B-DNJ will help elucidate the role of gangliosides in MPS brain disease and will be effective in treating CNS degeneration in the MPS disorders.

AIMS:

1. To characterise biochemical and functional CNS pathology in the severe MPS VII and attenuated MPS IIIA murine models in order to add to the current model of MPS brain disease and to identify an appropriate model for treatment with *N*B-DNJ.
2. To determine whether treatment with *N*B-DNJ initiated early or later in pathology is effective at decreasing brain ganglioside levels and improving CNS functional deficits in an MPS murine model.
3. To characterise other brain lipids, both structural and inflammatory, in order to determine whether they have a role to play in MPS brain disease and whether they are altered with *N*B-DNJ treatment.

SIGNIFICANCE: Understanding MPS brain disease and the development of *N*B-DNJ treatment of CNS degeneration in the MPS disorders is of great significance for patient survival and quality of life. *N*B-DNJ has the potential to treat all MPSs with CNS involvement and could eventually be used in conjunction with a systemic therapy (e.g. ERT) to target all disease symptoms.

Chapter Two: Materials and methods

2.1 Materials

A list of materials is included in Appendix 1.

2.2 Murine models

2.2.1 Animal husbandry

Studies using animals were approved by the Children, Youth and Women's Health Service and the University of Adelaide Animal Ethics committees. Mice were same-sex group housed, at a constant temperature and humidity, on a 14 hour light/ 10 hour dark cycle, with *ad libitum* food and water. Cage changes, monitoring of mouse condition and weight measurement were performed weekly. Mice of six to 15 weeks of age were mated to produce up to three litters. MPS VII colony mating occurred between heterozygous mice. Normal or homozygous affected pairs were mated in the MPS IIIA colony. Pups were toe tagged at seven days of age for genotyping (Chapter 2.2.2). Weaning of pups took place at three weeks, under the condition that mice weighed a minimum of 5g. Mice were humanely killed at experimental end points by carbon dioxide asphyxiation.

2.2.2 Genotyping

A polymerase chain reaction (PCR)-based genotyping protocol was performed on genomic DNA prepared from toe samples according to Wolfe and Sands (1996) (MPS VII mouse model) or Roberts *et al.* (2009) (MPS IIIA mouse model). Normal and MPS alleles were distinguishable by restriction enzyme digestion. The single-base-pair deletion mutation in the MPS VII model results in the abolition of an NciI restriction site (Sands and Birkenmeier 1993) and the G91A point mutation in the MPS IIIA model results in the abolition of a MSPAII restriction site (Bhattacharyya *et al.* 2001).

2.2.2.1 Toe lysis

Genomic DNA was generated from toe tissue lysed using Viagen lysis buffer containing 0.4mg/mL proteinase K as per the manufacturer's instructions (Viagen Biotech Inc., USA). Lysates were stored at -20°C.

2.2.2.2 MPS VII genotyping PCR

The PCR reaction mix contained 1µL tissue lysate, 200µM dNTPs, 1x PCR buffer (1.5mM magnesium chloride, 10mM Tris-HCl, 50mM potassium chloride), 1.25U Taq polymerase, 1mM magnesium chloride, 50ng intronic primer (5'-CCT GTG TCA TTT GCA TGT G-3') and 50ng mismatch primer (5'-GAT AAC ATC CAC GTA CCG C-3'), made up to a final volume of 25µL. Reactions were placed in a thermocycler (Biorad, USA) for one cycle at 95°C for 15 minutes, 33 cycles at 94°C for 30 seconds, 52°C for 90 seconds and 72°C for one minute and one cycle at 72°C for one minute. PCR samples were stored at 4°C until analysed.

2.2.2.3 MPS IIIA genotyping PCR

The PCR reaction mix contained 2µL tissue lysate, 200µM dNTPs, 1x PCR buffer (1.5mM magnesium chloride, 10mM Tris-HCl, 50mM potassium chloride), 1.25U Taq polymerase, 1x Q solution, 100ng forward primer (5'-TCC AAC TCC TGA GCA TCA CA-3') and 100ng reverse primer (5'-AAC AGC TGC TGA CAG ACG TG-3'), made up to a final volume of 25µL. Reactions were placed in a thermocycler (Biorad, USA) for one cycle at 95°C for 10 minutes, 35 cycles at 95°C for 45 seconds, 55°C for 45 seconds and 72°C for 40 seconds and one cycle at 72°C for five minutes. PCR samples were stored at 4°C until analysed.

2.2.2.4 Enzyme digestion

MPS VII PCR products were digested with NciI. In each reaction 5µL PCR product was digested with 2.5U NciI restriction enzyme in 1x NEB4 buffer (New England Biolabs Inc., USA) at 37°C overnight. MPS IIIA genotyping PCR products were MspA1 digested. In each reaction 6µL PCR product was digested with 5U MspA1 restriction enzyme in 1x NEB4 buffer (New England Biolabs Inc., USA) at 37°C for one hour. Digest products were then visualised on agarose gels.

2.2.2.5 Gel electrophoresis

MPS VII and MPS IIIA digests were run on a 5% agarose gel (5% w/v agarose, 40mM Tris-acetate, 2mM EDTA pH 8.5), or 3% agarose gel (3% w/v agarose, 40mM Tris-acetate, 2mM EDTA pH 8.5) respectively, in TAE buffer (40mM Tris-acetate, 2mM EDTA pH 8.5), at 100V, for 40 minutes, alongside a Puc19/HpaII molecular weight marker. Loading buffer (20% Ficoll 400, 0.01M EDTA, 0.025% bromophenol blue, 0.1% SDS) was added to samples prior to loading onto the gel. Gels were stained for five minutes in 50µg/mL ethidium bromide and destained for 30 minutes with deionised water, before being visualised under UV using an Uvitec GelDoc system (version 11.01). For MPS VII samples band sizes of 77bp indicated normal, 77 and 95bp indicated heterozygote and 95bp indicated MPS VII genotypes (Figure 2.1). For MPS IIIA samples band sizes of 114/115bp indicated normal, 114/115 and 229bp indicated heterozygote and 229bp indicated MPS IIIA genotypes (Figure 2.1).

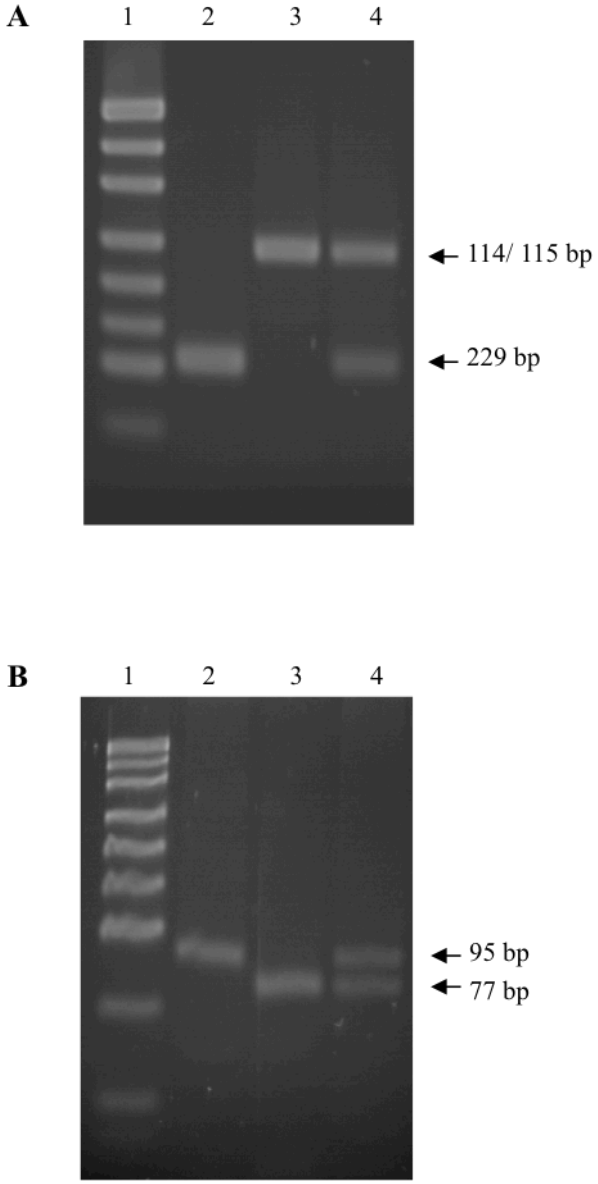

Figure 2.1: MPS genotyping.
The gene of interest was amplified from MPS IIIA (**A**) or MPS VII (**B**) tissue lysates by PCR, and digested with MspAI or NciI restriction enzymes respectively. Digests were run on 3% (**A**) or 5% (**B**) agarose gel. Lanes 1, 2, 3 and 4 contain a Puc19/ HpaII DNA marker, MPS, normal and heterozygote PCR digests respectively.

2.2.3 Behaviour tests

2.2.3.1 Vertical pole

Mice were placed in the centre of a 60cm long pole (1cm in diameter) over a cushioned surface (Figure 2.2). The pole was lifted at one end and raised from 0° to 90° (i.e. from horizontal to vertical) over 10 seconds and the angle at which mice fell off was recorded.

2.2.3.2 Inverted grid

The inverted grid test was performed as described by Macsai et al. (2012). Briefly, mice were placed on a 10cm by 18cm wire grid, which was inverted 50cm over a cushioned surface for a maximum of 120 seconds (Figure 2.3). The time to fall from the inverted grid was recorded.

2.2.3.3 Rotarod

The rotarod test was performed as described by Macsai et al. (2012). Briefly, mice were placed on the rotating barrel of a rotarod apparatus (Ugo Bassile S.r.l., Italy; Figure 2.4), which accelerated from five to 35rpm over two minutes and then maintained 35rpm for a further minute. As mice fell off, a lever was activated and the time was recorded using Communication Ugo Bassile version 3.0.15 software (Ugo Bassile S.r.l., Italy, 2005). Mice completed two trials 30 minutes apart each day for three consecutive days. All but the last trial were used to habituate the mice to the test. Performance on the second trial of the third day (the final trial) was used for comparison between ages and genotypes.

Figure 2.2: Vertical pole.
The vertical pole test measures neuromuscular strength. Mice are placed on a 60cm long pole, which is raised at one end from 0°to 90°over a cushioned surface. The angle at which mice fall off is recorded.

Figure 2.3: Inverted grid.
The inverted grid test is used to measure neuromuscular strength. Mice are placed on a 10 by 18cm wire grid, which is inverted 50cm over a cushioned surface for 120 seconds. The time that mice are able to remain on the grid, up to a maximum of 120 seconds, is recorded.

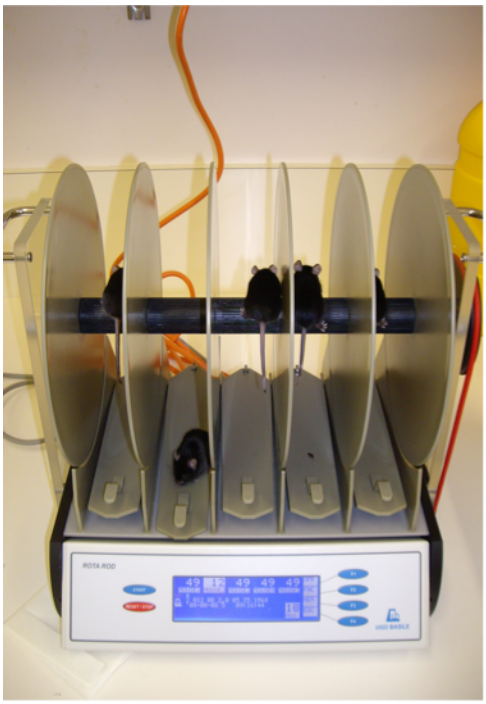

Figure 2.4: Rotarod.
The rotarod is used to measure motor coordination and balance. Mice are placed on a rotating barrel, which accelerates from 5 to 35rpm over two minutes and then maintains 35rpm for a further minute. As mice fall off, a leaver is activated and the time recorded by the apparatus.

2.2.3.4 Open field

The open field test was performed as described by Macsai et al. (2012). Briefly, mice were released in the front left hand corner of a Versamax animal activity monitor (AccuScan Instruments, Inc., USA; Figure 2.5). Horizontal and vertical sensor beam crosses over three minutes were recorded by the apparatus and Versamax 4.20 software (AccuScan Instruments, Inc., USA, 2005) was used to translate this to rearing events and centimeters traveled. A break down of activity in the center and margin of the apparatus was also determined using the above software. Rearing events at one month of age were determined manually as mice were too small to activate sensor beams.

2.2.3.5 Water cross-maze

The apparatus was set up such that a cross-shaped Perspex box with an arm length of 26cm and arm width of 20cm was placed inside a circular pool (130cm in diameter). The pool and cross were filled with water (14cm deep) at 23.5- 24.5°C made opaque with 500g of full cream milk powder. A 9.5cm x 13.5cm platform was submerged in one arm of the cross, with the position of the platform remaining constant. Constant visual cues were placed above each arm of the cross (Figure 2.6).

The water cross-maze test was performed as described by Roberts et al. (2007). After an initial day of habituation, the ability of mice to learn the position of the submerged platform was tested over six days. During habituation, the platform was removed and each mouse was placed in the cross for 60 seconds in order to become accustomed to the apparatus. During learning trials the platform was included. Six trials per mouse per day over six days were performed in which mice were released into a different arm for each trial and given 60 seconds to locate the platform via the cues. Time taken to find the platform (escape latency), number of entries into arms that did not contain the platform (incorrect entries) and trials in

A

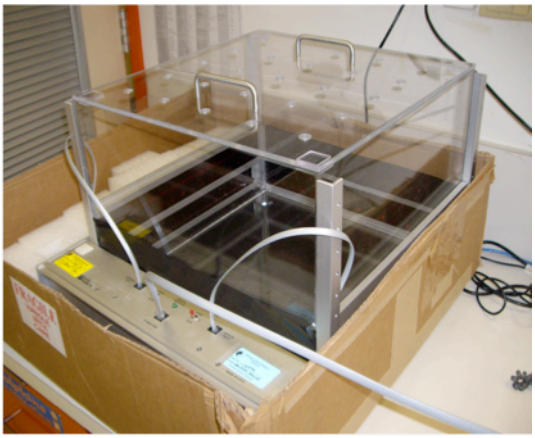

B

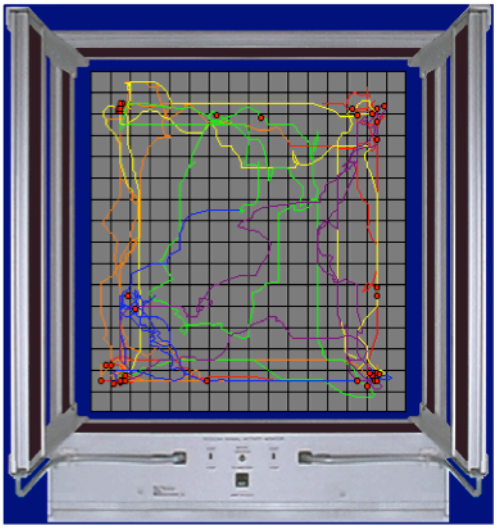

Figure 2.5: Open field.
The open field is used to measure activity and anxiety. Mice are placed in the front left hand corner of a Perspex box and horizontal and vertical sensor beam crosses recorded by the apparatus over three minutes (**A**). An example of an aerial map of mouse activity is shown (**B**), demonstrating the path travelled (coloured lines) and rearing events (red dots). Open field software can also be used to calculate time spent and distance travelled in the center of the apparatus compared with the margin.

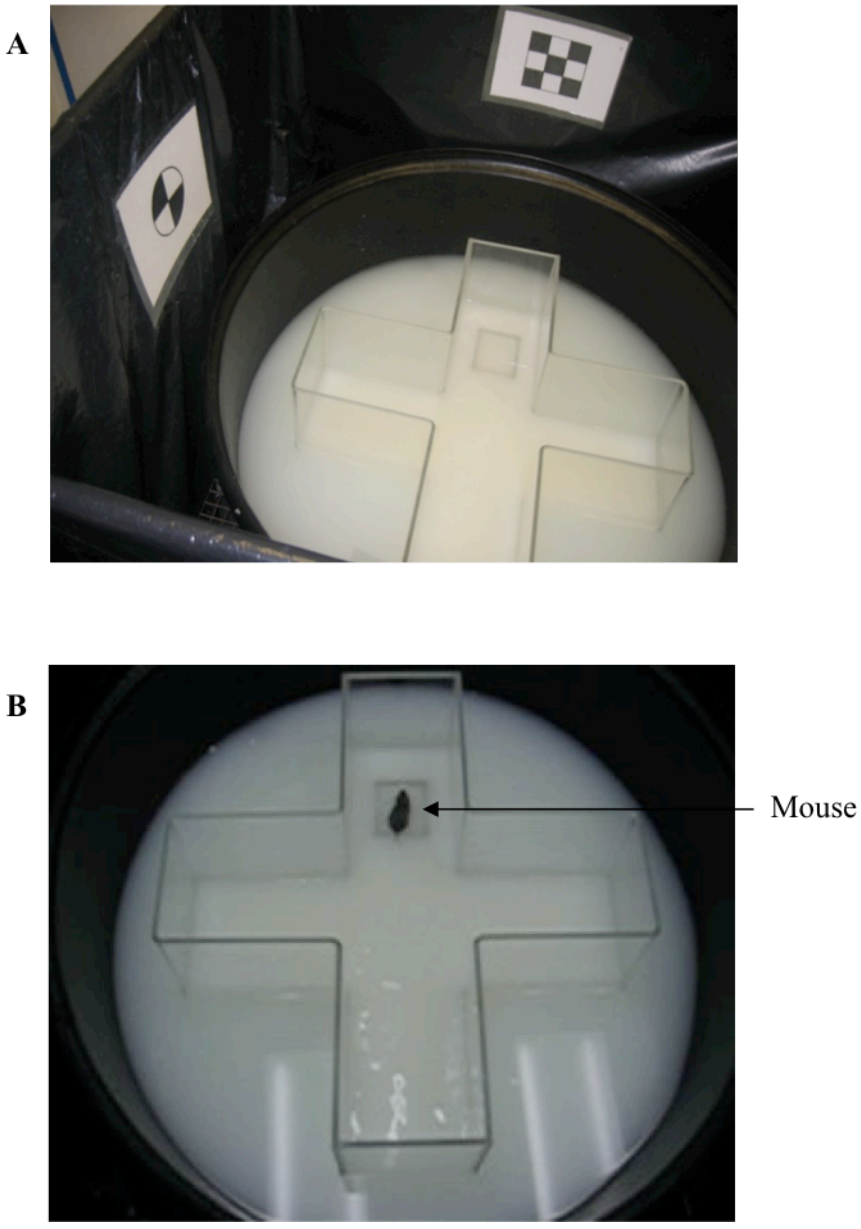

Figure 2.6: Water cross-maze.
The water cross-maze is used to measure spatial learning. The apparatus is made up of a cross shaped Perspex maze inside a circular pool. The pool is filled with water made opaque with milk powder and a platform is placed in one arm of the cross maze, the position of which remains constant. Constant visual cues are placed above each arm of the cross (**A**). Mice use these visual cues to learn the position of the platform. The relative sizes of the mouse and apparatus can be seen in **B**.

which the mouse traveled straight to the platform (correct entries) were recorded and the mean of all trials determined each day.

2.2.4 N*B-DNJ treatment*

2.2.4.1 Oral administration

Mice were fasted overnight (5pm to 9am) and fed with a daily intake of powdered chow, calculated at 5g chow/30g body weight/day, which was mixed with 4800mg/kg/day *N*B-DNJ. Fasting ensured that all food containing the daily dose of *N*B-DNJ was consumed. This dose was the highest described in the literature (Platt *et al.* 1997a). Treatment occurred from four to five weeks of age. Mice were humanely killed by carbon dioxide asphyxiation in the morning after the final fasting.

*2.2.4.2 Intravenous (*iv*) administration*

In the short-term mode of administration trial, mice were injected via the tail vein with 0.4μg/gm body weight *N*B-DNJ in 0.9% sterile saline, three times a week, from four to eight weeks of age. Although, blood samples were collected, a laboratory measuring *N*B-DNJ levels could not be sourced, therefore a theoretical blood concentration was determined. Given that mice have a blood volume 7% of total body weight, the dose of 0.4μg/gm body weight *N*B-DNJ was estimated to give a blood concentration of 25μM (Hoff 2000). This concentration was within the range of 18μM to 57μM previously described as therapeutically effective (Platt *et al.* 1997a; Platt *et al.* 1997b).

Mice were injected via the tail vein, three times per week from four weeks to six months of age (early treated mice) or from four to six months of age (late treated mice). In the early and

late treatment trials, the *iv* dose administered to mice was doubled to 0.8μg/gm body weight *N*B-DNJ in 0.9% sterile saline, for an even greater theoretical blood concentration of 50μM. Mice were humanely killed 24 hours after the final dose.

2.3 Biochemical analysis

Mouse brains were cut in half sagittally, along the cerebral fissure. For the comparative time course of MPS IIIA and MPS VII brain (Chapter Three and Chapter Five) the right hand side piece was used for lipid extraction and analysis (Chapter 2.3.1) and the left hand side piece was used for GAG isolation and measurement (Chapter 2.3.2). For the study of *iv N*B-DNJ treatment a central slice was taken from the right hand half of brain and frozen in OCT for the analysis of inflammatory mediators (Chapter 2.3.3). The remainder of the right hand half of the brain was used for lipid extraction and analysis (Chapter 2.3.1) and the left hand side piece was used for GAG isolation and measurement (Chapter 2.3.2).

2.3.1 Brain lipid analysis

2.3.1.1 Extraction of brain lipids

Lipids were isolated from the right hand side section of brain using the Folch method (Folch *et al.* 1957). Deionised water was added to each half brain such that the total weight was equal to 1gm, 400pmol N-octadecanoyl-d_3-monosialoganglioside 1 (d_3-G_{M1}) internal standard was added and samples were homogenised in 20 volumes of 2:1 (v/v) chloroform/methanol. Homogenates were incubated at room temperature for one hour, before 0.2 volumes of 0.1M potassium chloride were added and samples were shaken on a platform shaker (Patton industries, Australia) for five minutes. Aqueous (upper) and organic (lower) phases were separated by a five-minute 800 x *g* centrifugation.

The ganglioside-containing aqueous phase (Hakomori and Siddiqui 1974) was passed through a 200mg Bond Elut C18 column pre-wet with one column volume (3mL) of methanol, the column was washed with three column volumes of deionised water under vacuum and the gangliosides were eluted with one column volume of methanol. Samples were dried under nitrogen at 40-45°C, resuspended in 250µL methanol and stored at -20°C pending analysis. The organic phase containing all lipids other than gangliosides was dried under nitrogen at 40-45°C, resuspended in 250µL 2:1 chloroform/methanol and stored at -20°C pending analysis.

2.3.1.2 Thin layer chromatography (TLC)

Lipids were separated by TLC on 10cm by 20cm high performance TLC pre-coated silica gel plates. Ganglioside (aqueous phase) extracts (20µL of each) and G_{M1}, G_{M2}, and G_{M3} standards (10µg of each) were applied onto the plates at the origin and dried under nitrogen. Plates were placed into a chromatography module and run in chloroform/methanol/0.25% (w/v) calcium chloride (60:35:8) for 45 minutes. To visualise, the plate was sprayed evenly with 2M orcinol in 75% sulphuric acid, allowed to dry and developed at 125°C for five to ten minutes.

Organic phase lipids extracted from mouse brain were also analysed by TLC. Simple lipids were analysed alongside cholesterol, cholesterol ester, triglyceride and free fatty acid standards, using a solvent system of hexane/diethylether/acetic acid (85:15:1, v/v/v) for 30 minutes. Bands were visualised by spraying with 75% sulphuric acid and developing at 120°C for 10 to 15 minutes. Glycolipids in lower phase lipid extracts, including cerebroside, triglycosylceramide and sulphatide, were run alongside galactocerebroside, N-palmitoyl-DL-dihydro, ceramide trihexoside and sulphamide standards in chloroform/methanol/deionised water (65:25:4, v/v/v) for 45 minutes and visualised using 2M orcinol in 75% sulphuric acid spray developed at 120°C for five minutes. Phospholipids including cardiolipin (CL), phosphatidic acid (PA), phosphatidylethanolamine (PE), phosphatidylinositol (PI),

phosphatidylcholine (PC) and sphingomyelin (SM) were run alongside against SM, PC and PE standards in chloroform/methanol/deionised water (65:25:4, v/v/v) for 30 minutes and visualised using 0.025% (w/v) phosphomolybdic acid, 0.05% (v/v) sulphuric acid, 10% (v/v) deionised water in glacial acetic acid and developed at 100°C for two minutes. Densitometry was performed to determine the relative amount of each lipid using the UVitec gel documentation system (UK) and UVI photoMW software (version 11.01).

2.3.1.3 Ganglioside detection by liquid chromatography- electrospray ionisation tandem mass spectrometry (LC-ESI MS/MS)

Gangliosides were quantified by LC-ESI MS/MS in negative ion mode on a AB Sciex API 3000 triple-quadrupole mass spectrometer, with turbo spray ion source at a source temperature of 200°C and collision energy of -79. An Alltima C18 column (50mm x 2.1mm) was used on an on an Agilent 1100 G1312A pump with mobile phases A (MPA; 30% tetrahydrofuran, 20% methanol, 50% 5mM ammonium formate) and B (MPB; 70% tetrahydrofuran, 20% methanol, 10% 5mM ammonium formate) at a gradient of 100% MPB for 10 minutes, followed by 70% MPA and 30% of MPB for three minutes. Samples of 20µL were injected at a flow rate of 200µL/minute by a Gilson 233 autosampler. The flow was directed into waste for 2.4 minutes prior to MS/MS over 10.5 minutes. Multiple reaction monitoring (MRM) pairs (Q1/Q3) of 1573.0/290.1, 1383.0/290.1, 1180.1/290.1, 1547.9/290.1 were used to monitor ion intensities representing the molecular species of G_{M1} (d18:1/18:0), G_{M2} (d18:1/22:1), G_{M3} (d18:1/18:0) and d_3-G_{M1} (d18:1/18:0) respectively. Data was collected and integrated using Analyst 1.5.1 software (Applied Biosystems, USA). Each ganglioside was quantified against the d_3-G_{M1} internal standard and normalised to wet tissue weight.

2.3.1.4 Prostanoid LC-ESI MS/MS

Organic phase lipid extracts were diluted 1:20 in 5% acetonitrile/0.1% HCOOH (v/v) and internal standards 12(s)-HETE-d8, PGD2-d4, PGE2-d4, PGF2α-d4, 6-keto-PGF1α-d4, iso-PGF2α-d4, TXB2-d4, DHA-d5, EPA-d5 and AA-d8 added such that each was at a final concentration of 1μM. Metabolites 13(s)-hydroxyoctadecadienoic acid (13(s)-HODE), EPA, AA, 12(s)-hydroxyeicosatetraenoic acid (12(s)-HETE), 15(s)-hydroxyeicosatetraenoic acid (15(s)-HETE), DHA, prostoglandin D2 and prostoglandin E2 (PGD2/E2), prostoglandin F2 alpha (PGF2α), thromboxane B2 (TXB2), 6-keto-prostogmandin F1 alpha (6-keto-PGF1α) and resolvin D1 alpha (RVD1α) were detected by LC-ESI MS/MS as described by Unterwurzacher et al. (2008) and quantified against the above deuterated internal standards.

2.3.1.5 Ceramide glucosyltransferase activity assay

Brain samples were homogenised in 2.5 volumes of 0.1% (v/v) Triton X-100. Homogenates were centrifuged at 700 x *g* and supernatants isolated. Ceramide glucosyltransferase activity was measured in supernatant samples as described by Ichikawa *et al.* (1996), with some modifications. Briefly, C6-NBD-ceramide fluorescent substrate and L-α-phosphatidylcholine were mixed in ethanol and the solvent evaporated, before being sonicated in deionised water to form liposomes. Each brain supernatant sample (10μL) was incubated with 20mM Tris-HCl (pH 7.5), 500μM UDP-Glucose and liposomes at 30°C for 24 hours. Lipids were extracted with 20 volumes of 2:1 chloroform/methanol and free C6-NBD-ceramide separated from glucose bound C6-NBD-ceramide by TLC, on 10cm by 20cm high performance TLC pre-coated silica gel plates, in 65:25:4 chloroform/methanol/deionised water and visualised by UV illumination. Bands representing C6-NBD-glucosylceramide were scraped from the plate and resuspended in 2:1 chloroform/methanol and the fluorescence measured at λ_{ex} 466 and λ_{em} 539nm.

2.3.2 Analysis of brain GAG

2.3.2.1 Extraction of brain GAG for quantification

The left hand side pieces of mouse brain were homogenised in 2.5 volumes 0.1% (v/v) Triton X-100. The supernatant was removed, 2.5 volumes cetylpyridinium chloride/citrate buffer were added (0.1% (w/v) cetylpyridinium chloride/0.054M citrate, pH 4.8) and incubated at 37°C for 30 minutes. Samples were centrifuged at 700 x *g* for 10 minutes and the supernatant aspirated. Pellets were resuspended in 2M lithium chloride, before 5.3 volumes of absolute ethanol were added and samples were incubated at -20°C for one hour. Samples were centrifuged at 700 x *g* for 10 minutes, the supernatant was aspirated and the pellet dried at room temperature overnight. Pellets were resuspended in 100µL deionised water and samples spun at 700*g* for one minute to pellet solids. Supernatant was transferred to a new microfuge tube and GAG content measured by uronic acid assay.

2.3.2.2 Uronic acid assay

The uronic acid (UA) assay was performed as described by Blumenkrantz and Asboe-Hansen (1973). In short, six volumes of 0.0125M tetraborate in concentrated sulphuric acid were added to the samples and incubated at 100°C for 10 minutes. Samples were cooled on ice, 20µL colour reagent (0.15% (w/v) 3-phenylphenol/0.5% (w/v) sodium hydroxide) was added, the colour was developed over five minutes and absorbance (520nm) was measured using a 1234 Delfia research fluorometer (Wallac, Finland).

2.3.2.3 Extraction and purification of brain GAGs for characterisation

Mouse brains were minced and rotated at 4°C with two volumes 0.5M sodium hydroxide for 48 hours. The brain extract was spun at 700 x *g*, at 4°C, for 20 minutes, before the supernatant

was isolated and the pH neutralised to between seven and nine. Brain GAG was bound to 1mL DEAE Sephacel equilibrated with 0.1M sodium acetate (pH 5) overnight on a 4°C rotator. The resin bound sample was put into a 10mL Biorad column, washed with 10mL 0.1M sodium acetate (pH 5) and eluted with 10 washes of 0.5mL 0.1M sodium acetate/2M sodium chloride, pH 5. GAG containing fractions (determined by uronic acid assay; Chapter 2.3.2.2) were pooled and desalted over a PD-10 column equilibrated with 0.1M sodium acetate, pH 5.

GAGs were either visualised on cellulose acetate sheets (Chapter 2.3.2.4) or were further processed to isolate HS. A chondroitinase ABC digestion was performed as per the manufacturer's instructions (Sigma, USA), before the sample was run over a PD-10 column equilibrated with 0.1M sodium acetate, pH 5, to separate HS from CS/DS disaccharides. The isolated HS was hydrolysed for GAG chain characterisation (Chapter 2.3.2.5).

2.3.2.4 Cellulose acetate electrophoresis

GAG extracts (3µg) were run on 94mm by 76mm cellulose acetate sheets alongside CS, DS and HS standards (3µg of each). The electrophoresis was performed in 1M barium acetate at 200V for 45 minutes. GAGs were stained with 0.5% (w/v) alcian blue for 15 minutes, destained with three 15 minute washes in 0.1% (v/v) acetic acid and three 15 minute washes with deionised water.

2.3.2.5 Hydrolysis

Normal brain HS was hydrolysed using a method adapted from Hook *et al.* (1974) and Bame and Robson (1997). HS (0.1mg) hydrolysis to monosaccharides was begun in 2M trifluoroacetic acid (TFA) at 100°C for three hours, before being evaporated to dryness. Samples were resuspended in 3.9M sodium nitrite in 0.28M acetic acid and after 10 minutes

10 volumes of 1M acetic acid were added. Samples were then passed through a column (1cm by 3cm) of Dowex 50 (X8; H^+ form) equilibrated with 1M acetic acid and the flow through along with three column volumes collected. An equal volume of 100% methanol was added to the flow through and evaporated to dryness. 2M TFA was then added and incubated at 100°C for four hours and once again evaporated to dryness (Hook *et al.* 1974). Samples were then incubated in 1.5M ammonium hydroxide for 90 minutes to convert free lactones to acids (Bame and Robson 1997), evaporated to dryness, resuspended in deionised water and passed through a column (1cm by 3cm) of Dowex 1 (X8; acetate form) equilibrated with deionised water. The column was washed with three column bed volumes of deionised water and glucuronic acid (GlcA)/iduronic acid (IdoA) was eluted with three column volumes of 2.5% (v/v) formic acid. The samples were evaporated to dryness, and once again incubated in 1.5M ammonium hydroxide for 90 minutes at room temperature. Finally, it was evaporated to dryness and resuspended in deionised water.

GlcA and IdoA (in 9µg hydrolysed sample) were visualised on 94mm by 76mm cellulose acetate alongside GlcA and IdoA standards (3µg of each). The electrophoresis was performed in 0.1M zinc acetate at 200V for 50 minutes and monosaccharides were stained with silver nitrate as per Miyamoto and Nagase (1981).

2.3.3 Analysis of inflammatory mediators

An inflammatory gene expression and astroglial activation study was performed in early and late treated MPS IIIA mouse brains at six months of age. A central, sagittal slice of brain was frozen in OCT and stored at -80°C. Frozen sections were cut and immunohistochemistry performed (Chapter 2.3.3.1), before cDNA was generated from the remainder of the tissue for real time PCR (Chapter 2.3.3.2).

2.3.3.1 Immunohistochemistry

Immunohistochemistry of glial fibrillary acidic protein (GFAP) was performed on 10μm frozen brain sections on superfrost plus microscope slides. Slides were defrosted at room temperature, fixed in 10% neutral buffered formalin at room temperature for 30 minutes and washed three times in PBS at room temperature. Antigen retrieval was performed in 1% SDS at room temperature for five minutes before washing three times in PBS at room temperature. Slides were incubated in blocking solution (2% (w/v) bovine serum albumen in PBS) at 4°C for one hour. Incubation in rabbit anti-GFAP primary antibody (diluted 1:50 in blocking solution) was performed at 37°C for 30 minutes, apart from the negative control, which was incubated in blocking solution under the same conditions. Slides were once again washed three times in PBS at room temperature, before being incubated in the secondary antibody (anti-rabbit FITC conjugated; diluted 1:1000 in blocking solution) at room temperature for one hour. Another wash was performed and slides were mounted in ProLong Gold antifade reagent with DAPI. Staining was viewed using an upright fluorescence microscope and photographed at a magnification of x40.

2.3.3.2 Real-time PCR

Brain pieces were washed three times in TRIzol to remove OCT. The tissue was manually homogenised in TRIzol reagent and total RNA extracted following the TRIzol manufacturer's instructions (Invitrogen, USA) and quantified using a nanodrop 1000 spectrophotometer (Thermo Scientific, USA). cDNA was generated from 1μg of total RNA using the Qiagen QuantiTec reverse transcription kit as per the manufacturer's instructions (Qiagen, Germany).

The expression levels of ten inflammatory mediator genes were determined: *Gfap*, tumor necrosis factor family receptor superfamily member 1a (*Tnfrs1α*), chemokine (C-C motif) ligand 3 (*Ccl3*; *Mip1a*), interleukin 1 beta (*Il1β*), transforming growth factor beta 1 (*Tgfβ1*),

CD68 antigen (*Cd68*), interferon gamma (*Ifnγ*), synuclein alpha (*α Syn*), cathepsin B (*Ctsb*) and tumor necrosis factor alpha (*Tnfα*) (Table 2.1). Forward and reverse primers for each gene of interest were chosen using NCBI primer-BLAST (www.ncbi.nlm.nih.gov/tools/primer-blast), ensuring that primers crossed an exon-exon boundary and were specific to the gene of interest.

Each reaction contained 1μL of brain cDNA, 1x CYBR green real-time PCR master mix, 45pmol forward primer and 45pmol reverse primer (one inflammatory gene primer set per reaction; Table 2.1). A reaction with cyclophilin A (*Cypa*) real-time PCR primers was also made for each sample for normalising data (Table 2.1). Reactions were carried out on a thermocycler (Applied Biosystems 7300), with one cycle at 50°C for two minutes, one cycle at 95°C for ten minutes, 40 cycles at 95°C for 15 seconds and 60°C for one minute and a dissociation step of one cycle at 95°C for 15 seconds, 60°C for 30 seconds and 95°C for 15 seconds. The $2^{-\Delta\Delta Ct}$ method was used to calculate the fold change in gene expression (Livak and Schmittgen 2001).

2.4 Statistical analysis

Statistical differences between means were determined by one-way or two-way analysis of variance (ANOVA) with Tukey's or Dunn's HSD post-hoc test, as appropriate (SigmaStat, 3.0, SPSS Inc., USA).

Table 2.1: Inflammatory genes.
Inflammatory gene expression levels were determined by real-time PCR using forward and reverse primer sets designed using NCBI primer-BLAST.

Gene symbol	Gene name	Function	Genbank access number	Forward primer	Reverse primer
Gfap	Glial fibrillary acidic protein	marker of astroglial activation	NM_010277.2	TGGAGCTCAATGACCGCTTT	TCTCCTCCTCCAGCGATTCA
Tnf	Tumor necrosis factor	expressed by astroglia and microglia	NM_013693.2	ATGGCCTCCCTCTCATCAGT	CTTGGTGGTTTGCTACGACG
Tnfrsf1α	Tumor necrosis factor family receptor superfamily member 1α	Tnf receptor	NM_011609.3	CGAGGTCCTGGAGGACTGTA	ATGGAGTAGACTTCGGGCCT
Ccl3 (*Mip1α)*	Chemokine (C-C motif) ligand 3	macrophage chemoattractant	NM_011337.2	AGGATACAAGCAGCAGCGAG	TCAGGAAAATGACACCTGGC
Il1β	Interleukin 1 beta	cytokine secreted by astroglia and microglia	NM_008361.3	AGCTTCCTTGTGCAAGTGTC	TGGGTGTGCCGTCTTTCATT
Tgfβ1	Transforming growth factor beta 1	expressed by macrophages	NM_011577.1	ACCGCAACAACGCCATCTAT	TGCCGTACAACTCCAGTGAC
Cd68	CD68 antigen	expressed by monocytes, granulocytes and activated T-cells	NM_009853.1	CTTAAAGAGGGCTTGGGGCA	ACTCGGGCTCTGATGTAGGT
Ifnγ	Interferon gamma	expressed by T-cells	NM_008337.3	CTGGCAAAAGGATGGTGACA	ATCTGAGTTCAGTCAGCCGC
α Syn	Synuclein alpha	neurodegenerative marker	NM_009221.2	ATCTATCTGCGCGTGTGCTT	TGCTCCACACTTTCCGACTT
Ctsb	Cathepsin B	lysosomal protease released by activated astroglia	NM_007798.3	ACTTAGGAGTGCACGGGAGA	TAGCCACCATTACAGCCGTC
Cypa	Cyclophilin A	housekeeping gene	NM_008907.1	GGTTGGATGGCAAGCATGTG	TGCTGGTCTTGCCATTCCTG

Chapter Three: CNS disease in murine models of MPS IIIA and MPS VII

3.1 Introduction

CNS degeneration is a major obstacle to current therapies for the MPSs. To date, the only clinical option for improving brain disease has been with BMT for MPS I patients, when initiated prior to the onset of clinical manifestations (Whitley *et al.* 1993). In order to develop new therapeutic options for the brain, it is important that a better understanding of the progression of MPS neurodegeneration is established. This chapter focuses on mapping the onset and progression of the primary storage of GAG, the secondary storage of ganglioside and associated behavioural deficits in two animal models of MPS disease.

MPS models exist in a range of species, however only murine models offer the advantage that large numbers can be generated over a short period and a range of behaviour tests can be performed to provide a comprehensive analysis of functional deficits. Two MPS murine models have been chosen for this purpose: a MPS IIIA and a MPS VII model. MPS IIIA mice represent the most common subset of the MPS III disorders (Table 1.2), which predominantly have CNS symptoms. MPS IIIA mice have 3-4% of normal sulphamidase function and consequently have an attenuated form of the disease. They store both GAG and ganglioside and display abnormal brain function (Bhaumik *et al.* 1999; Bhattacharyya *et al.* 2001; Neufield and Muenzer 2001; McGlynn *et al.* 2004; Roberts *et al.* 2007). MPS VII mice also exhibit GAG storage, ganglioside storage and brain disease, as well as skeletal disease (McGlynn *et al.* 2004; Tomatsu *et al.* 2009; Macsai *et al.* 2012). In addition, this model results from a null mutation that leads to 0.1% residual enzyme activity, which suggests that storage and brain dysfunction is severe (Tomatsu *et al.* 2009). Thus, the characterisation of MPS VII mice covers this end of the MPS disease spectrum.

The characterisation of brain biochemistry and behaviour is also important for the selection of an appropriate model for a therapeutic trial aimed at reducing ganglioside levels in MPS. An

ideal model for ganglioside-targeted treatment would have high brain ganglioside levels and exhibit easily detectable behavioural deficits. Whether these features are present in the MPS IIIA or MPS VII murine model is identified through the characterisation of brain disease in this chapter.

3.2 CNS storage

In the MPS brain, the accumulation of GAG is the primary result of lysosomal enzyme dysfunction, while gangliosides G_{M2} and G_{M3} are secondary storage products (Neufield and Muenzer 2001). A time-course experiment was conducted in order to understand the relative timing and level of accumulation of GAG and ganglioside. These molecules were measured in MPS IIIA and MPS VII brains at one, two, three and six months of age. In addition, two further time points of five days and 12 months were included for MPS IIIA mice. The five day time point was included as MPS IIIA mice are bred from homozygous mice, meaning that the genotype is known from birth, while MPS VII mice must be bred from heterozygous mice and genotype is not determined until three weeks of age (Chapter 2.2.2). The 12 month time point was included as MPS IIIA mice can survive to this age, while MPS VII mice have a maximum life span of eight months (Birkenmeier *et al.* 1989; Crawley *et al.* 2006).

3.2.1 Primary storage of brain GAG

The brains of MPS IIIA, MPS VII and age matched normal mice were homogenised in Triton X-100 and supernatant GAG levels were measured using an UA assay and normalised to wet tissue weight (Chapter 2.3.2.1 and 2.3.2.2). Despite some variation with age, there was no significant change in normal brain GAG levels (Figure 3.1). MPS IIIA brain GAG levels increased significantly by 234% from five days to 12 months of age (two-way ANOVA, Tukey's HSD; Figure 3.1A). MPS VII brain GAG levels increased significantly by 156% from one to six months of age (two-way ANOVA, Tukey's HSD; Figure 3.1B). At six months

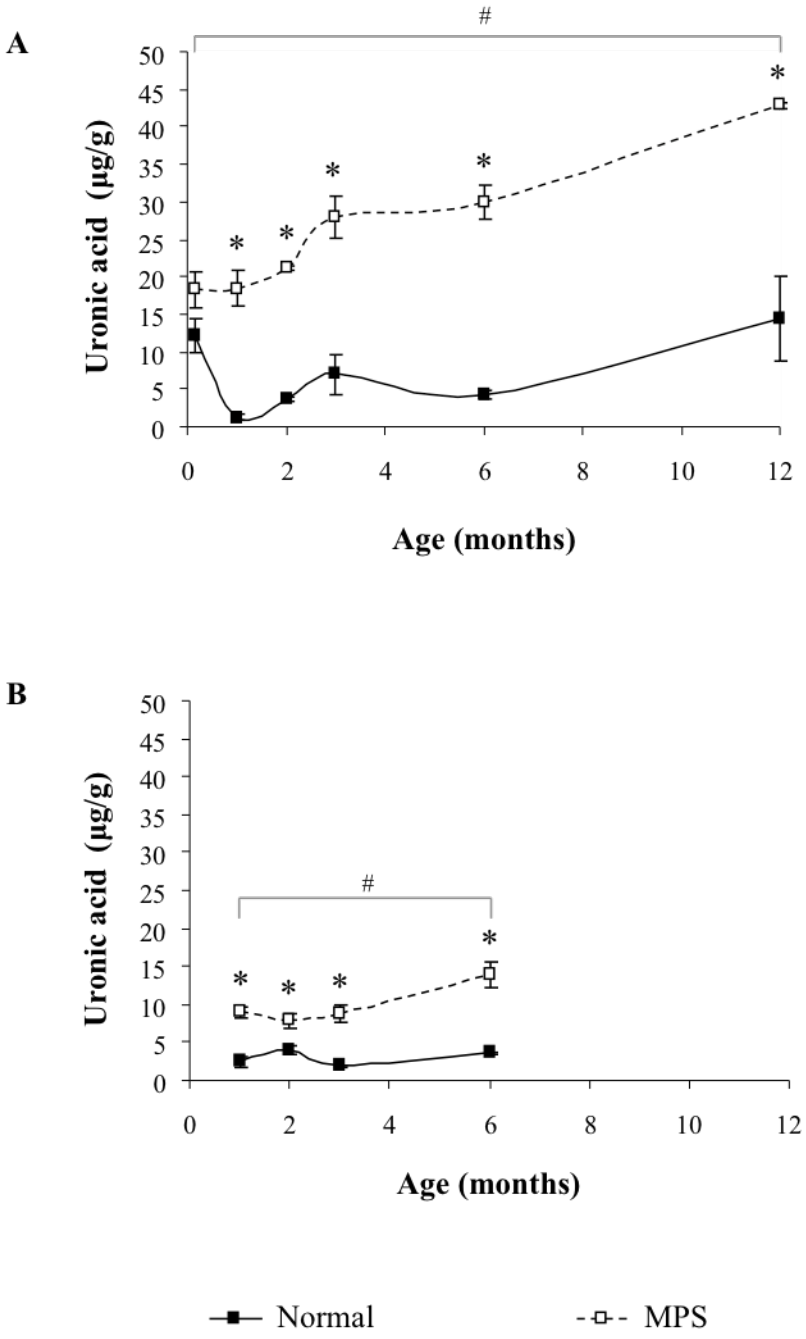

Figure 3.1: Time course of brain GAG levels.
Brain GAG content was determined in Triton X-100 extractions of five day to 12 month old normal, MPS IIIA (**A**) and MPS VII (**B**) brains and measured by uronic acid assay. Results were expressed as mean ± standard deviation of n=3-21. * Significantly different from same age normal ($p<0.05$), # significant difference between MPS time points ($p<0.05$) (two-way ANOVA, Tukey's HSD).

of age GAG levels were far greater in the MPS IIIA brain than in the MPS VII brain (723% of normal and 385% of normal, respectively; two-way ANOVA, Tukey's HSD; Figure 3.1).

The types of GAG that predominated in normal, MPS IIIA, and MPS VII mouse brain at six months of age was demonstrated by cellulose acetate electrophoresis of brain sodium hydroxide extracts, visualised using alcian blue (Chapter 2.3.2.4). In normal mouse brain, CS was the GAG in greatest abundance, while much lower amounts of HS were observed and DS was too low for detection (Figure 3.2). In the MPS IIIA mouse brain CS was similar to normal, however, a substantial increase in HS was observed. DS was not detected (Figure 3.2). In the MPS VII mouse brain, an increase in CS compared to normal was the greatest change, while HS and DS were only slightly greater than normal (Figure 3.2).

The qualitative analysis of brain GAG profiles in normal, MPS IIIA and MPS VII mouse brain (Figure 3.2) was consistent with the increase in overall brain GAG levels observed via UA assay (Figure 3.1). The surprising finding from these data was that brain GAG storage in the MPS IIIA mice (specifically HS) exceeded that of MPS VII mice, despite a greater residual enzyme activity in the MPS IIIA model (3-4%) than in the MPS VII model (<1%) (Birkenmeier *et al.* 1989; Bhaumik *et al.* 1999). Thus, it was hypothesised that the substrate for the enzyme deficient in MPS VII, GlcA, may be at low levels in brain HS. This would mean a greater level of the alternative UA molecule, IdoA, in mouse brain HS.

3.2.1.1 Murine brain HS UA composition

In order to determine the relative levels of GlcA and IdoA in murine brain HS, normal, MPS IIIA and MPS VII brain GAG was extracted by sodium hydroxide, digested with chondroitinase ABC, and run over a size exclusion column in order to separate HS from other GAGs. The HS was hydrolysed (Chapter 2.3.2.5) and cellulose acetate electrophoresis

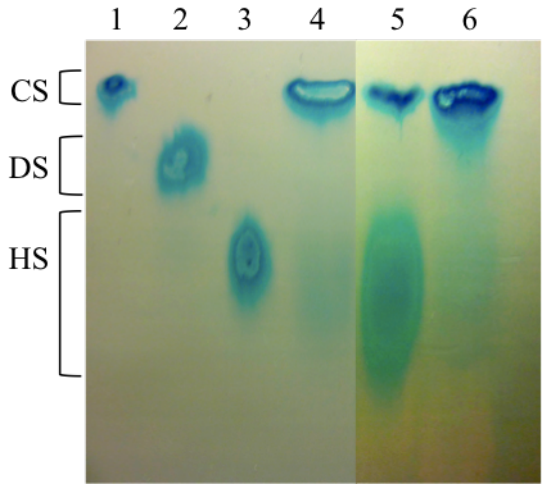

Figure 3.2: Brain GAG.
Cellulose acetate electrophoresis of six-month-old normal, MPS IIIA and MPS VII mouse brain GAG in lanes four, five and six respectively, alongside CS (lane one), DS (lane two), and HS (lane three) standards.

followed by silver nitrate staining was used to observe levels of GlcA and IdoA residues (Chapter 2.3.2.5).

As expected, the amount of GlcA was similar in normal and MPS IIIA HS, but was greater in MPS VII, where its metabolism is deficient (Figure 3.3). However, HS IdoA from all three genotypes was too low to be detected, demonstrating that GlcA was the predominant UA residue in mouse brain HS, and refuting our hypothesis (Figure 3.3). The validity of these results was supported by the presence of both GlcA and IdoA in hydrolysed control HS (Figure 3.3).

3.2.2 Secondary storage of brain ganglioside

The importance of HS GAG in particular for the MPSs is that its storage in the brain is associated with the secondary storage of G_{M2} and G_{M3} gangliosides and CNS degeneration (Neufield and Muenzer 2001). In order to better understand the relationship between primary and secondary storage, a time-course of ganglioside levels was conducted using normal, MPS IIIA and MPS VII brains at ages equivalent to those used in the time-course of GAG storage (Chapter 3.2).

Brain gangliosides were extracted in 2:1 (v/v) chloroform/methanol as per the Folch method (Folch *et al.* 1957) in the presence of 400pmol d_3-G_{M1} internal standard (Chapter 2.3.1.1). The brain ganglioside levels of six month old mouse brains were initially qualitatively measured by TLC alongside standards of each of the three monosialogangliosides: G_{M1}, G_{M2}, and G_{M3} (Chapter 2.3.1.2). As expected, bands representing G_{M1} did not differ between normal and MPS IIIA, or normal and MPS VII brain extracts (Figure 3.4). Both MPS IIIA and MPS VII brain G_{M2} and G_{M3} levels were greater than normal and this increase was observed to be greater for MPS IIIA brain extracts (Figure 3.4). This was consistent with the greater level of brain GAG storage in the MPS IIIA model (Figure 3.1).

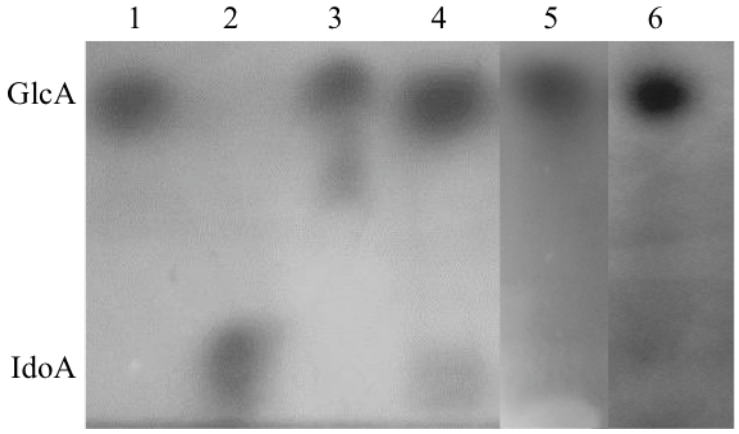

Figure 3.3: Comparison of mouse brain GlcA and IdoA.
HS was extracted from normal (lane three), MPS IIIA (lane five) and MPS VII (lane six) mouse brains using sodium hydroxide. These along with an HS control (lane four) were hydrolysed with trifluoroacetic acid, separated by cellulose acetate electrophoresis alongside a GlcA (lane one) and IdoA (lane two) standard and visualised using silver nitrate.

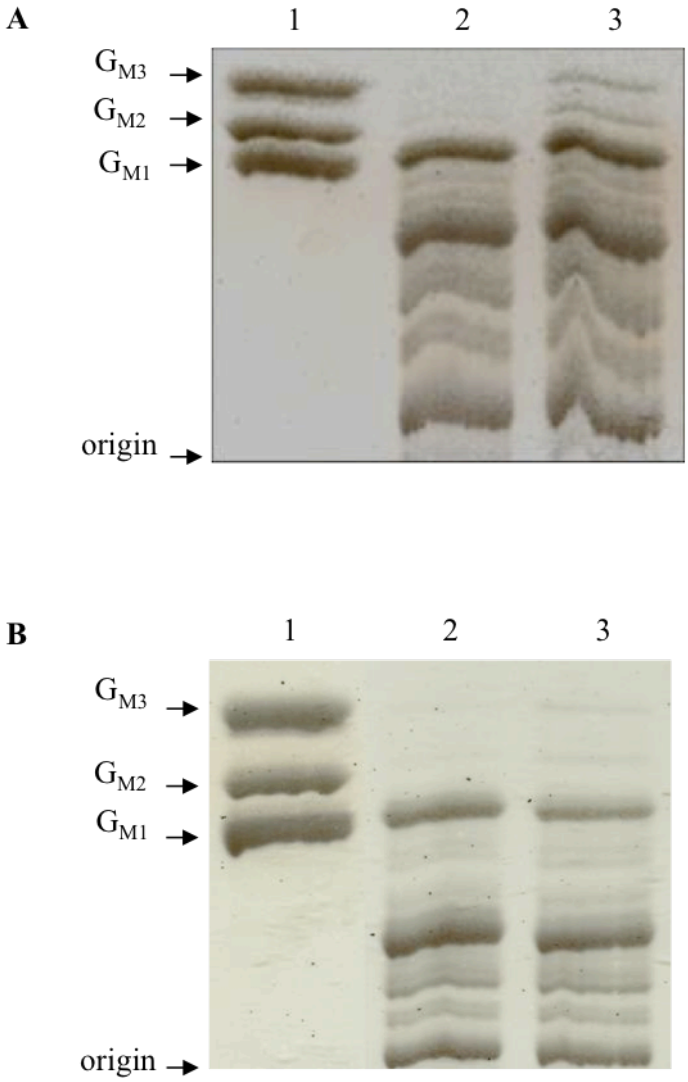

Figure 3.4: Qualitative brain ganglioside analysis.
Gangliosides were extracted from six month old normal, MPS IIIA (**A**) and MPS VII (**B**) mouse brains into 2:1 (v/v) chloroform/methanol and visualised by TLC. G_{M1}, G_{M2}, and G_{M3} standards were run in lane one, normal brain extract in lane two and MPS brain extract in lane three.

The quantitative analysis of monosialoganglioside accumulation in normal, MPS IIIA and MPS VII mouse brains was then determined. The most common brain ganglioside species, G_{M1} d18:1/18:0, and the two ganglioside species affected in the MPS brain, G_{M2} d18:1/22:1 and G_{M3} d18:1/18:0, were measured by LC-ESI MS/MS and quantified against the d_3-G_{M1} internal standard, before being normalised against wet tissue weight (Chapter 2.3.1.3). As expected, MPS IIIA and normal brain G_{M1} levels did not differ, both increasing significantly between five days and two months of age before stabilising (Figure 3.5A). Normal brain G_{M2} levels remained unchanged with age whereas MPS IIIA brain G_{M2} was significantly raised at all time points (two-way ANOVA, Tukey's HSD; Figure 3.5B). At five days of age levels were 348% of normal and continued to increase to a maximum of 548% of normal at six months. Normal brain G_{M3} was constant at all ages, and while MPS IIIA brain G_{M3} was at normal levels at five days of age, it then significantly increased from one month onwards (two-way ANOVA, Tukey's HSD; Figure 3.5C). By two months of age MPS IIIA G_{M3} levels were 484% of normal before a plateau to 12 months of age.

G_{M1} levels were consistent between MPS VII and normal at all ages as expected (Figure 3.5D). MPS VII G_{M2} was significantly greater than normal at all ages, averaging an increase of 219% (two-way ANOVA, Tukey's HSD; Figure 3.5E). MPS VII brain G_{M3} was significantly greater than normal at two months (172% increase) and six months (313% increase) of age (two-way ANOVA, Tukey's HSD; Figure 3.5F).

Again, brain storage of both G_{M2} and G_{M3} were demonstrated to be greater in the MPS IIIA model compared with the MPS VII model (Figure 3.5).

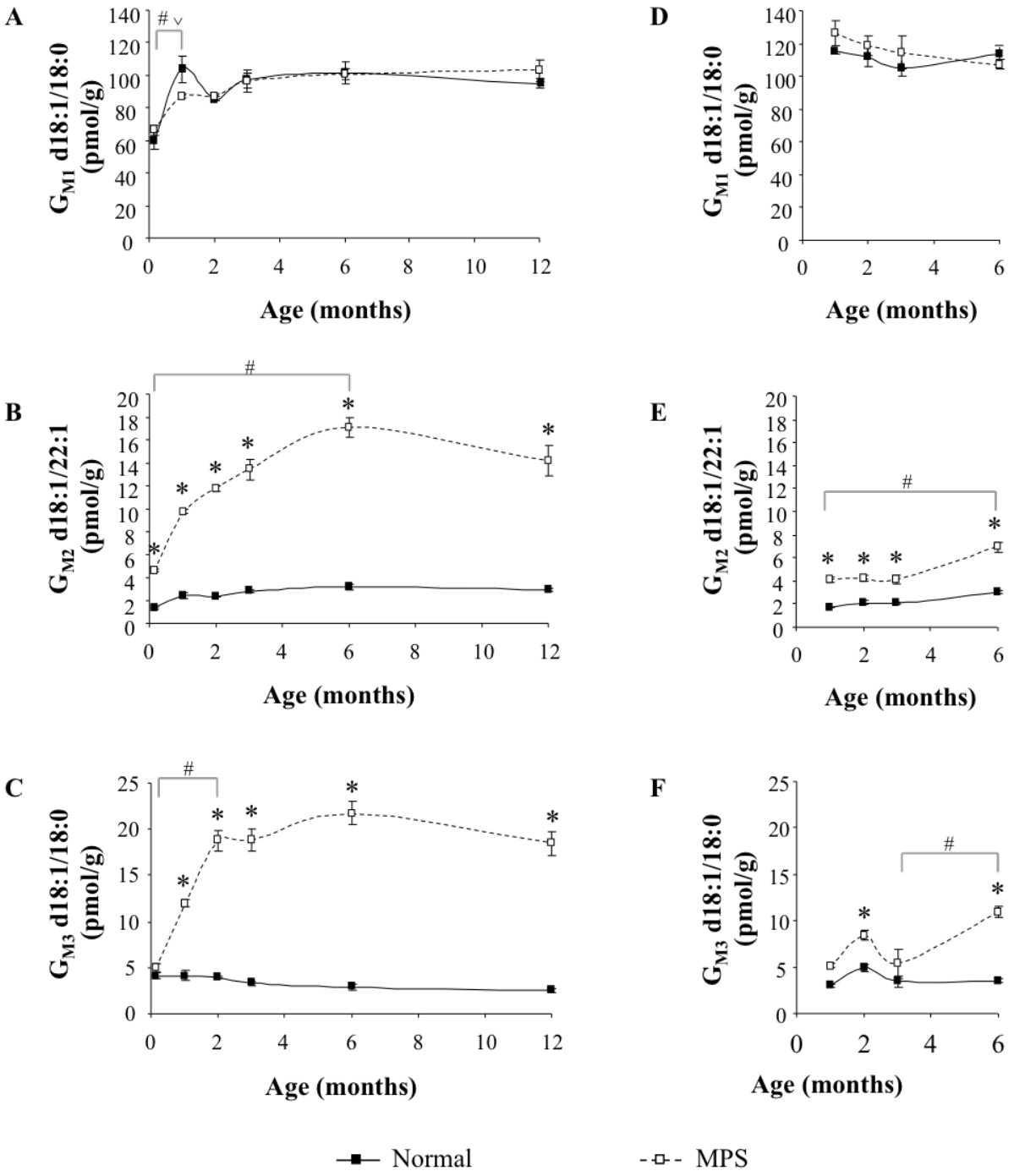

Figure 3.5: Time course of brain monosialoganglioside levels.
Gangliosides were chloroform/methanol extracted from normal, MPS IIIA (**A-C**) and MPS VII (**D-F**) mouse brains of five days to 12 months of age. G_{M1} (d18:1/18:0) (**A**, **D**), G_{M2} (d18:1/22:1) (**B**, **E**) and G_{M3} (d18:1/18:0) (**C**, **F**) levels were quantified by LC-ESI MS/MS against a d_3-G_{M1} internal standard and normalised to tissue weight. Results are the mean ± standard error of n=3-6. * Significant difference from same age normal ($p<0.05$), $^{\#}$ significant difference between MPS of indicated ages ($p<0.05$) (two-way ANOVA, Tukey's HSD). ^{v} significant difference between normal of indicated ages ($p<0.05$) (two-way ANOVA, Tukey's HSD).

3.3 Development of behavioural abnormalities

To determine whether brain dysfunction was relative to the level of primary and secondary storage, both of which were greater in the MPS IIIA brain, a series of behaviour tests were used. Behaviour testing began at two months of age when brain levels of GAG, G_{M2} and G_{M3} were elevated in both the MPS IIIA and MPS VII model.

3.3.1 Neuromuscular strength

Neuromuscular strength was measured monthly from two to six months of age using the vertical pole (Chapter 2.2.3.1) and inverted grid (Chapter 2.2.3.2) tests. In the vertical pole test, normal mice were able to reach an angle of 90° at all ages tested (Figure 3.6). MPS IIIA average latency to fall was significantly reduced compared to normal at six months (90% of normal; two-way ANOVA, Tukey's HSD; Figure 3.6A). A greater deficit was observed in MPS VII average latency to fall, which was first evident at three months of age. This progressed from 85% of normal at three months to 61% of normal by six months (Figure 3.6B). In the inverted grid test, MPS IIIA average latency to fall was normal at all ages, apart from at the five-month time point (90% of normal; two-way ANOVA, Tukey's HSD; Figure 3.7A). MPS VII latency to fall was significantly lower compared with normal at all ages, with an average performance of 16% of normal (two-way ANOVA, Tukey's HSD; Figure 3.7B).

3.3.2 Motor coordination and balance

Motor coordination and balance were assessed monthly from two to six months of age using the accelerating rotarod (Chapter 2.2.3.3). MPS IIIA average latency to fall did not diverge significantly from normal until six months of age (83% of normal; two-way ANOVA, Tukey's HSD; Figure 3.8A). MPS VII mice displayed significant deficits in average latency to fall from the apparatus from three months of age (49% of normal), which remained

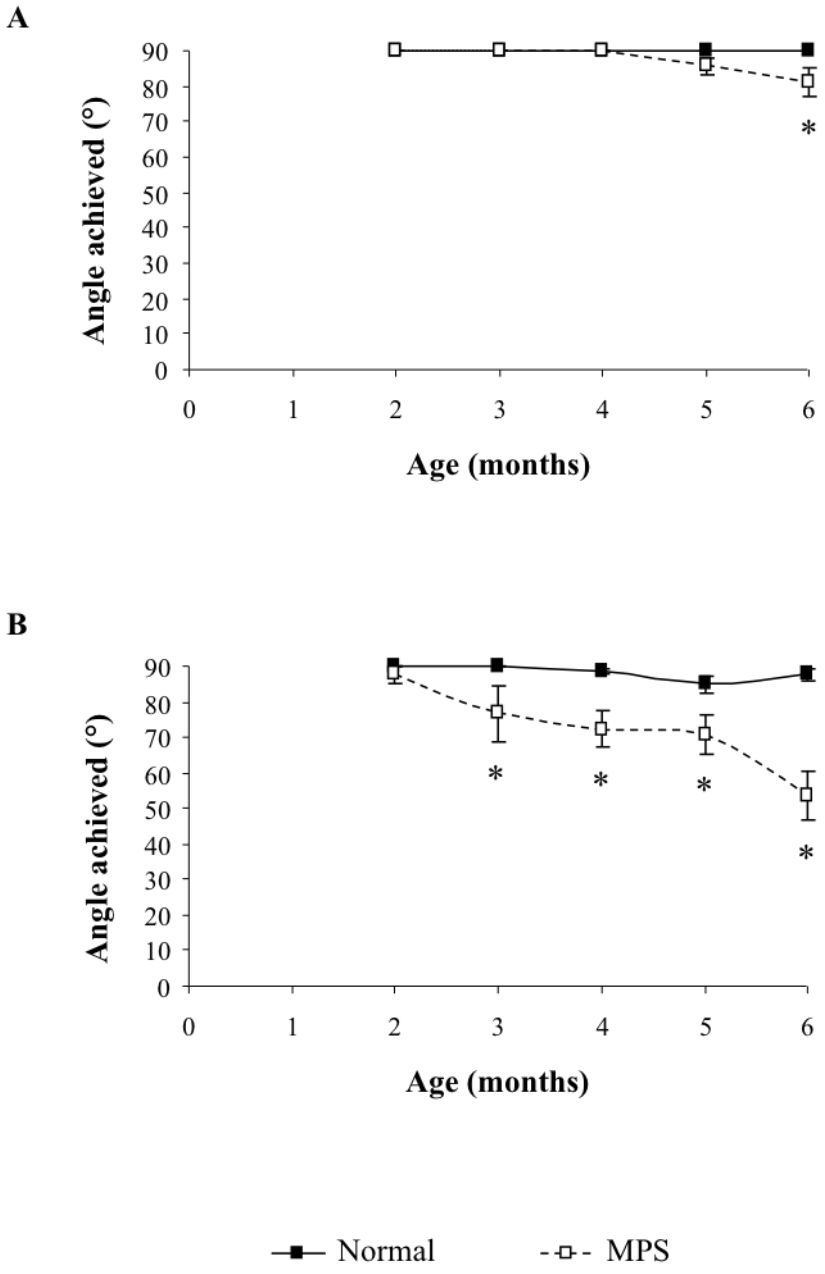

Figure 3.6: Vertical pole.
Normal, MPS IIIA (**A**) and MPS VII (**B**) mice were placed on a horizontal pole which was raised at one end such that the angle increased from 0° to 90°. The angle at which the mice fell off was determined. Results were expressed as mean ± standard error of n=9-25. * Significant difference between normal and MPS, $p<0.05$ (two-way ANOVA, Tukey's HSD.

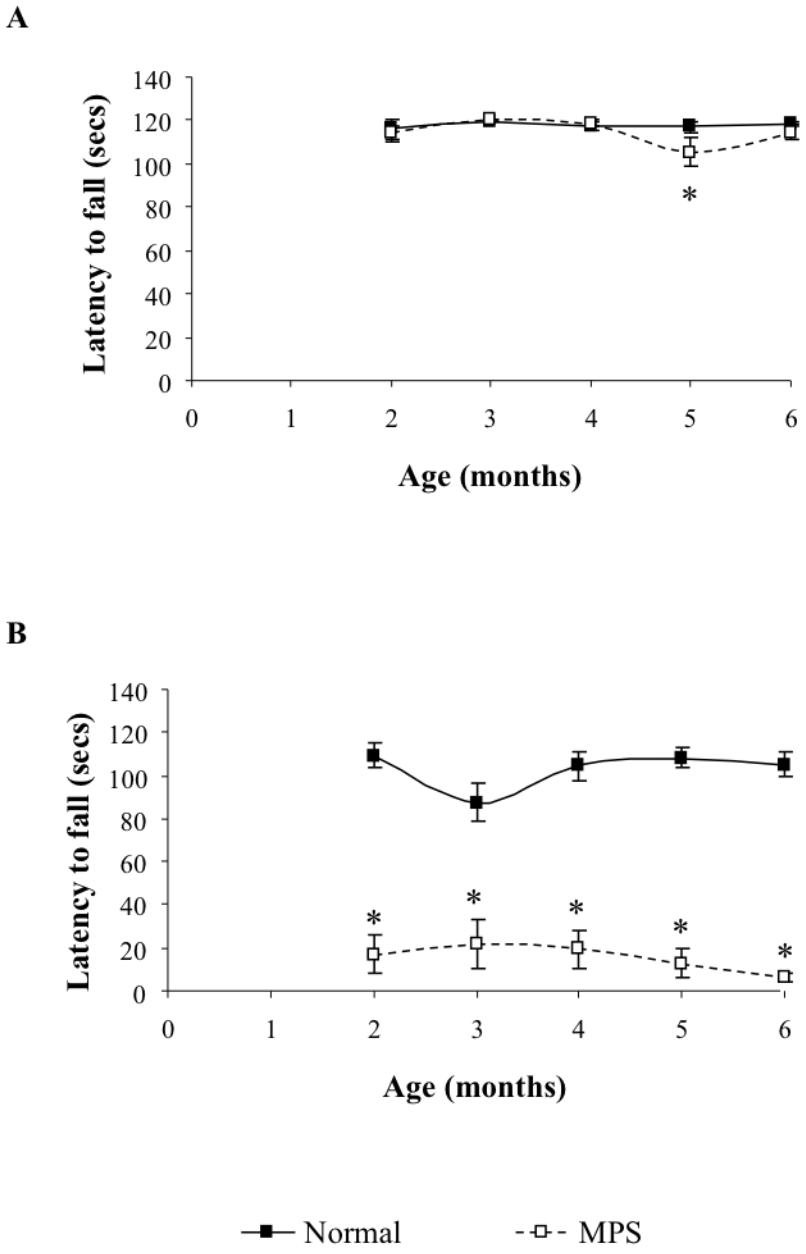

Figure 3.7: Inverted grid.
Normal, MPS IIIA (**A**) and MPS VII (**B**) mice were placed on a wire grid, which was inverted over a cushioned surface. Latency to fall up to a maximum of 120 seconds was recorded. Results were expressed as mean ± standard error of n=9-25. * Significant difference between normal and MPS, $p<0.05$ (two-way ANOVA, Tukey's HSD).

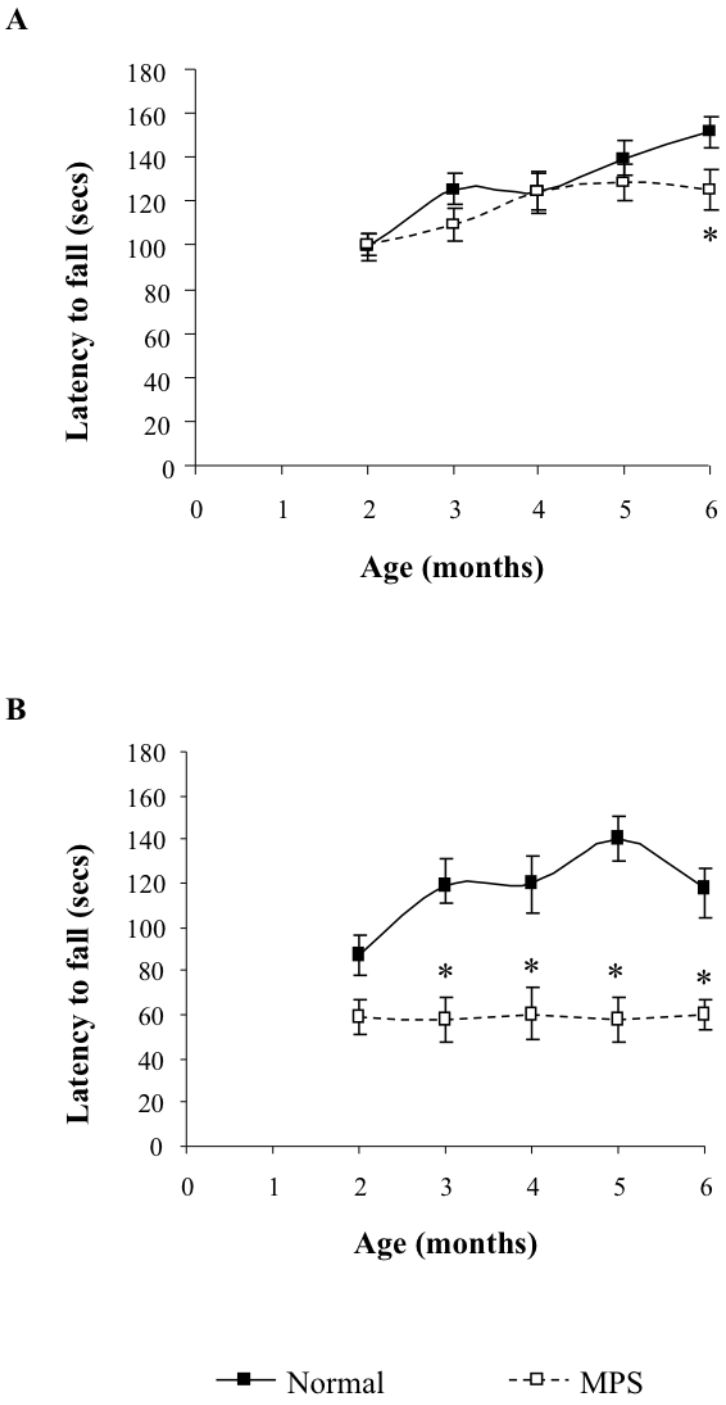

Figure 3.8: Rotarod.
Normal, MPS IIIA (**A**) and MPS VII (**B**) mice were placed on a rotating barrel, which accelerated form five to 35 rpm over two minutes and then maintained 35 rpm for a further minute. Latency to fall was recorded and results were expressed as mean ± standard error of n=7-22. * Significant difference between normal and MPS, $p<0.05$ (two-way ANOVA, Tukey's HSD).

relatively constant to six months of age (51% of normal; two-way ANOVA, Tukey's HSD; Figure 3.8B).

3.3.3 Activity and anxiety

Normal, MPS IIIA and MPS VII activity and anxiety were measured using the open field test (Chapter 2.2.3.4) from one to six months of age. The parameters tested included distance travelled and rearing (measures of activity) and the percentage of distance travelled and time spent in the centre of the apparatus (measures of anxiety). The performance of normal mice age matched to MPS IIIA or MPS VII was quite different for all these parameters, demonstrating the sensitivity of the test to outside stimuli and the importance of only making comparisons of mice tested in the same session.

The MPS IIIA average distance travelled over three minutes was significantly lower than normal levels from three months of age (averaging 54% of normal; two-way ANOVA, Tukey's HSD; Figure 3.9A), as were rearing events (averaging 38% of normal; two-way ANOVA, Tukey's HSD; Figure 3.9B). The percentage distance travelled by MPS IIIA mice in the centre of the apparatus was significantly lower than normal at one and six months of age (66% and 58% respectively; two-way ANOVA, Tukey's HSD; Figure 3.9C). The time that MPS IIIA mice spent in the centre of the apparatus was 41% of normal at one month of age, but was normal at all other time points (two-way ANOVA, Tukey's HSD; Figure 3.9D).

The average MPS VII distance travelled over three minutes was below normal from two months of age and this reduction was significant at two, three and four months of age (64%, 19% and 4% of normal distance travelled respectively; two-way ANOVA, Tukey's HSD; Figure 3.9E). The average number of MPS VII rearing events over three minutes was also below normal from two months of age, this being significant at two, three, and four months of age (38%, 0% and 0% of normal respectively; two-way ANOVA, Tukey's HSD; Figure

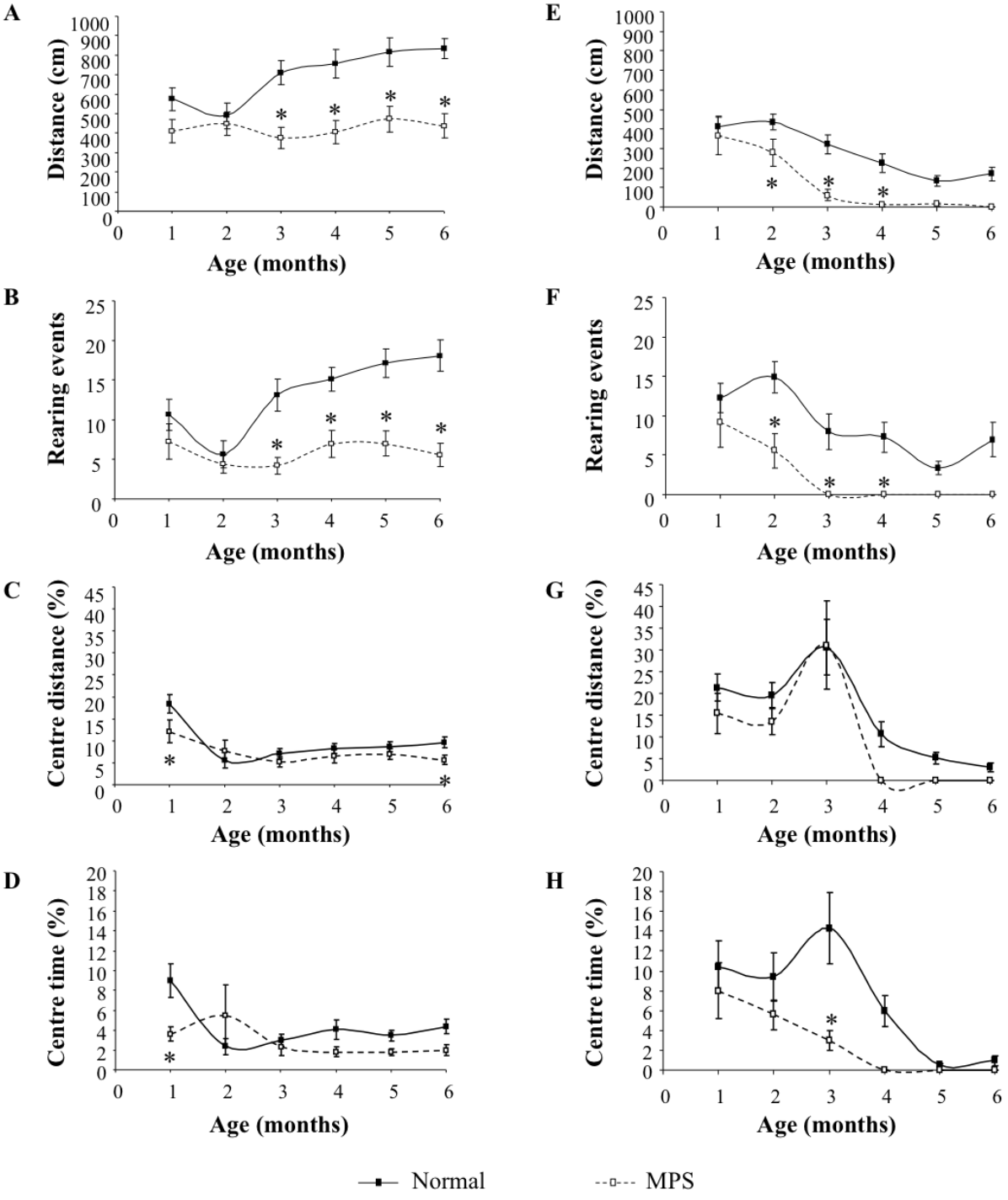

Figure 3.9: Open field.
Normal, MPS IIIA (**A**, **B, C, D**) and MPS VII (**E, F, G, H**) mice were placed in the front left hand corner of the open field apparatus and distance traveled (**A**, **E**), number of rearing events (**B**, **F**), distance traveled in the centre (**C, G**) and time spent in the centre (**D, H**) were recorded. Results were expressed as mean ± standard error of n=6-23. * Significant difference between normal and MPS, $p<0.05$ (two-way ANOVA, Tukey's HSD).

3.9F). The percentage distance travelled (Figure 3.9G) and time (Figure 3.9H) that MPS VII mice spent in the centre of the apparatus was normal, apart from time spent in the centre at three months of age, which was significantly reduced (21% of normal; two-way ANOVA, Tukey's HSD).

3.3.4 Learning

The water cross-maze was used to test learning ability over a period of six days. The task required two, four and six month old naïve normal, MPS IIIA and MPS VII mice to locate a submerged platform via visual cues (Chapter 2.2.3.5). Data at day six was expressed as a percentage of normal.

The average number of trials in which MPS IIIA mice travelled straight to the platform (correct entries) were normal at two and four months of age but were significantly decreased at six months of age (78% of normal respectively; two-way ANOVA, Dunn's HSD; Figure 3.10A). MPS IIIA entries into cross-maze arms that did not contain the platform (incorrect entries) were normal at two and four months of age and were raised over normal at six months of age (189% of normal), however this was not significant (Figure 3.10B). MPS IIIA escape latency was at normal levels at two and four months of age, but increased significantly to 166% of normal six months of age (two-way ANOVA, Dunn's HSD; Figure 3.10C).

MPS VII average correct entries were less than normal at two and four months of age, however this was not significant. At six months of age, MPS VII correct entries were significantly reduced (57% of normal; two-way ANOVA, Dunn's HSD; Figure 3.10A). MPS VII incorrect entries were greater than normal at all ages tested (160%, 145% and 251% at two, four and six months respectively) and this was significant at four and six months (two-way ANOVA, Dunn's HSD; Figure 3.10B). MPS VII escape latency was significantly greater than normal at two, four and six months of age (157%, 175% and 297% respectively; two-

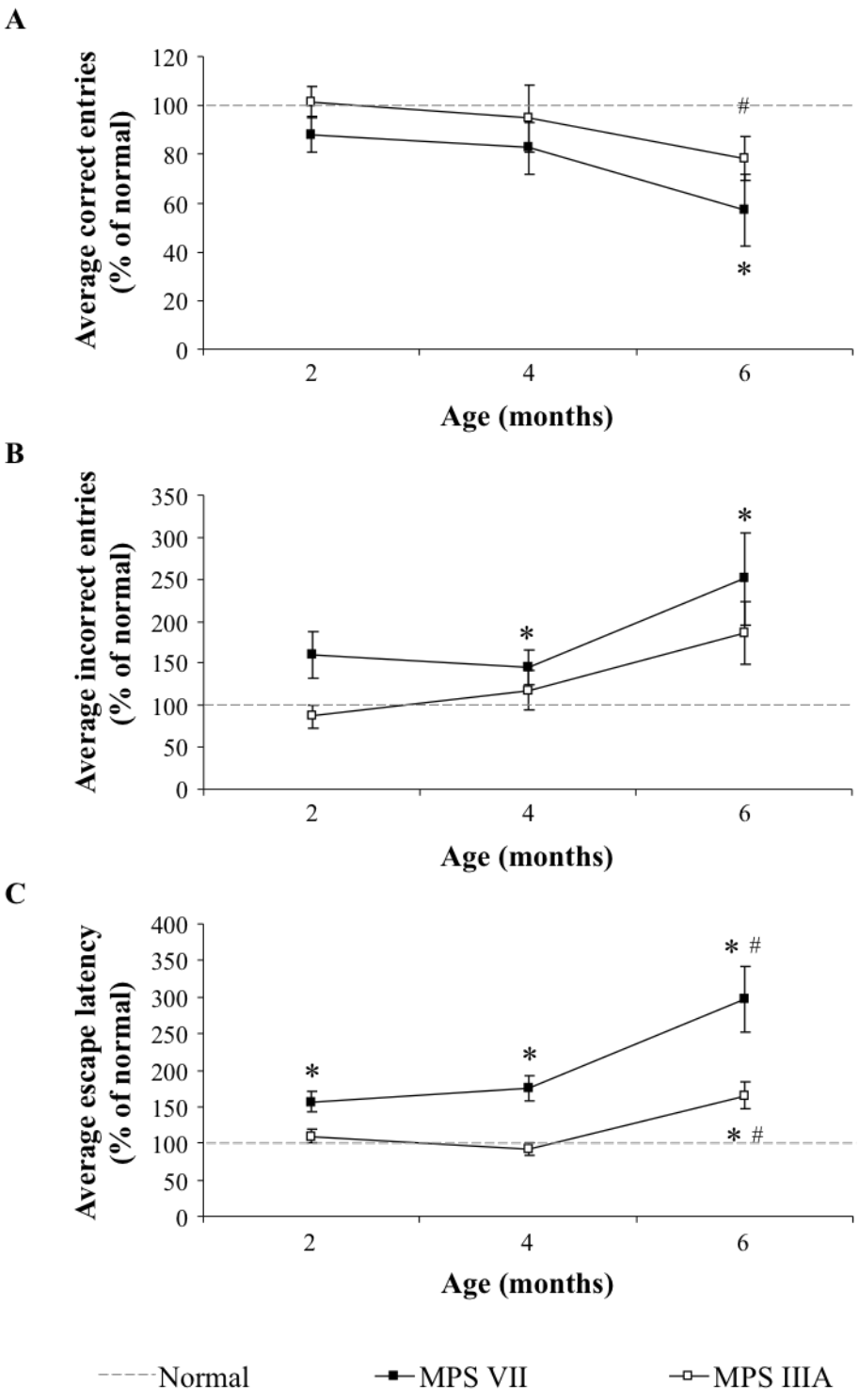

Figure 3.10: Water cross-maze.
Normal, MPS IIIA and MPS VII mice were placed in a cross shaped pool filled with opaque water and used constant visual cues to locate a submerged platform. Correct entries (**A**), incorrect entries (**B**) and escape latency (**C**) were measured and converted to a percentage of normal. Results were expressed as mean ± standard error of n=66-120 trials. * Significant difference between normal and MPS ($p<0.05$), # significantly different from the same MPS type at younger ages ($p<0.05$) (two-way ANOVA, Dunn's HSD).

way ANOVA, Dunn's HSD; Figure 3.10C). In addition, MPS VII escape latency increased significantly between learning trials at four and six months of age (two-way ANOVA, Dunn's HSD).

3.4 Discussion

Understanding MPS neurodegeneration is important for the development of CNS targeted therapies and to provide a baseline against which they can be measured. We have mapped the onset and progression of GAG, G_{M2} and G_{M3} accumulation and behavioural deficits in murine models of MPS IIIA and MPS VII. Both these models store HS and display the characteristic ganglioside storage and CNS degeneration observed in HS storing MPSs (Neufield and Muenzer 2001; McGlynn *et al.* 2004).

The MPS VII and MPS IIIA murine models are both naturally occurring, resulting from <1% of normal GUSB activity and 3-4% of normal sulphamidase activity respectively (Birkenmeier *et al.* 1989; Bhaumik *et al.* 1999). In the MPSs, this small difference in enzyme levels can have considerable effects on disease onset and progression, and an enzyme activity level of 10% can give a normal phenotype (Perkins *et al.* 2001). Thus, MPS IIIA represents an attenuated model and MPS VII a severe model of disease. However, characterisation of brain GAG levels demonstrated that the overall level of brain GAG was greater in MPS IIIA than in MPS VII, reaching 723% and 385% of normal at six months, respectively. Consistent with this data, HS GAG which is associated with CNS pathology in the MPSs, was also observed to be greater in MPS IIIA brain tissue compared with MPS VII (Neufield and Muenzer 2001).

Relative GAG levels in the MPS IIIA and MPS VII model were not as expected given their enzyme activities. This prompted a structural analysis of normal brain HS in order to gain an understanding of how inhibition of different parts of the HS degradative pathway in MPS IIIA

and MPS VII could lead to a significant difference in storage levels (Neufield and Muenzer 2001). It was hypothesised that the difference in storage was due to mouse brain HS having low levels of the substrate for the enzyme deficient in MPS VII, GlcA, and higher levels of the alternative UA residue, IdoA (Neufield and Muenzer 2001). However, the characterisation of brain HS demonstrated that GlcA levels were in fact far greater than IdoA. Thus, the composition of HS UA could not be responsible for the lower level of storage in the MPS VII brain compared with MPS IIIA.

An alternative hypothesis is that HS is highly N-sulphated leading to a greater level of GAG accumulation in the MPS IIIA brain. Studies have demonstrated that approximately 40%, 45%, 42% and 41% of normal mouse, rat, bovine and porcine brain HS disaccharides respectively are N-sulphated (Toida *et al.* 1997; Park *et al.* 1999; Shi and Zaia 2009; Wilkinson *et al.* 2012). Furthermore, it has been suggested that under inflammatory conditions, as are observed in the MPS brain, expression of N-deacetylase/N-sulphotransferase-1 increases, resulting in a subsequent increase in HS N-sulphation (Carter *et al.* 2003). As the removal of N-sulphate residues is deficient in MPS IIIA, this would in turn lead to an increase in total HS storage in the MPS IIIA mouse brain.

In addition to GAG levels, G_{M2} and G_{M3} secondary storage levels were also raised earlier and to greater levels in the MPS IIIA mouse model (reaching 548% and 484% of normal, respectively) compared with the MPS VII model (reaching 219% and 313% of normal, respectively). This suggests that ganglioside levels are dependent on GAG levels; however, the mechanism linking them is currently unknown. While studies have shown that GAG chains can inhibit the degradation of ganglioside (Avila and Convit 1975; Constantopoulos *et al.* 1976; Constantopoulos and Dekaban 1978; Constantopoulos *et al.* 1980; McGlynn *et al.* 2004), these storage materials do not co-localise (McGlynn *et al.* 2004). G_{M2} and G_{M3} are typically present in the developing brain before decreasing to negligible levels shortly after

birth (Rosenberg and Stern 1966; Hogan *et al.* 1988; Kotani *et al.* 1993; Kotani *et al.* 1994; Kotani *et al.* 1995), therefore these dramatic increases in ganglioside levels post birth suggest a change in ganglioside synthesis and/or degradation.

Gangliosides have been suggested to be responsible for neurodegeneration in the MPSs rather than the primary GAG storage, due to the similar pattern of progressive CNS degeneration and neuronal morphology observed between the MPSs and the primary ganglioside storing disorders: Tay-Sachs and Sandhoff disease (Purpura and Suzuki 1976; Levy *et al.* 1996; Walkley *et al.* 2000; McGlynn *et al.* 2004; Walkley *et al.* 2005). The characterisation of MPS IIIA and MPS VII behaviour was conducted to determine the onset and progression of brain disease associated with varying residual enzyme activities and to determine a point of reference for CNS function against which treated mice could be compared. A series of behaviour tests designed to assess brain function were performed to characterise MPS IIIA and MPS VII models. However, it became apparent that MPS VII performance in the majority of tests was influenced by their severe skeletal disease, making comparisons between the two models difficult. MPS VII mice performed poorly in neuromuscular strength, balance and coordination tasks, due to their poor ability to grip and to move quickly. In addition MPS VII hypo-activity, demonstrated using the open field test, may also have been the result of difficulty with movement caused by skeletal disease. All of these behaviour tests demonstrated that onset of a behavioural phenotype occurred earlier in MPS VII mice (deficits by two months of age) than MPS IIIA mice (first evident at three months of age).

MPS VII open field data presented in this chapter is consistent with a recent study by Macsai et al. (2012) who demonstrated deficits in distance travelled and rearing events at six months of age. However, other studies that have tested the activity of MPS VII (Bielicki *et al.* 2010) and MPS IIIA (Hemsley and Hopwood 2005; Crawley *et al.* 2006; Lau *et al.* 2008) mice in the open field have not shown any significant difference from normal activity, apart from

hyperactivity in three week old MPS IIIA mice (Hemsley and Hopwood 2005). However, Bielicki et al. (2010) combined line crosses and rearing events for a general measure of activity. Furthermore, the above studies measured activity manually, while the open field activity test conducted in these experiments and by Macsai et al. (Macsai *et al.* 2012) used an automated system, and therefore, removed user subjectivity and the influence of the researcher being visible to the mice. Despite this, we have previously demonstrated deficits in MPS VII activity using the manual system, which are consistent with these current results (unpublished data). As a measure of anxiety, the open field has been used previously to determine activity in the centre of the apparatus versus the margin for MPS IIIA mice, but we did not observe any changes in this parameter in our time-course experiment (Malinowska *et al.* 2010; Langford-Smith *et al.* 2011a).

The water cross-maze was one behaviour test in which not all parameters tested were influenced by skeletal pathology. MPS VII mice took much longer to locate the submerged platform (escape latency), which was not unexpected as their skeletal pathology makes swimming difficult. However, MPS VII mice were still able to swim and respond to the negative stimulus of the water, thus their ability to learn where the platform was located (correct and incorrect entries) was a reliable measure of CNS function. MPS VII learning ability was found to diverge from normal from four months of age, consistent with a study by Macsai *et al.* (2012), while MPS IIIA learning began to differ from normal at six months of age. The only other study to use the water cross-maze to test MPS IIIA spatial learning was by Roberts *et al.* (2007), demonstrating that MPS IIIA mice displayed significant deficits in learning at seven months of age. Others have used the Morris water maze, which has indicated that deficits in special learning are present at five months of age (Gliddon and Hopwood 2004; Crawley *et al.* 2006). These studies are consistent with the finding in this chapter that MPS IIIA special learning ability is significantly reduced at six months but not at four months of age.

Data in this chapter suggests that the levels of storage in the MPS VII brain, although lower than MPS IIIA, were sufficient for CNS pathology to occur. In fact, MPS VII CNS function declined earlier than MPS IIIA. It is possible that the skeletal pathology present in the MPS VII model had a greater effect on water cross-maze correct and incorrect entries than expected, as it would have required a greater effort for MPS VII mice to remain afloat, which may have distracted them from learning the task. Thus, it is recommended that other tests are investigated to better characterise the onset and progression of CNS pathology in the MPS VII mouse model.

Taken together, our data spanning five days to twelve months in the MPS IIIA model and one to six months in the MPS VII model has provided a base line for disease onset and progression in these models. We have demonstrated that the first indication of CNS pathology is an increase in overall brain GAG and G_{M2} levels. This is observed from the earliest time points tested and continues to increase over time. It is known that as the enzyme deficiencies of the two MPSs examined are GAG specific and that G_{M2} accumulation is obviously a secondary phenomenon (Neufield and Muenzer 2001). The two storage materials must be closely connected as the comparison of the two MPS models demonstrates that G_{M2} is elevated to greater levels when GAG levels are greater; however, GAG storage is not likely directly responsible for G_{M2} storage as the two do not co-localise (McGlynn *et al.* 2004). The second ganglioside to be affected was G_{M3}, which increased later than G_{M2} but to far greater levels. It is therefore possible that G_{M3} accumulation occurs in response to a build up of G_{M2}, particularly as the two molecules are so closely connected in the GSL metabolic pathway (Figure 1.1 and 1.2) (Kolter *et al.* 2002). Functional pathology was not observed until after all these biochemical changes had begun, suggesting that the degenerative process takes time to develop and/or a storage threshold to be reached. It is unknown whether the storage products themselves cause direct damage to the brain, or whether there is a downstream cascade of

cellular damage, such as inflammation, apoptosis and oxidative stress (Villani *et al.* 2007; Richard *et al.* 2008; DiRosario *et al.* 2009; Arfi *et al.* 2011).

This chapter presents a time-course of GAG storage, ganglioside storage and behaviour using murine models of MPS IIIA and MPS VII. There is currently no way to separate the effects of GAG and ganglioside storage on CNS degeneration in the MPSs. By decreasing ganglioside synthesis using the inhibitor of GSL synthesis, *N*B-DNJ, the specific impact of ganglioside levels on CNS pathology can be elucidated. Furthermore, this could have positive therapeutic outcomes for MPS brain disease. Of the two models characterised, the MPS IIIA model was chosen for use in a ganglioside targeted therapeutic trial as ganglioside accumulation occurred earlier and was more pronounced than that observed in the MPS VII model and all functional pathology could be attributed to CNS degeneration. Therefore, a trial of *N*B-DNJ treatment in MPS IIIA mice was conducted.

Chapter Four: *N*B-DNJ treatment of MPS IIIA mice

4.1 Introduction

While the primary accumulation of G_{M3} has not been described in any known LSD, G_{M2} accumulates in the G_{M2} gangliosidoses (Tay Sachs disease, Sandhoff disease and G_{M2}-activator protein deficiency) due to a dysfunction in a lysosomal enzyme or activator protein responsible for its degradation and is associated with severe brain pathology (Sandhoff *et al.* 1971; Conzelmann and Sandhoff 1978). LSDs with secondary ganglioside storage, such as the MPSs and NPC, have CNS degeneration and neuronal morphology that is similar to that of the gangliosidoses, suggesting that gangliosides may contribute significantly to brain pathology in these diseases (Constantopoulos and Dekaban 1978; Constantopoulos *et al.* 1980; Zervas *et al.* 2001a). It is unknown whether this is due to the burden of additional storage material on the lysosome interfering with lysosomal function, or through the downstream signalling of stored gangliosides; however, it is likely that a combination of these processes contribute to MPS brain pathology.

To date, the individual effect of ganglioside storage on MPS brain function has not been investigated. All GAG targeted ERT, GT, BMT and SDT trials that have improved behaviour have not only decreased levels of GAG storage products but gangliosides as well (Frisella *et al.* 2001; Ellinwood *et al.* 2007; Malinowska *et al.* 2010; Vite *et al.* 2011; Wolf *et al.* 2011). In order to assess the role of gangliosides alone in MPS CNS disease, we have used the iminosugar *N*B-DNJ to reduce the synthesis of all GSLs, including gangliosides (Platt *et al.* 1994; Platt *et al.* 1997a; Platt *et al.* 1997b). This allows for the analysis of biochemical and functional CNS disease progression with a reduction in ganglioside storage and can add to the current understanding of the sequence of events that lead to MPS brain dysfunction.

Decreasing brain ganglioside levels using *N*B-DNJ also has the potential to treat this component of MPS disease. The development of a treatment is of great importance to children

with MPS associated CNS degeneration, as in the majority of cases, this aspect of disease is currently untreatable (Neufield and Muenzer 2001). In the past, *N*B-DNJ has demonstrated some effect in improving CNS degeneration in clinical trials for children with NPC and is now in clinical use for this LSD (Chien *et al.* 2007; Patterson *et al.* 2007; Santos *et al.* 2008; Pineda *et al.* 2009; Wraith *et al.* 2009; Patterson *et al.* 2010; Pineda *et al.* 2010; Wraith *et al.* 2010; Fecarotta *et al.* 2011; Zarowski *et al.* 2011; Patterson *et al.* 2012). We now test whether *N*B-DNJ can also be used to improve brain disease in the MPS IIIA mouse model. This model was chosen for its significant accumulation of brain G_{M2} and G_{M3} and for its association with behavioural deficits that result from CNS dysfunction (Chapter Three).

4.2 *N*B-DNJ dose and mode of administration

Previous *N*B-DNJ treatment trials in LSD mouse models have used oral delivery (Platt *et al.* 1997a; Jeyakumar *et al.* 1999; Jeyakumar *et al.* 2001; Zervas *et al.* 2001b). However, *iv* administration of *N*B-DNJ has the advantage that smaller amounts of drug can be used, as the entire dose enters the bloodstream. In order to identify whether similar decreases in ganglioside levels could be achieved with the two methods of drug delivery, a comparative study was conducted, in which oral or *iv N*B-DNJ was administered to normal mice (Chapter 2.2.4).

For the oral treatment regimen, normal mice were fed with 4800mg/kg/day *N*B-DNJ mixed into their daily intake of powdered chow, for seven days, from four to five weeks of age (Chapter 2.2.4.1). Within the first few days of initiating the oral *N*B-DNJ treatment, it was observed that all mice were having difficulty with temperature regulation, being inactive and cool to touch. Temperature and activity returned to normal after mice were placed in a humidity crib, where they stayed for the remainder of the treatment period. The treatment was

stopped after seven days due to concern over the wellbeing of the mice. These side effects have not been previously described.

For the intravenous treatment of normal mice, a dose of 0.4μg/gm mouse weight *N*B-DNJ was administered via the tail vein, three times per week, from four to eight weeks of age (Chapter 2.2.4.2). Mice treated with *iv N*B-DNJ did not display any side effects, thus the treatment was continued for the full four week protocol.

4.2.1 Ganglioside levels after short-term N*B-DNJ treatment of normal mice*

Brain gangliosides were isolated from the brains of orally treated normal mice at five weeks of age and measured by LC-ESI MS/MS (Chapter 2.3.1.1 and 2.3.1.3). G_{M1}, G_{M2}, and G_{M3} were reduced by 15%, 20% and 42% respectively, with the decrease in G_{M3} reaching statistical significance (one-way ANOVA, Tukey's HSD; Figure 4.1).

Brain gangliosides were isolated from the brains of *iv* treated normal mice at eight weeks of age and measured by LC-ESI MS/MS (Chapter 2.3.1.1 and 2.3.1.3). G_{M1}, G_{M2}, and G_{M3} were reduced by 39%, 31% and 42% respectively, with the decreases in G_{M1} and G_{M3} reaching statistical significance (one-way ANOVA, Tukey's HSD; Figure 4.1). This demonstrated that brain ganglioside levels could be reduced with *iv N*B-DNJ treatment and that these reductions were comparable to the oral treatment regimen.

4.2.2 Weights after short-term N*B-DNJ treatment of normal mice*

The body and tissue weights of *N*B-DNJ treated and untreated normal mice were measured, as treatment with oral *N*B-DNJ is known to cause weight loss due to diarrhoea and decreased spleen volume (Platt *et al.* 1997b; Andersson *et al.* 2000). At five weeks of age the average body weight of mice treated orally with *N*B-DNJ was significantly less than that of untreated

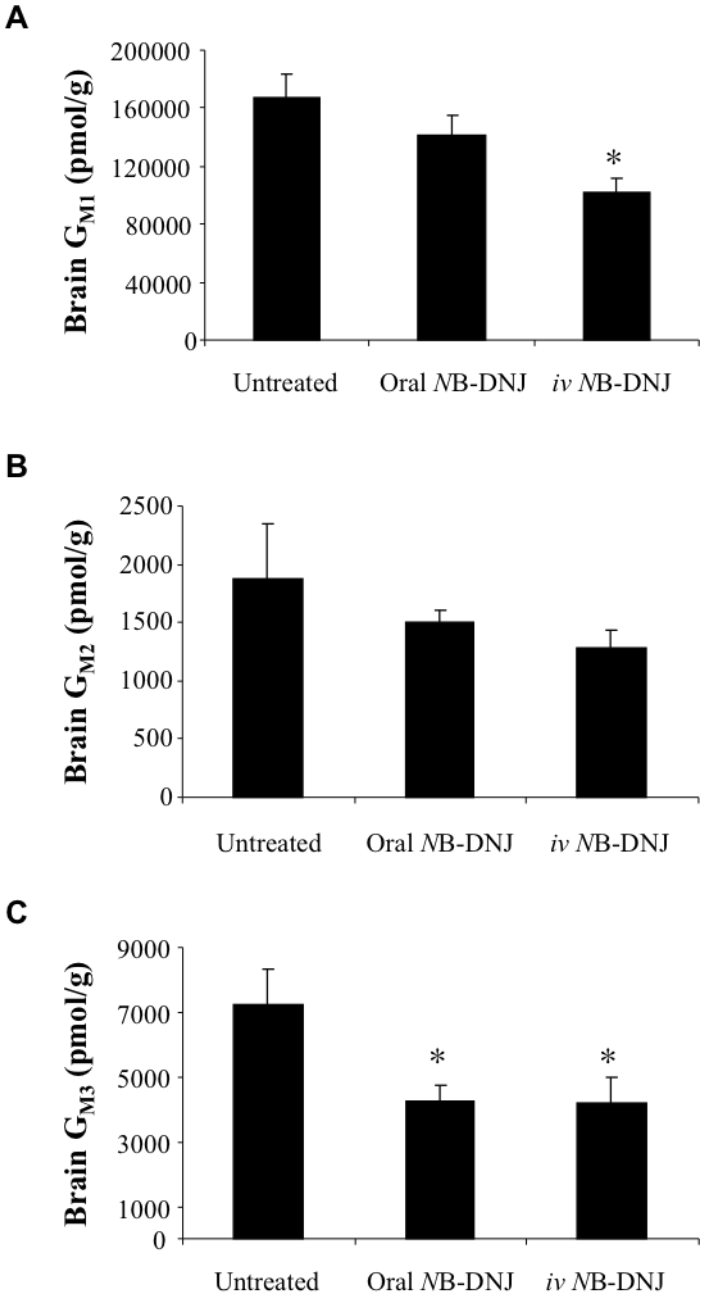

Figure 4.1: Ganglioside levels after short-term *N*B-DNJ treatment of normal mice.

Gangliosides were chloroform/methanol extracted from normal mouse brains treated with oral or *iv N*B-DNJ from four to five or four to eight weeks of age, respectively. G_{M1} (d18:1/ 18:0) (**A**), G_{M2} (d18:1/22:1) (**B**), and G_{M3} (d18:1/18:0) (**C**) levels were quantified by LC-ESI MS/MS against a d_3-G_{M1} internal standard and normalised to tissue weight. Results were expressed as mean ± standard error of n=5. * Significantly different from untreated normal, $p<0.05$ (one-way ANOVA, Tukey's HSD).

mice (63% of untreated; one-way ANOVA, Tukey's HSD; Figure 4.2A), although no diarrhoea was observed. Liver, kidney, spleen, heart, lung, and brain weights were also significantly less than untreated mice (64%, 74%, 22%, 67%, 75%, and 96% of untreated weights respectively; one-way ANOVA, Tukey's HSD; Figure 4.2B).

The body and tissue weights of untreated normal and *iv N*B-DNJ treated normal mice were determined when mice were humanely killed at eight weeks of age. Body weight with treatment was no different from untreated mice (Figure 4.2C). Liver, kidney, spleen, heart, lung, and brain weights also did not differ between treated and untreated normal mice (Figure 4.2D). This demonstrated that *iv N*B-DNJ treatment did not have the same side effects as oral treatment, perhaps due to the lower dose required and that *iv* treatment bypassed the gastrointestinal system.

4.3 *In vivo iv N*B-DNJ treatment trials

Based on the preliminary results described above and observation of severe side effects with oral treatment, the *iv* delivery method was chosen for MPS IIIA *N*B-DNJ treatment trials. In addition, the dose was doubled from 0.4μg/gm mouse weight to 0.8μg/gm mouse weight in order to achieve a dose consistent with high dose oral *N*B-DNJ studies and maximise the effect of treatment on ganglioside synthesis. Two groups of MPS IIIA mice were treated with 0.8μg/gm mouse weight *N*B-DNJ intravenously, three times per week. The treatment of one group was initiated early (four weeks of age; Chapter 2.2.4.2) when brain G_{M2} and G_{M3} levels were 72% and 38% of the affected maximum, respectively (Chapter Three). Treatment of the second group was initiated later (four months of age; Chapter 2.2.4.2) when G_{M2} and G_{M3} were already at the MPS IIIA brain maximum (Chapter Three). A normal treatment group was also included to determine whether *N*B-DNJ altered normal mouse behaviour. Brain function was monitored throughout the treatment period using behaviour tests at two, four and

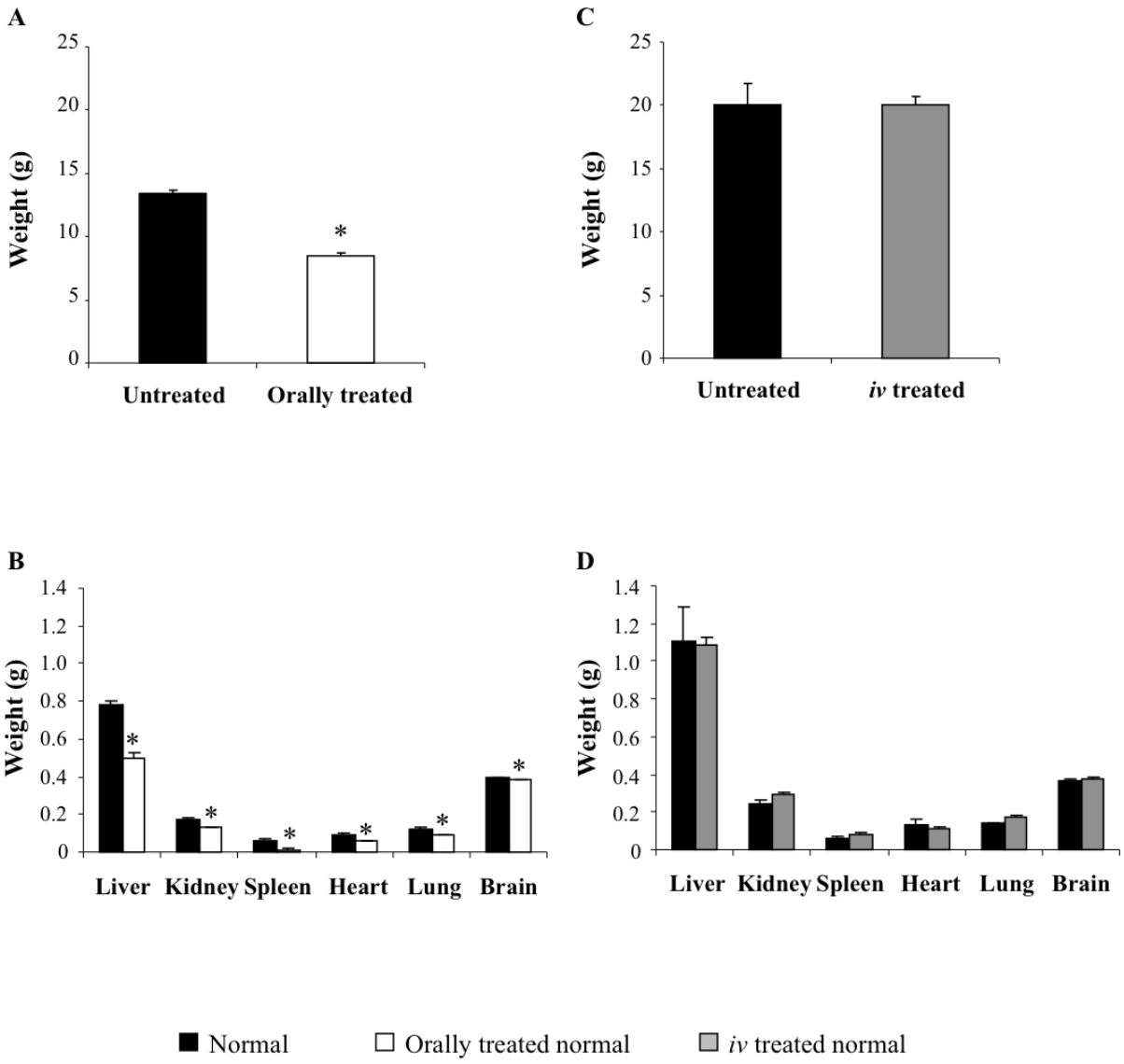

Figure 4.2: Body and tissue weights with short-term *N*B-DNJ treatment.
Mice were treated with oral or *iv* *N*B-DNJ from four to five or four to eight weeks of age, respectively. Body (**A, C**) and tissue (**B, D**) weights were determined. Results were expressed as mean ± standard error of n=2-5. * Significantly different from untreated normal, $p<0.05$ (one-way ANOVA, Tukey's HSD).

six months of age for early treated MPS IIIA and normal mice and at six months for late treated MPS IIIA mice. Biochemical changes were measured at the trial end point (six months for all groups).

4.3.1 Animal and tissue weights

To determine the effect of *N*B-DNJ treatment on body weight, mice were weighed weekly over the treatment period (19 to 26 weeks for late treated mice, four to 26 weeks for all other groups). Average female MPS IIIA mouse weights were significantly greater than normal from eight weeks of age (one-way ANOVA, Tukey's HSD; Figure 4.3A). Average male MPS IIIA mouse weights were greater than normal from seven weeks of age, becoming significant from 19 weeks (one-way ANOVA, Tukey's HSD; Figure 4.3B). Neither male nor female MPS IIIA body weights changed with *N*B-DNJ treatment compared with untreated MPS IIIA controls (Figure 4.3). Normal mouse body weights also did not change with treatment (Figure 4.3C). Thus, *iv N*B-DNJ treatment did not impact on mouse body weight.

The effect of *N*B-DNJ treatment upon brain, liver, kidney, spleen, heart and lung weights were determined at six months of age. *N*B-DNJ treatment did not alter organ weights of normal mice (Figure 4.4). A comparison of organ weights of female mice demonstrated that the average spleen and heart weights of untreated MPS IIIA mice were significantly greater than normal (281% and 158% of normal respectively), but were not significantly different form normal with either early or late *N*B-DNJ treatment (one-way ANOVA, Tukey's HSD; Figure 4.4B and E). Although they were not significantly different, there appeared to be a slight reduction in spleen weight with late treatment and an even greater reduction in spleen weight with early treatment compared with untreated MPS IIIA mice. This suggests that there is some effect of *iv N*B-DNJ on spleen weight, which increases over time. No other changes in female mouse organ weights were observed. A comparison of male organ weights demonstrated that the average liver weights of untreated MPS IIIA mice were significantly

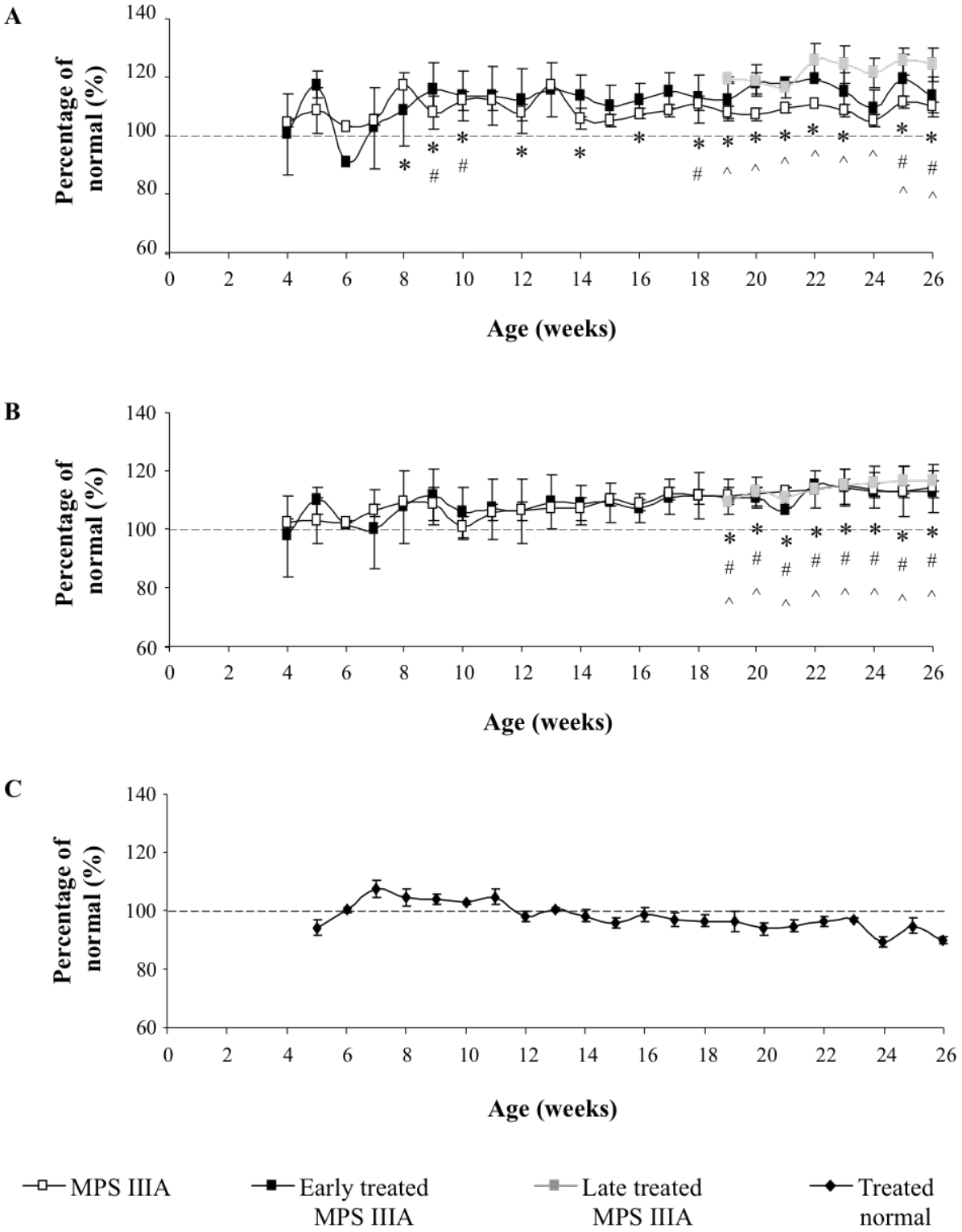

Figure 4.3: Body weights of mice treated with *N*B-DNJ.
Female (A, C) and male (B) mouse weights were measured weekly. Results were expressed as mean ± standard error of n=2-6. Significant differences between normal and MPS IIIA (*), normal and early treated MPS IIIA (#) and normal and late treated MPS IIIA (^), $p<0.05$ (one-way ANOVA, Tukey's HSD).

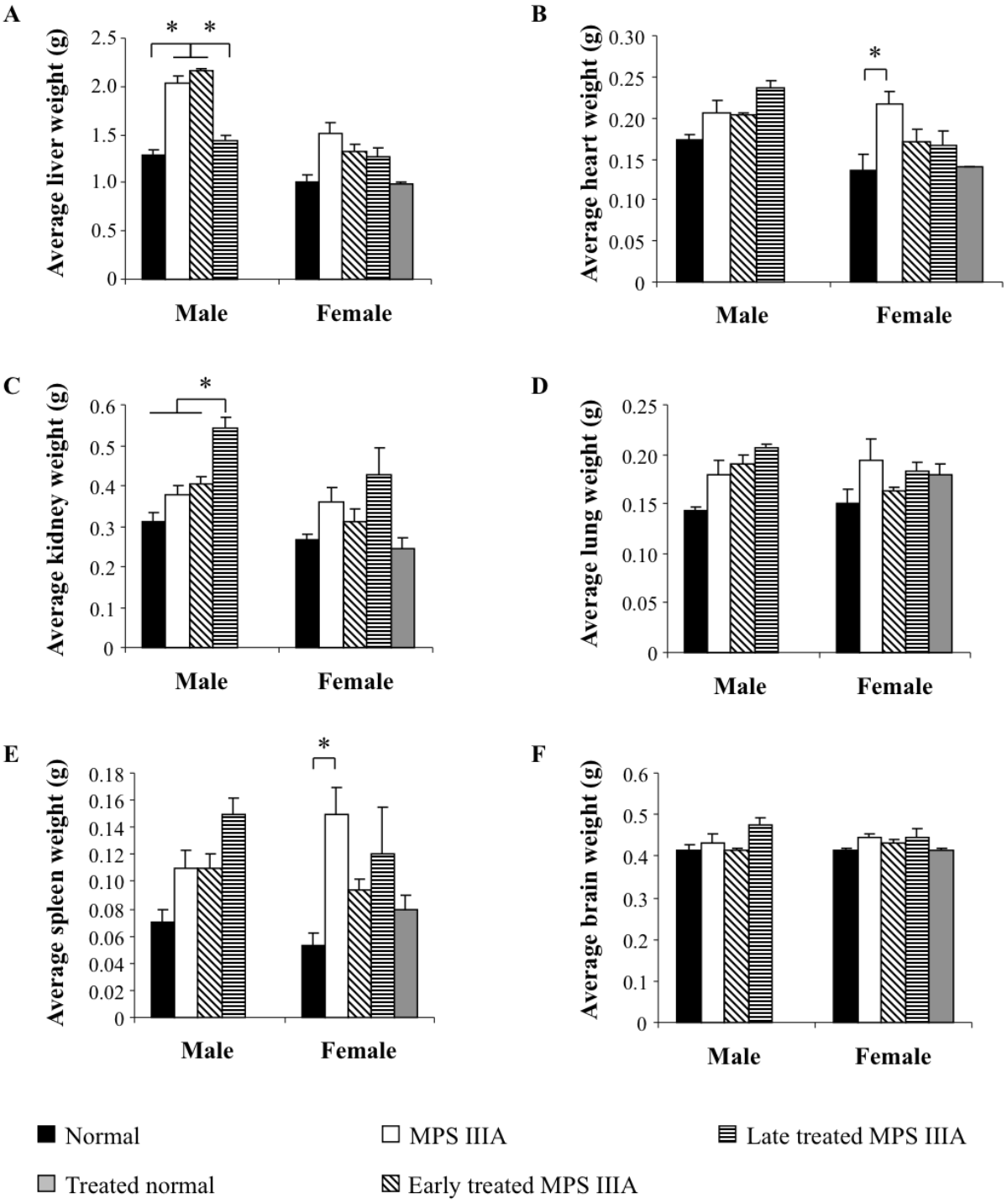

Figure 4.4: Tissue weights.
Mice were humanely killed at six months of age and tissue weights determined. Results were expressed as mean ± standard error of n=2-4. * Significant difference between indicated groups, $p<0.05$ (one-way ANOVA, Tukey's HSD).

greater than normal (158% of normal; one-way ANOVA, Tukey's HSD, Figure 4.4A) and were significantly reduced with late, but not early, *N*B-DNJ treatment. It was also observed that the average kidney and spleen weights of male, late treated MPS IIIA mice were increased compared with untreated MPS IIIA control mice, this being significant for kidney (143% of normal mice; one-way ANOVA, Tukey's HSD; Figure 4.4C and E). No other changes in male organ weight were observed. These results demonstrate some differences between early and late treated MPS IIIA male organ weights, however, the reason for this is unknown.

4.3.2 Behavioural outcomes with N*B-DNJ treatment*

In order to determine the effect of *N*B-DNJ treatment on brain function, motor coordination, activity, anxiety and learning ability were measured using a series of behavioural tests.

4.3.2.1 Motor coordination with N*B-DNJ treatment*

At six month of age, motor coordination of normal, MPS IIIA, and early *N*B-DNJ treated MPS IIIA mice was measured using the rotarod (Chapter 2.2.3.3). Latency to fall did not differ between groups (Figure 4.5). As no deficit in untreated MPS IIIA motor coordination was identified compared to normal, the rotarod was not an appropriate test with which to identify behavioural improvements, therefore late treated MPS IIIA mice were not tested.

4.3.2.2 Activity and anxiety with N*B-DNJ treatment*

The activity and anxiety of MPS IIIA and normal mice was measured using the open field test (Chapter 2.2.3.4). Early-treated mice were tested at two, four and six months of age, while late-treated mice were tested at six months of age. The number of rearing events and total distance travelled over three minutes was not significantly different between ages or treatment

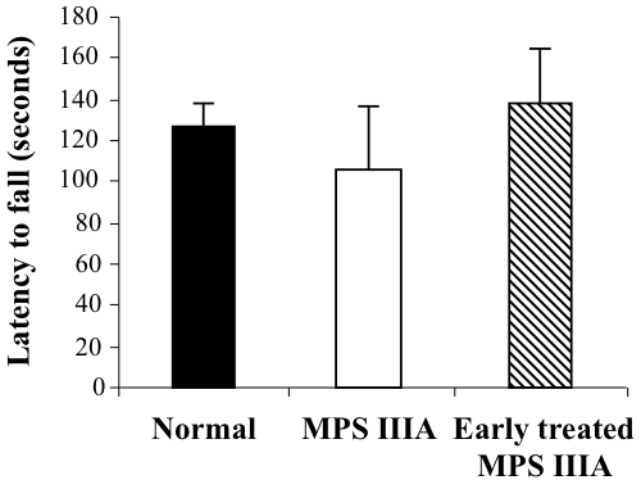

Figure 4.5: Motor coordination with *N*B-DNJ treatment.
Normal, MPS IIIA and early *N*B-DNJ treated MPS IIIA mice were placed on a rotating barrel, which accelerated form five to 35 rpm over two minutes and then maintained 35 rpm for a further minute. Latency to fall was recorded and results were expressed as mean ± standard error of n=4-6.

groups (one-way ANOVA, Tukey's HSD; Figure 4.6A and B). Centre activity (percentage of distance travelled and time spent in the centre of the apparatus) of untreated MPS IIIA mice was significantly greater than normal from four months of age (202% and 307% of normal for distance and time respectively) and this was normalised with early *N*B-DNJ treatment (one-way ANOVA, Tukey's HSD; Figure 4.6C and D). At six months of age, centre activity (both percentage of distance travelled and time spent in the centre) for both early and late *N*B-DNJ treated MPS IIIA mice was significantly reduced compared with untreated MPS IIIA (one-way ANOVA, Tukey's HSD; Figure 4.6C and D). Six month old untreated normal mice spent less time in the centre compared with untreated MPS IIIA mice, however the percentage of distance travelled in the centre was not significantly different to untreated MPS IIIA mice (one-way ANOVA, Tukey's HSD; Figure 4.6C and D). Average normal activity did not change with *N*B-DNJ treatment (Figure 4.6).

4.3.2.3 Learning ability with N*B-DNJ treatment*

The water cross-maze was used to test the learning ability of mice from all treatment groups at six months of age. Normal, MPS IIIA and early and late *N*B-DNJ treated MPS IIIA mice were given six days to learn the location of a submerged platform via visual cues (Chapter 2.2.3.5). Parameters measured included the average number of correct entries, where mice travelled straight to the platform, incorrect entries, where mice entered maze arms that did not contain the platform, and escape latency, which was the time taken to locate the platform. The performance of normal treated and untreated mice did not differ for any of these parameters (Figure 4.7). Surprisingly, untreated MPS IIIA mouse performance was also not significantly different compared with untreated normal mice (Figure 4.7). However, MPS IIIA incorrect entries and escape latency appeared to be greater than normal and to normalise with both early and late *N*B-DNJ treatment (Figure 4.7).

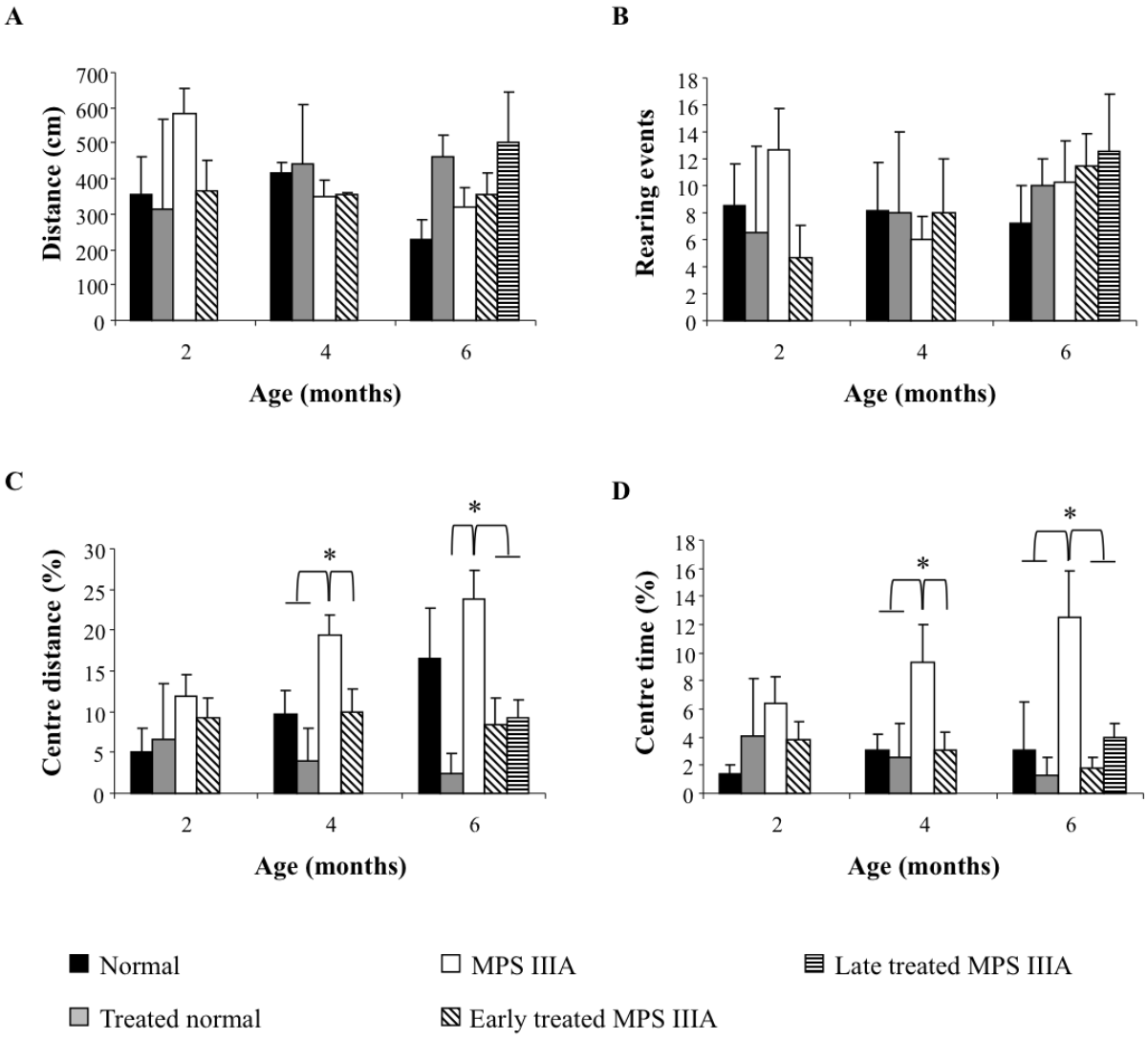

Figure 4.6: Activity with *N*B-DNJ treatment.
Mice were placed in the front left hand corner of the open field apparatus and distance traveled (**A**), number of rearing events (**B**), percentage of overall distance traveled in the central zone (**C**) and percentage of time spent in the central zone (**D**) were recorded. Results were expressed as mean ± standard error of n=6 (normal, MPS IIIA, and early and late treated MPS IIIA) or n=2 (treated normal). * Significant difference between groups, $p<0.05$ (one-way ANOVA, Tukey's HSD).

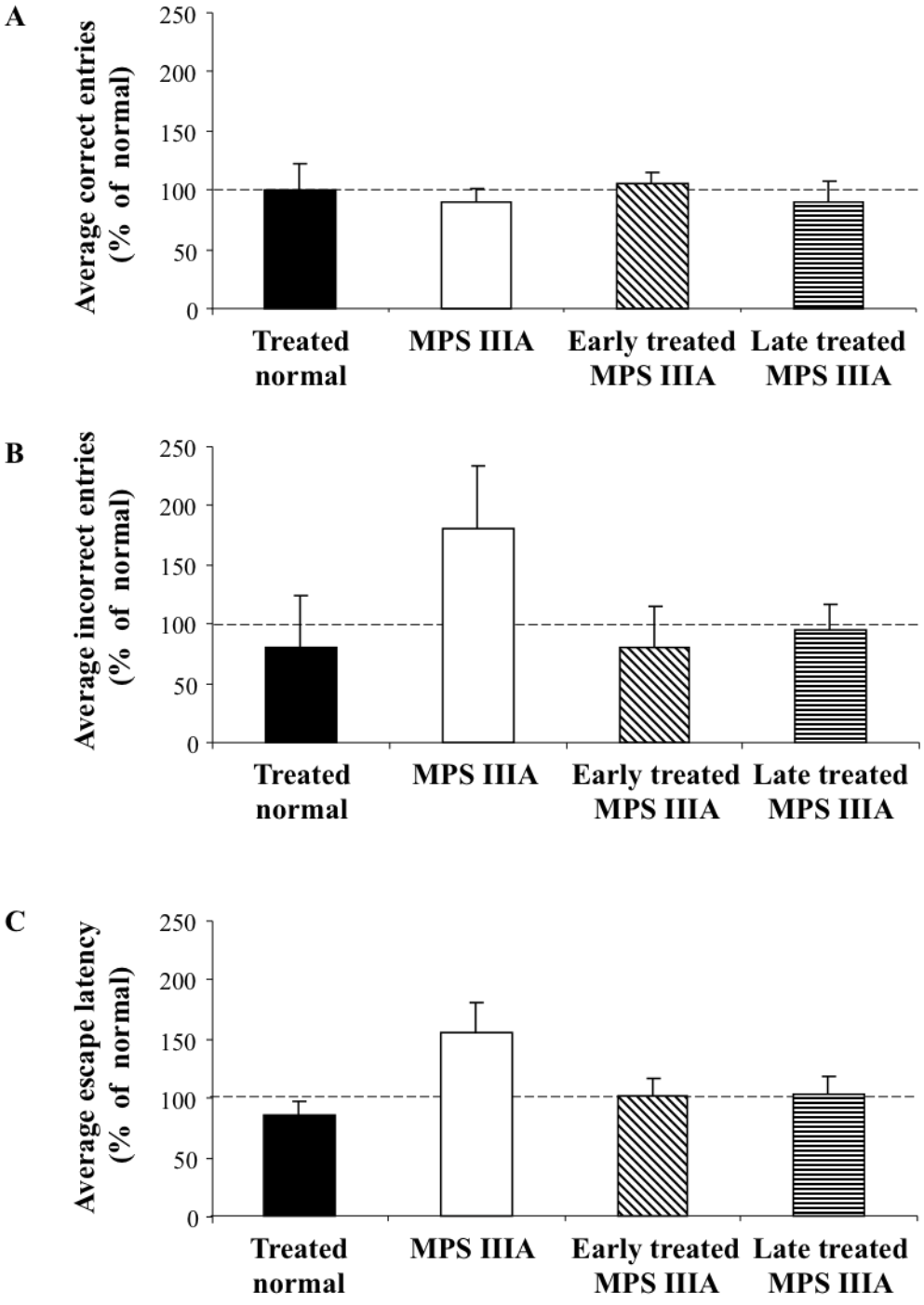

Figure 4.7: Learning ability after *N*B-DNJ treatment.
Mice were placed in a cross shaped pool filled with opaque water and used constant visual cues to locate a submerged platform. Correct entries, incorrect entries and escape latency were measured, normalised to normal values and expressed as mean ± standard error of n=6 (normal, MPS IIIA, and early and late treated MPS IIIA) or n=2 (treated normal).

4.3.3 N*B-DNJ treatment effects on the GSL synthesis pathway*

Following the measurement of behavioural changes with *N*B-DNJ treatment, the effect of treatment on the GSL synthesis pathway was determined in mouse brain tissue. Ceramide glucosyltransferase activity was measured to determine whether *N*B-DNJ was successful in decreasing enzyme activity in the brain. In addition, brain G_{M2} and G_{M3} levels were measured as these lipids are downstream products of the GSL synthesis pathway and were the targets of this study. Levels of a control monosialoganglioside, G_{M1}, which does not accumulate in the MPS brain but was still expected to decrease with *N*B-DNJ treatment was also measured.

4.3.3.1 Ceramide glucosyltransferase activity with N*B-DNJ treatment*

Brain ceramide glucosyltransferase activity was measured in 0.1% (v/v) Triton X-100 brain extracts (Chapters 2.3.1.5 and 2.3.2.1). Decreases in brain enzyme activity were observed in all treatment groups compared to untreated mice, with ceramide glucosyltransferase activity in brains from both early and late treated MPS IIIA mice being significantly lower than untreated normal (one-way ANOVA, Tukey's HSD; Figure 4.8). Ceramide glucosyltransferase activity did not differ significantly between early and late treatment groups (one-way ANOVA, Tukey's HSD; Figure 4.8).

4.3.3.2 Brain ganglioside levels with N*B-DNJ treatment*

At six months of age, brain gangliosides were extracted (Chapter 2.3.1.1) and quantified by LC-ESI MS/MS (Chapter 2.3.1.3). G_{M1} levels did not differ between normal, treated normal, MPS IIIA and early treated MPS IIIA brains, but were significantly reduced in late-treated MPS IIIA brains compared with untreated normal brains (one-way ANOVA, Tukey's HSD; Figure 4.9A). The level of G_{M2} in treated and untreated normal mouse brain did not differ (one-way ANOVA, Tukey's HSD; Figure 4.9B). MPS IIIA mouse brain G_{M2} was

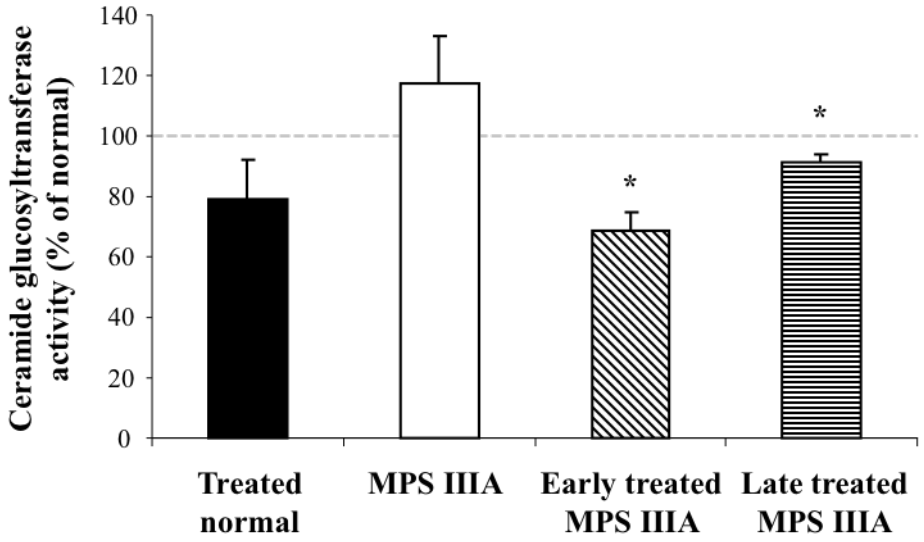

Figure 4.8: Brain ceramide glucosyltransferase activity.
A fluorometric assay was used to measure ceramide glucosyltransferase activity in six-month-old untreated normal, *N*B-DNJ treated normal, MPS IIIA and early and late *N*B-DNJ treated MPS IIIA brains homogenised in 0.1% (v/v) Triton X-100. Results were normalised to normal values and expressed as mean ± standard error of n=2-9. * Significantly different from normal, $p<0.05$ (one-way ANOVA, Tukey's HSD).

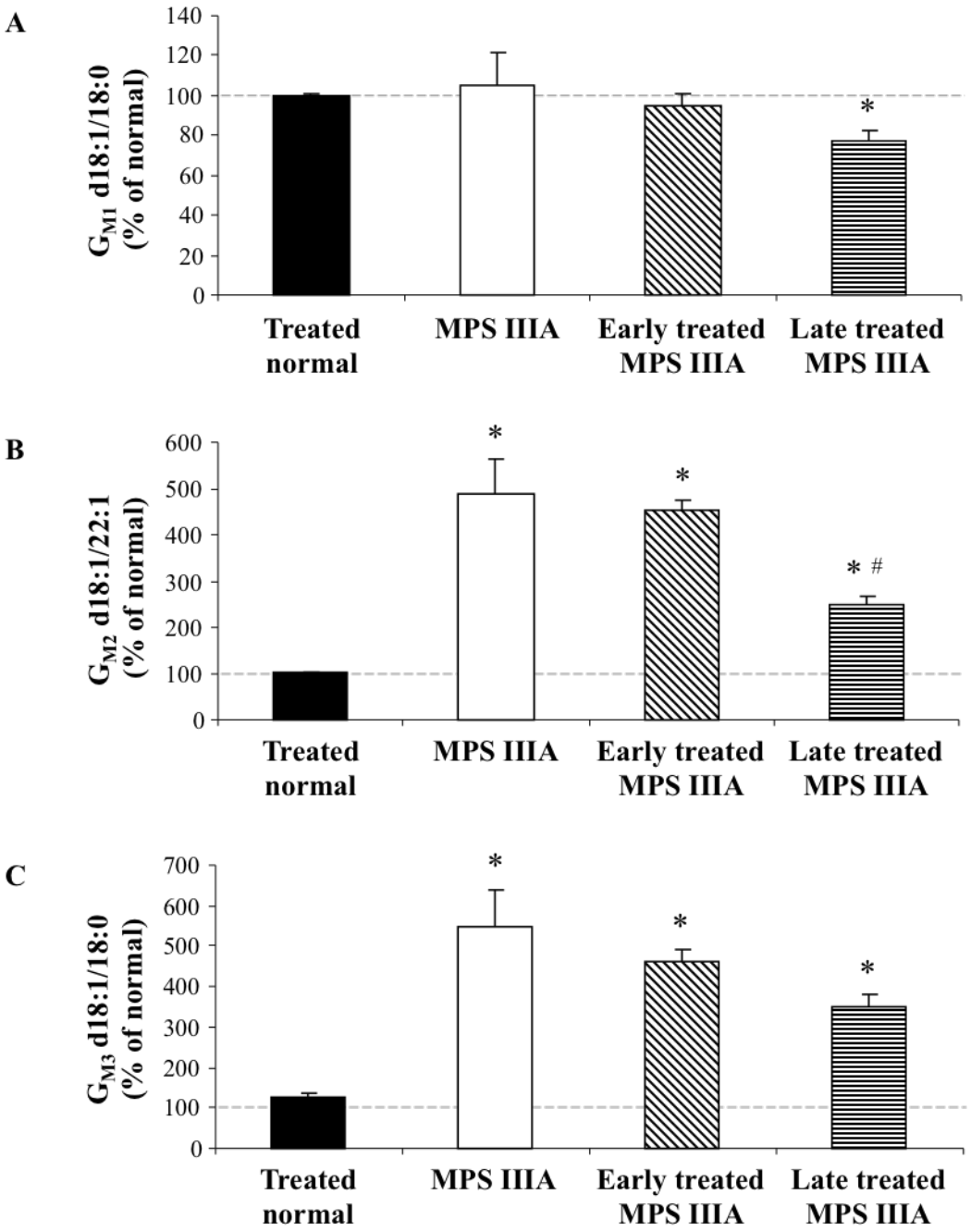

Figure 4.9: Quantification of brain gangliosides with *N*B-DNJ treatment.
Gangliosides were chloroform/methanol extracted from six-month-old untreated normal, *N*B-DNJ treated normal, MPS IIIA and early and late *N*B-DNJ treated MPS IIIA mouse brains. G_{M1} (d18:1/18:0) (**A**), G_{M2} (d18:1/22:1) (**B**) and G_{M3} (d18:1/18:0) (**C**) levels were quantified by LC-ESI MS/MS against a d_3-G_{M1} internal standard and normalised to tissue weight. Results were expressed as mean ± standard error of n=6. Significantly different from normal (*) or untreated MPS IIIA ($^{\#}$), $p<0.05$ (one-way ANOVA, Tukey's HSD).

significantly elevated to 461% of normal and this did not change with early *N*B-DNJ treatment (475% of normal; one-way ANOVA, Tukey's HSD; Figure 4.9B). However, brain G_{M2} levels were significantly decreased to 249% of normal in the brains of late-treated MPS IIIA mice (one-way ANOVA, Tukey's HSD; Figure 4.9B). G_{M3} levels did not differ between treated and untreated normal mouse brain (one-way ANOVA, Tukey's HSD; Figure 4.9C). G_{M3} was significantly raised to 512% of normal in untreated MPS IIIA mouse brains and this did not change significantly with early *N*B-DNJ treatment (484% of normal; one-way ANOVA, Tukey's HSD; Figure 4.9C). In late-treated MPS IIIA mouse brains, G_{M3} brain levels were decreased to 277% of normal, but were not significantly different from untreated MPS IIIA levels (one-way ANOVA, Tukey's HSD; Figure 4.9C). Overall, these results indicate that late treatment was more effective than early treatment at decreasing brain ganglioside levels, despite both treatment regimens being effective at reducing ceramide glucosyltransferase activity, as shown above.

4.3.4 Brain GAG levels with treatment

Brain GAG levels were measured to determine whether *N*B-DNJ treatment had an effect on primary GAG storage. At six months of age brain GAG was extracted (Chapter 2.3.2.1) and GAG levels determined by UA assay (Chapter 2.3.2.2). Normal brain GAG levels were unchanged with *N*B-DNJ treatment, while untreated, early and late treated MPS IIIA brain GAG levels were significantly raised over normal (238%, 280% and 336% respectively; one-way ANOVA, Tukey's HSD; Figure 4.10).

4.4 Discussion

While the MPSs are primarily GAG storing disorders, neuronal storage of G_{M2} and G_{M3} is also observed, which is associated with CNS degeneration in other LSDs (Constantopoulos and Dekaban 1978; Constantopoulos *et al.* 1980; McGlynn *et al.* 2004). The extent to which

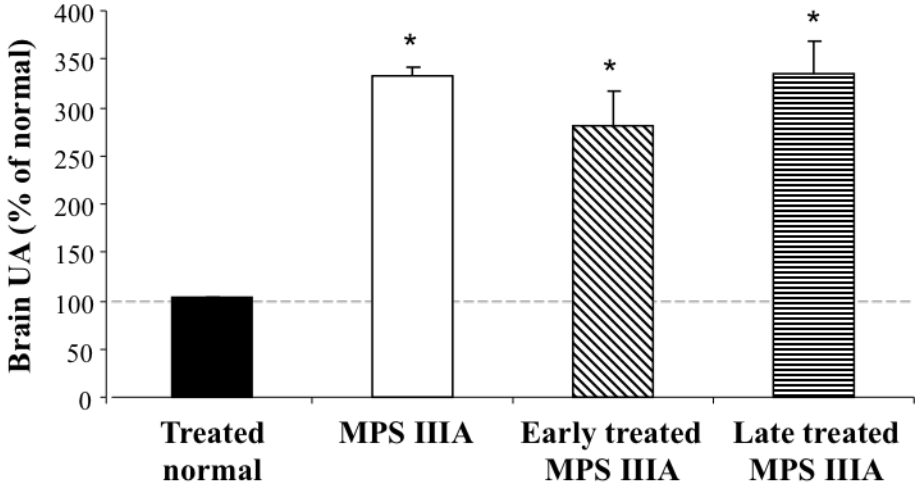

Figure 4.10: Quantification of brain GAG with *N*B-DNJ treatment.
GAGs were 0.1% (v/v) Triton X-100 extracted from six-month-old untreated normal, *N*B-DNJ treated normal, MPS IIIA and early and late *N*B-DNJ treated MPS IIIA brains and measured by uronic acid (UA) assay. Results were normalised to normal values and expressed as mean ± standard error of n=6. * Significantly different from normal, $p<0.05$ (one-way ANOVA, Tukey's HSD).

gangliosides are responsible for the deterioration of MPS brain function has been investigated for the first time in this study, using *N*B-DNJ to decrease brain ganglioside synthesis in the MPS IIIA mouse model.

Typically, whether in the clinic or in animal trials, *N*B-DNJ is administered orally (Jeyakumar *et al.* 1999; Cox *et al.* 2000; Treiber *et al.* 2007). This has the advantage of being the easiest route of administration, as well as allowing for a slow diffusion of the compound into the circulation and reducing its rate of clearance (Treiber *et al.* 2007). However, in order to get adequate circulating levels of *N*B-DNJ, an oral method of treatment requires very high doses (Fischl *et al.* 1994; Platt *et al.* 1997a; Cox *et al.* 2000). Trials in murine models require even greater dosages than in humans in order to obtain the therapeutically effective serum concentration (5-50μM) due to the increased rate of renal clearance, which is approximately two fold that of humans (Platt *et al.* 1997a; Platt *et al.* 1997b; Treiber *et al.* 2007). Therefore, *iv* versus oral *N*B-DNJ treatment was investigated in this chapter to determine whether *iv* treatment was effective.

A comparison was made between normal mice treated orally with the highest described murine dose of *N*B-DNJ (4800mg/kg/day), previously shown to give a serum concentration in the region of 50μM (Platt *et al.* 1997a), and normal mice treated three times a week with 0.4mg/kg of *iv N*B-DNJ. Although serum samples were collected for the determination of *N*B-DNJ levels, a laboratory performing this test was unable to be sourced. The *iv* dose was calculated according to the mouse blood volume being 70μl/g of body weight (Hoff 2000), aiming to achieve a theoretical 25μM blood concentration with each treatment (Chapter 2.2.4.2). The result of brain ganglioside quantification following treatment in these normal mice demonstrated comparable results between the two groups, with a similar decrease in G_{M2} and G_{M3} levels and a slightly greater decrease in G_{M1} levels seen with *iv* treatment. Mice were also monitored for *N*B-DNJ side-effects, which include weight-loss, diarrhoea and atrophy of

lymphoid organs (Platt *et al.* 1997a). Normal mice treated orally with a high dose of *N*B-DNJ displayed below average body weights compared with age matched untreated normal mice and had difficulty with temperature regulation, though no diarrhoea was observed. In addition, organ weights were significantly reduced, with the reduction in spleen weight being most dramatic. On the other hand, no side-effects were observed in mice treated with *iv N*B-DNJ, perhaps due to the lower dose delivered and because *iv* treatment bypassed the gastrointestinal system. Given these preliminary treatment outcomes, *iv N*B-DNJ was chosen for the long term treatment of MPS IIIA mice. In order to maximise the effect of treatment on ganglioside levels, the dose used was also raised further to 0.8mg/kg three times per week to achieve an estimated 50μM blood concentration. There were no adverse effects of longer-term *iv* treatment with this treatment regimen

Mouse weights with long-term *N*B-DNJ treatment were equivalent to untreated mice of the same genotype, with MPS IIIA mice (both treated and untreated) being slightly heavier than age matched normal mice as previously described (Roberts *et al.* 2006). In addition, no spleen atrophy was observed. In fact, for an unknown reason, the spleens of late treated males appeared to be heavier than those of untreated MPS IIIA mice, as were the kidney, heart, and lung weights in this treatment group. This increase was significant for kidney weights. Hepatomegaly is another characteristic of MPS IIIA (Roberts *et al.* 2006), though this was only observed for MPS IIIA untreated and early treated male mice. Late-treated MPS IIIA mouse liver weights were reduced compared to untreated MPS IIIA mice, but again, the reason for this is unknown. As these same observations were not made in the early treatment group (i.e. in those mice treated for longer), it is suggested that organ weights stabilised with continued *N*B-DNJ treatment.

Improvements in brain function in the MPS IIIA mice treated with *N*B-DNJ were demonstrated through the use of the open field and water cross-maze behaviour tests. Activity

and anxiety, measured as total distance travelled, the number of rearing events and the percentage of time spent and distance travelled in the centre was measured at two, four and six months of age using the open field apparatus. No differences in total distance travelled or number of rearing events were observed between groups. This was consistent with some previous studies, which have shown no significant difference in these parameters between normal and MPS IIIA mice (Crawley *et al.* 2006; McIntyre *et al.* 2010; Langford-Smith *et al.* 2011a). Other studies have demonstrated hyperactivity in female MPS IIIA mice (Crawley *et al.* 2006; Langford-Smith *et al.* 2011a), however, the current study did not have sufficient numbers of mice of each sex to enable analysis of sex differences.

Differences in activity between normal and MPS IIIA mice were observed in the time spent and distance travelled in the centre. These behavioural differences appeared at two months of age, becoming significant by four months of age. This indicated that MPS IIIA mice lost the innate, protective fear response that causes mice to avoid open spaces (Simon *et al.* 1994). This behaviour is consistent with eight month old MPS IIIB mice, which had a greater frequency of entry into the centre of the open field (Malinowska *et al.* 2010). In the MPS IIIB study, mice were also treated with Genistein, a GAG targeting SDT agent, which normalised this behaviour (Malinowska *et al.* 2010). While the previous study demonstrated that a reduction in GAG levels could normalise the fear response, data presented in this chapter also demonstrates that the fear response can be restored with ganglioside-targeted SDT. Given that it has been shown in many MPS models that reducing GAG levels also results in a reduction in brain ganglioside levels, the observations that the protective fear response was normalised by GAG-targeted SDT in the study by Malinowska et al. (2010) may have been in response to reduced ganglioside (Frisella *et al.* 2001; Vite *et al.* 2011; Wolf *et al.* 2011). These observations from previous studies support the contention that gangliosides play a role in MPS IIIA brain pathology. Furthermore, improvements in the fear response were observed with both long and short-term *N*B-DNJ treatment, indicating that whether treatment was

initiated when G_{M2} and G_{M3} were at 72% and 38% of the affected mouse maximum respectively, or whether it was initiated when G_{M2} and G_{M3} were at maximum levels, activity was still restored to that of normal mice. This suggests that ganglioside accumulation does not cause irreversible changes to activity.

The open field parameters that emphasised MPS IIIA versus normal genotype differences in the *N*B-DNJ treatment trial were not consistent with those demonstrated in Chapter Three, in which MPS IIIA mice displayed a smaller total distance travelled and less rearing events compared with normal mice, but no change in activity in the centre of the apparatus. An explanation for this is the difference in mouse handling, with mice used in Chapter Three being handled only during behaviour testing and mice used in this chapter being handled daily for weighing and *N*B-DNJ injections. This highlights the potential for variability between groups in murine behaviour tests, despite best efforts to maintain apparatus, testing protocol and researcher consistency. This variability has been described previously in a comparative review of the open field performance of MPS IIIA mice (Langford-Smith *et al.* 2011a). Despite this concern, mice tested in the *N*B-DNJ study were done so in a single group, thus we are confident with the validity of internal comparisons within this data group presented in this chapter.

Learning ability for normal, MPS IIIA and treated mice was also determined at six months of age, when a deficit in this behaviour had previously been observed, both in Chapter Three (Figure 3.10) and in a previous study by our group (Roberts *et al.* 2007). Unfortunately, this study failed to replicate the significant deficit in MPS IIIA learning ability, perhaps due to smaller numbers. Thus, we were not able to conclude whether NB-DNJ treatment had an effect on MPS IIIA learning.

Rotarod testing was also performed at six months of age to test motor coordination and balance, as a small, significant deficit in this test had previously been observed in MPS IIIA mice at six months of age (Figure 3.8). However, as no deficit was observed in this group of affected MPS IIIA mice, no further rotarod testing was performed in the *N*B-DNJ treatment trials.

To correlate the behavioural outcomes of *N*B-DNJ treatment with biochemical changes, the effects of early and late treatment on brain GSL synthesis were determined. Ceramide glucosyltransferase activity was significantly reduced in both early and late *N*B-DNJ treated MPS IIIA mice. However, only late *N*B-DNJ treatment of MPS IIIA mice had reduced brain ganglioside levels (significant for G_{M2}) at six months of age. Furthermore, we had previously shown that ganglioside levels were reduced at eight weeks of age after short-term treatment, even though these mice were treated with half the *N*B-DNJ dose. Taken together, these results demonstrate that the inhibition of brain ceramide glucosyltransferase activity by *iv N*B-DNJ persists over time, but that the decrease in ganglioside levels is transient. This is consistent with previous reports of brain gangliosides of Sandhoff mice being decreased with short-term, but not with long-term, *N*B-DNJ use (Jeyakumar *et al.* 1999; Jeyakumar *et al.* 2001; Ashe *et al.* 2011). It is possible that another part of the GSL metabolic cascade eventually corrects itself after a long period of inhibition of ceramide glucosyltransferase by *N*B-DNJ. It is important to note that despite the transient decrease in brain ganglioside levels, significant behavioural improvements were observed with *N*B-DNJ treatment, suggesting a delay between ganglioside storage and functional deficits. This finding was also seen in the Sandhoff studies described above (Jeyakumar *et al.* 1999; Jeyakumar *et al.* 2001).

In addition to the measurement of brain monosialoganglioside levels, GAG levels at six months of age were determined. Given that GAG levels remained unchanged with *N*B-DNJ treatment while MPS IIIA activity was no different to normal, it is suggested that MPS IIIA

deficits in activity was not due to GAG accumulation. The storage of gangliosides is an alternative potential cause for these behavioural deficits, given decreasing brain gangliosides for a short period was associated with restoring activity to normal. Another contributing factor could have been that *N*B-DNJ treatment had an anti-inflammatory effect. While the mechanism is unknown, it has been observed *in vitro* in an artificial model of G_{M2} gangliosidosis, as well as in normal, Sandhoff, and G_{M1} gangliosidosis mice (Platt *et al.* 1997b; Jeyakumar *et al.* 2003; Elliot-Smith *et al.* 2008; Boomkamp *et al.* 2010). This effect is not likely related to the drug's effect on GSL synthesis, as another iminosugar inhibitor of GSL synthesis, *N*-butyldeoxygalactonojirimycin (*N*B-DGJ), does not have the same anti-inflammatory properties (Andersson *et al.* 2000; Elliot-Smith *et al.* 2008). Whether *N*B-DNJ has also acted as an immune modulator in this study has been investigated further in Chapter Five.

In this chapter, the analysis of behaviour demonstrated an improvement in MPS IIIA activity with both long and short term *iv N*B-DNJ treatment. For the first time, this study has separated GAG and ganglioside involvement in the development of functional changes to the MPS brain. However, due to the dual role of *N*B-DNJ in decreasing ganglioside synthesis and modulating the immune system, we are now unable to determine whether CNS dysfunction is the result of ganglioside storage or neuro-inflammation. Despite this, the improvement of murine MPS IIIA behaviour has demonstrated that *N*B-DNJ may also be effective in treating CNS pathology in MPS patients, which is of great importance to patient quality of life.

Chapter Five: The role of structural lipids and inflammatory mediators in MPS brain disease

5.1 Introduction

The secondary storage of ganglioside has long been observed in the MPS brain in both human disease and in animal models (Constantopoulos and Dekaban 1978; Constantopoulos *et al.* 1980; McGlynn *et al.* 2004). Gangliosides accumulate in MPS IIIA and MPS VII mouse brain prior to the manifestation of behavioural changes (Chapter Three) and a reduction in ganglioside synthesis restores the normal fear response in MPS IIIA mice (Chapter Four). The storage of cholesterol has also been observed in MPS neurons (McGlynn *et al.* 2004), however, it is not know whether any other lipids are affected.

Gangliosides are normally found in cell membrane rafts, where they are closely associated with a heterogeneous population of simple, phospho- and glyco-lipids (Molander-Melin *et al.* 2005; Allen *et al.* 2007; Ohmi *et al.* 2009b; Sanchez-Wandelmer *et al.* 2009; Martin *et al.* 2010; Singh *et al.* 2010; Ohmi *et al.* 2011). From their positions in the membrane these lipids have both structural and cell signalling roles, such as membrane trafficking and axonal integrity (Pettegrew *et al.* 2001; Molander-Melin *et al.* 2005; Wheeler *et al.* 2008; Martin *et al.* 2010; Cheng *et al.* 2011; Fabelo *et al.* 2011; Chan *et al.* 2012). However, they can also signal systemically, for example, polyunsaturated fatty acids (PUFAs) can be released from phospholipids and mediate inflammation and its resolution (Peterson *et al.* 1998; Esposito *et al.* 2008).

Due to the close association between gangliosides and other lipids, an alteration in ganglioside levels may also indicate a change in other membrane raft components (Molander-Melin *et al.* 2005; Ohmi *et al.* 2009b; Singh *et al.* 2010; Fabelo *et al.* 2011; Ohmi *et al.* 2011; Ohmi *et al.* 2012). Alterations in structural lipid profiles have been implicated in brain disease in a series of other neurodegenerative diseases, such as Alzheimer's disease, Parkinson's disease and multiple sclerosis and may also contribute to CNS disease in the MPSs (Pettegrew

et al. 2001; Molander-Melin *et al.* 2005; Esposito *et al.* 2008; Wheeler *et al.* 2008; Martin *et al.* 2010; Cheng *et al.* 2011; Fabelo *et al.* 2011; Chan *et al.* 2012).

Phospholipid derived PUFAs are also of interest, not only because of potential alterations in membrane components in the MPS brain, but also due to the significant inflammatory element in MPS brain disease (Richard *et al.* 2008; DiRosario *et al.* 2009; Arfi *et al.* 2011). MPS neuro-inflammation is reduced with aspirin treatment, which may suggest that the inflammatory lipid oxidation pathway is up-regulated in the MPS brain (Arfi *et al.* 2011).

*N*B-DNJ treatment may also modulate MPS IIIA membrane lipid profiles and PUFA oxidation given its potential dual action: inhibition of GSL synthesis and reduction of inflammation (Platt *et al.* 1997a; Jeyakumar *et al.* 2003; Elliot-Smith *et al.* 2008; Boomkamp *et al.* 2010). Although *N*B-DNJ appears to reduce inflammatory cytokine expression in other LSD mouse models, it is not yet known whether it has the same effect in MPS IIIA mouse brain (Platt *et al.* 1997a; Jeyakumar *et al.* 2003; Elliot-Smith *et al.* 2008; Boomkamp *et al.* 2010).

This study will contribute to the current model of MPS neurodegeneration by determining whether alterations in membrane lipids and inflammatory mediators exist in the MPS brain. Thus, levels of simple, phospho- and glyco-lipids, as well as phospholipid derived PUFAs, are investigated in the MPS IIIA and MPS VII mouse models (characterised in Chapter Three). As brain lipids have the potential to act as markers of MPS brain disease and be affected by treatment, membrane lipids and inflammatory lipid and cytokine profiles of MPS IIIA mice, treated both early and late, with *N*B-DNJ (Chapter Four) have also been investigated.

5.2 MPS brain membrane lipids

The homeostasis of membrane lipids is important for normal neuronal function, such as membrane trafficking and axonal integrity (Pettegrew *et al.* 2001; Molander-Melin *et al.* 2005; Esposito *et al.* 2008; Wheeler *et al.* 2008; Martin *et al.* 2010; Cheng *et al.* 2011; Fabelo *et al.* 2011; Chan *et al.* 2012). In order to identify whether levels of these lipids are altered in the MPS brain or with *N*B-DNJ treatment, an analysis of organic lipids using TLC was performed on six month old normal, MPS VII, MPS IIIA and both early and late *N*B-DNJ treated MPS IIIA brain lipid extracts (Chapter 2.3.1.1). Simple, phospho- and glyco- lipids were separated using different solvent systems and visualised using stains specific for each lipid type (Chapter 2.3.1.2). No change in levels of any lipid was observed between normal, MPS VII or MPS IIIA brain samples (Figure 5.1). In addition, brain lipid profiles did not change with early or late *N*B-DNJ treatment of MPS IIIA mice (Figure 5.1).

5.3 MPS brain inflammatory mediators

Given the involvement of inflammation in MPS brain disease, levels of inflammatory lipids were measured in MPS IIIA and MPS VII mouse brain (DiRosario *et al.* 2009; Arfi *et al.* 2011). In addition, PUFAs, inflammatory gene expression and astroglial activation were determined in MPS IIIA mice, treated either early or late with *N*B-DNJ, in order to determine whether treatment had an effect on MPS IIIA brain inflammation.

5.3.1 Inflammatory lipids in the MPS brain

Brain PUFAs and their metabolites were quantified in normal, MPS VII, MPS IIIA and both early- and late- *N*B-DNJ treated MPS IIIA mouse organic lipid samples extracted using the Folch method (Chapter 2.3.1.1). Measurement of PUFAs and their derivatives (Table 5.1) was performed by LC-ESI MS/MS detection and quantification against deuterated standards (Chapter 2.3.1.4).

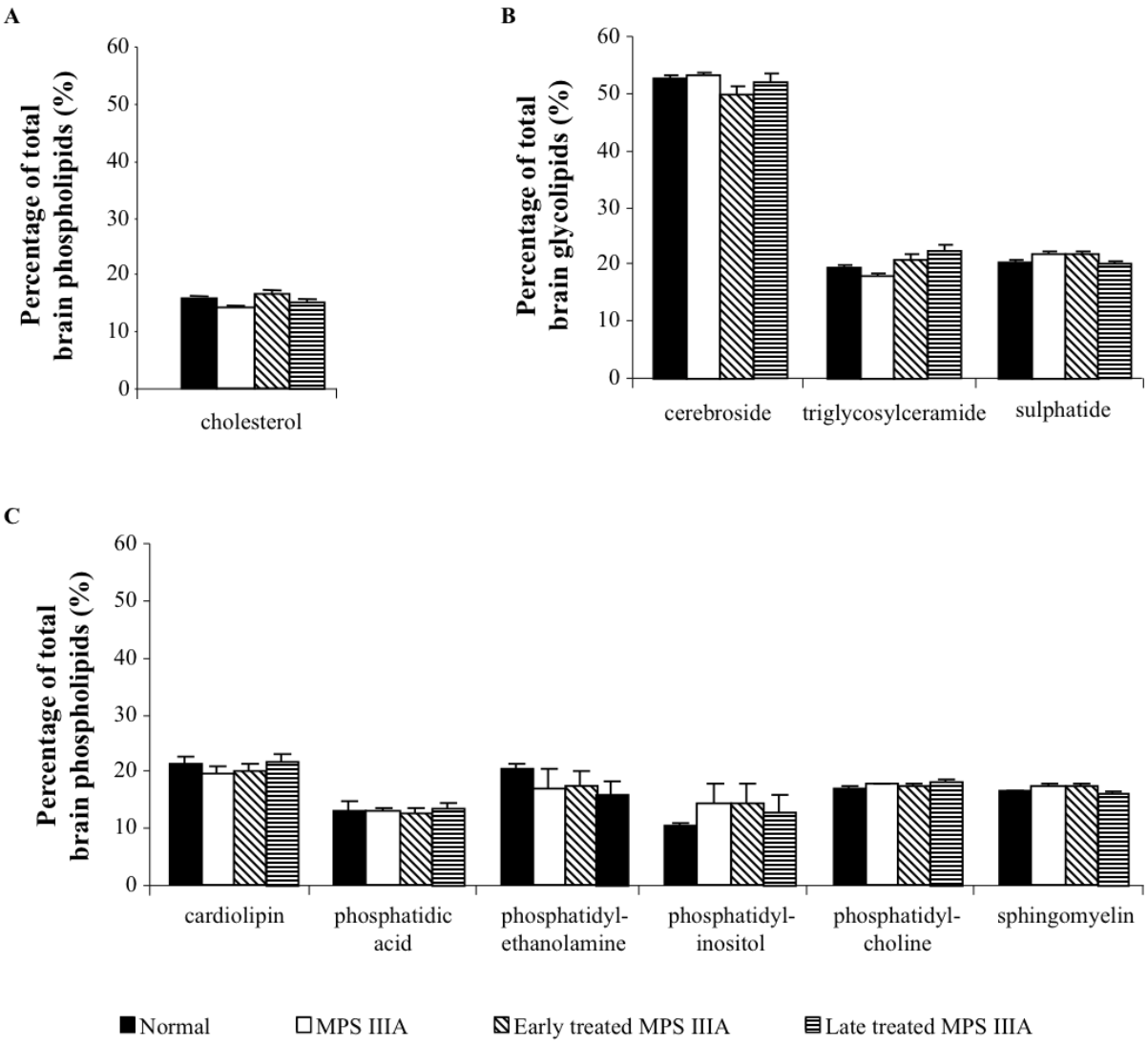

Figure 5.1: Brain lipid profiles.
Organic phase lipids extracted from the brains of six-month-old normal, MPS IIIA, MPS VII and both early and late *N*B-DNJ treated MPS IIIA mice using the Folch method were separated by high performance TLC and visualised with stains specific to each lipid type. Densitometry was used to determine simple (A), glyco- (B) and phospho-lipid (C) levels as a percentage of total phospholipids (A and C) or glycolipids (B) and expressed as mean ± SEM of n=3.

A

Promotion of inflammation	
PUFA	**Derivatives**
arachidonic acid (AA)	13(s)-hydroxyoctadecadienoic acid (13(s)-HODE)
	12(s)-hydroxyeicosatetraenoic acid (12(s)-HETE)
	15(s)-hydroxyeicosatetraenoic acid (15(s)-HETE)
	prostoglandin D2 (PGD2)
	prostoglandin E2 (PGE2)
	prostoglandin F2 alpha (PGF2α)
	thromboxane B2 (TXB2)
	6-keto-prostogmandin F1 alpha (6-keto-PGF1α)

B

Resolution of inflammation	
PUFA	**Derivatives**
docosahexaenoic acid (DHA)	resolvin D1 alpha (RVD1α)
eicosapentaenoic acid (EPA)	-

Table 5.1: PUFAs and their derivatives.
A series of PUFAs and their derivatives were measured in normal, MPS VII, MPS IIIA and both early and late *N*B-DNJ treated MPS IIIA mouse brain lipid extracts by LC-ESI MS/MS. These have roles in either the promotion (**A**) or resolution (**B**) of inflammation.

AA/DHA and AA/EPA PUFA ratios did not differ with genotype or with age (Figure 5.2). In addition, the time-course of PUFA derivative levels did not demonstrate any significant changes in MPS VII and MPS IIIA brains compared with normal, apart from an increase in 15(s)-HETE in untreated MPS IIIA at 12 months of age (44% greater than normal; one-way ANOVA, Tukey's HSD; Figure 5.3).

While there was little difference in levels of PUFAs and their derivatives between genotypes or with age, their levels were changed with *N*B-DNJ treatment. Analysis of brain lipid metabolites in six month old early and late *N*B-DNJ treated MPS IIIA mice demonstrated some significant differences between these, untreated MPS IIIA and normal controls. AA/DHA was significantly greater in early-treated than in untreated MPS IIIA brains (34% increase; one-way ANOVA, Tukey's HSD), but did not differ from normal and late-treated brain (Figure 5.4A).

Levels of TXB2, 6-keto-PGF1 alpha and RVD1α in brain were all greater in early-treated mice than in either MPS IIIA (by 299%, 66% and 505% respectively; one-way ANOVA, Tukey's HSD) or normal mice (by 349%, 139% and 475% respectively; one-way ANOVA, Tukey's HSD; Figure 5.4B). Increases in these same three metabolites were observed in late-treated mice, however this was only significant for RVD1α, which was 404% and 379% greater than untreated MPS IIIA and normal respectively (one-way ANOVA, Tukey's HSD; Figure 5.4B). Some reductions in metabolite levels were also observed with early- and late-treatment for 12(s)-HETE, which was significantly lower than in both untreated MPS IIIA and normal brain levels (early treatment decreased by 65% and 67% respectively and late treatment decreased by 76% and 78% respectively; one-way ANOVA, Tukey's HSD; Figure 5.4B).

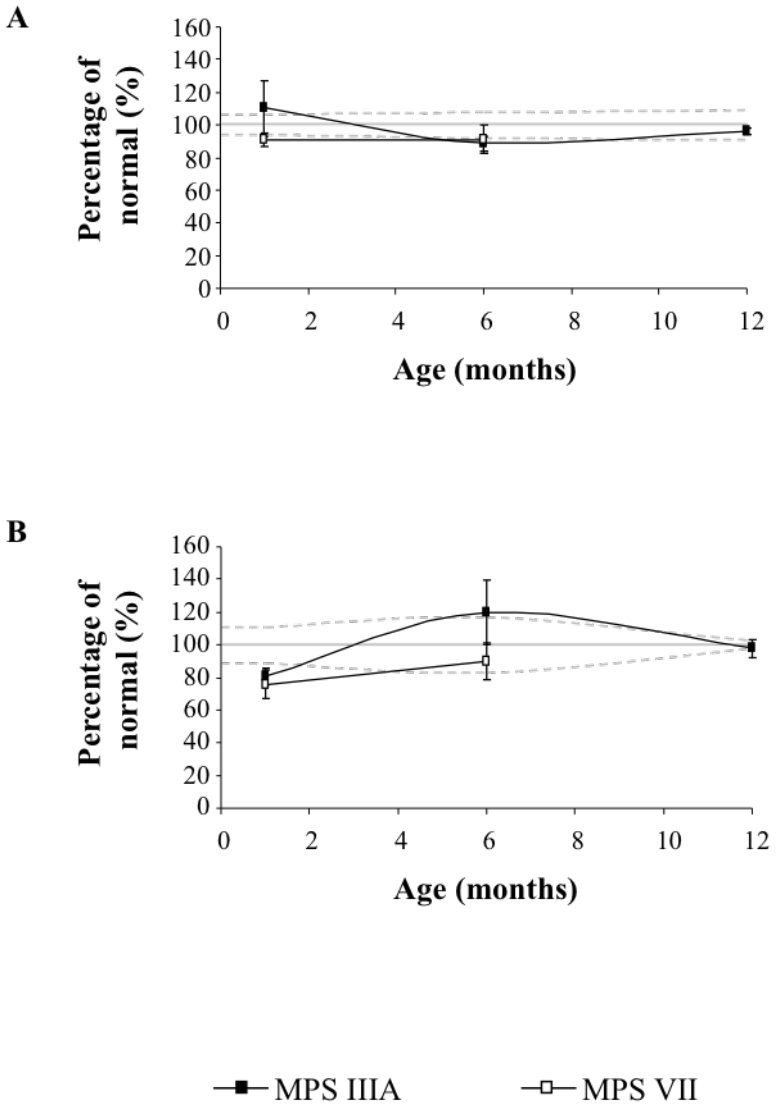

Figure 5.2: Brain PUFA ratios.
Organic lipids were extracted from the brains of normal, MPS IIIA and MPS VII mice using the Folch method and PUFAs were measured by LC ESI-MS/MS. PUFA measurements were expressed as AA/DHA (**A**) or AA/EPA (**B**) and results of n=4-6 presented as mean percentage of normal ± SEM. Grey lines indicate normal ± SEM.

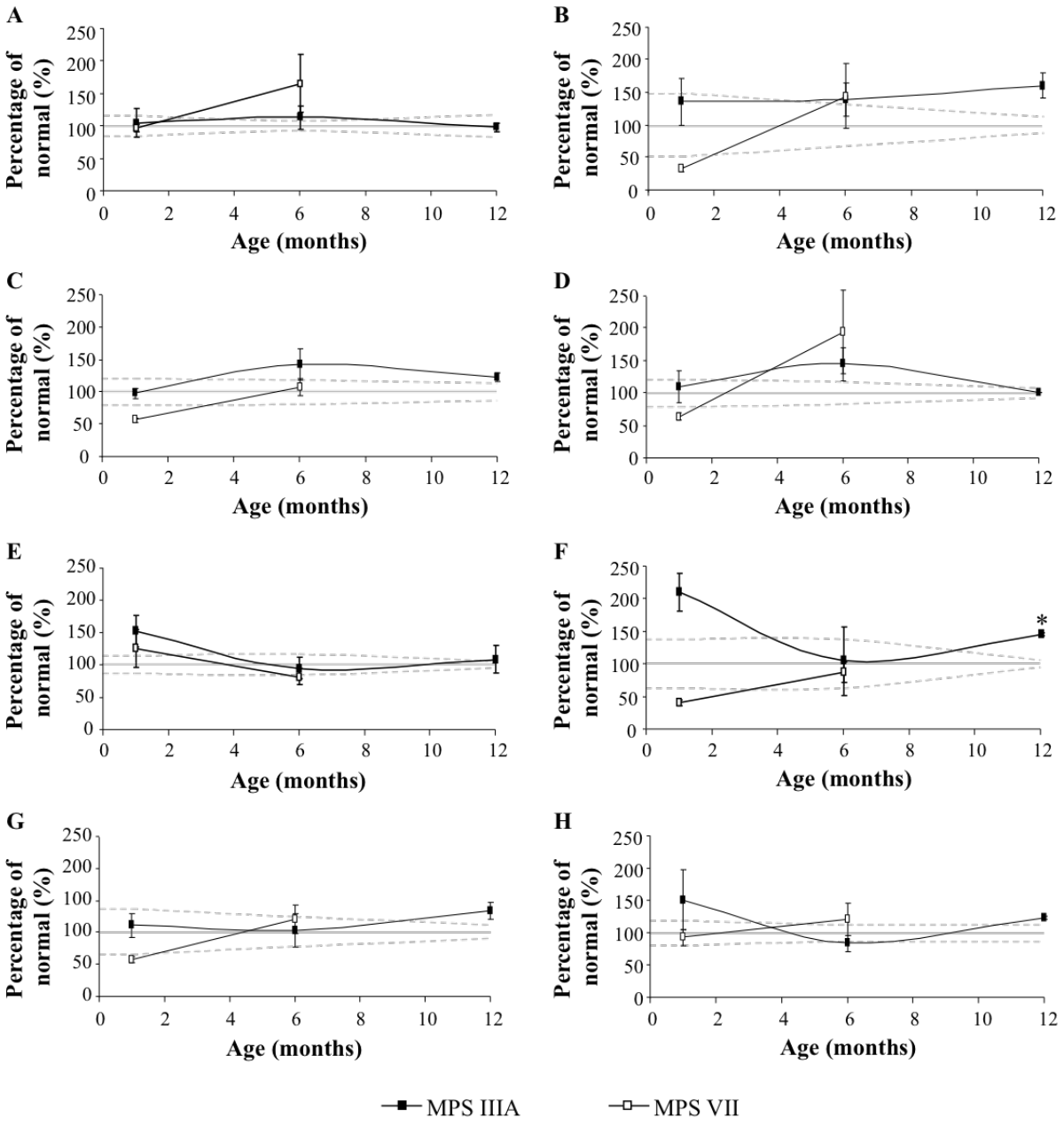

Figure 5.3: Brain PUFA metabolites ratios.
PUFAs and their derivatives: TXB2 (**A**), PGD2/E2 (**B**), PGF2α (**C**), 6-keto-PGF1α (**D**), 12(s)-HETE (**E**), 15(s)-HETE (**F**), 13(s)-HODE (**G**) and RVD1α (**H**) were measured by LC ESI-MS/MS in Folch extracted normal, MPS IIIA and MPS VII brain lipid samples. Metabolite levels were expressed as a ratio with the parent PUFA (DHA for RVD1α and AA for all others) and presented as a mean percentage of normal (n=4-6) ± SEM. * Significantly different from normal, $p<0.05$ (two-way ANOVA, Tukey's HSD). Grey lines indicate normal ± SEM.

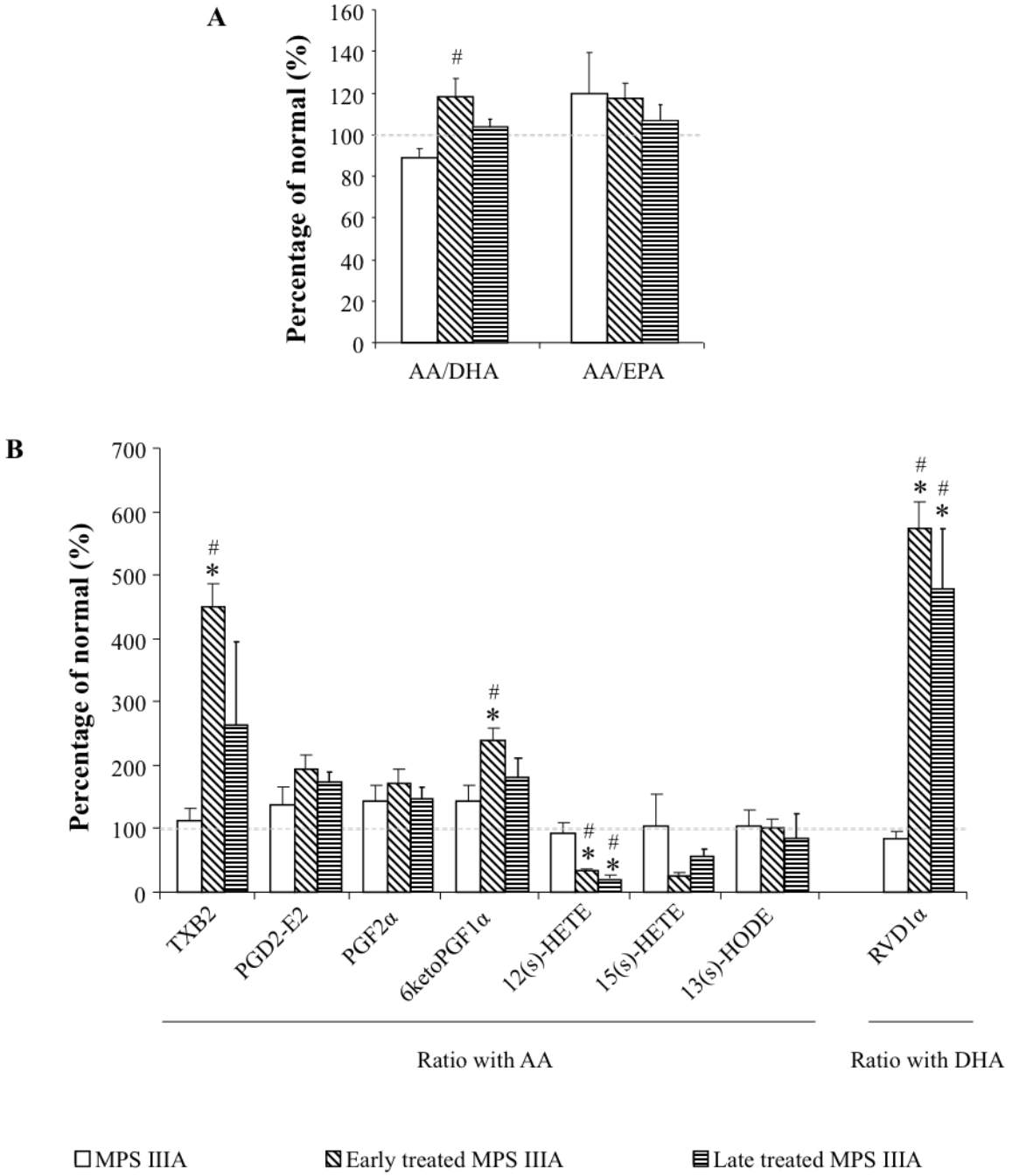

Figure 5.4: Brain PUFAs and their metabolites after *N*B-DNJ treatment.
Organic lipids were extracted from the brains of six-month-old normal, MPS IIIA and both early and late *N*B-DNJ treated MPS mice using the Folch method. PUFAs and their derivatives were measured by LC ESI-MS/MS. PUFA measurements were expressed as AA/DHA or AA/EPA (**A**), derivatives were expressed as a ratio with the parent PUFA (**B**) and results of n=4-6 were presented as mean percentage of normal ± SEM. Significant differences from normal (*) or untreated MPS IIIA (#) are indicated, $p<0.05$ (one-way ANOVA, Tukey's HSD).

5.3.2 Inflammatory gene expression and astroglial activation in the MPS brain

Inflammatory gene expression and astroglial activation have been previously described in MPS brain disease. For the first time, we investigate the effect of *N*B-DNJ treatment on MPS IIIA brain inflammation. cDNA was generated form six month old normal, MPS IIIA and both early and late treated MPS IIIA mouse brain and the expression levels of a number of inflammatory genes measured by real-time PCR (Chapter 2.3.3.2).

There was an overall increase in inflammatory gene expression in the MPS IIIA brain, compared with normal (Figure 5.5). This increase was significant for *Ccl3, Gfap*, *Cd68, Il1β* and *Tgfb1*, which were 5.1, 5.5, 5.8, 3.9 and 1.5 fold greater than normal, respectively (one-way ANOVA, Tukey's HSD; Figure 5.5). In general there was a suppression of inflammation with *N*B-DNJ treatment, which in many cases, was greater with early (longer term) than with late treatment. *Ccl3* expression in MPS IIIA brain decreased significantly with early (by 2.9 fold) but not late *N*B-DNJ treatment (one-way ANOVA, Tukey's HSD; Figure 5.5). *Gfap* expression in MPS IIIA brain was reduced with early and late treatment by 2.7 and 2.3 fold, respectively (one-way ANOVA, Tukey's HSD; Figure 5.5). *Il1β* expression in MPS IIIA brain was decreased significantly with both early and late *N*B-DNJ treatment (by 1.6 and 1.3 fold respectively; one-way ANOVA, Tukey's HSD; Figure 5.5). *Tgfb1* expression in MPS IIIA brain was reduced with both early and late *N*B-DNJ treatment, by 0.9 and 0.4 fold respectively (one-way ANOVA, Tukey's HSD; Figure 5.5). *Cd68* expression in MPS IIIA brain was not affected by either early or late treatment (one-way ANOVA, Tukey's HSD; Figure 5.5).

Astroglial activation was demonstrated with GFAP-targeted immunohistochemistry on formalin-fixed, frozen, sagittal sections of six month old normal, MPS IIIA and both early- and late- *N*B-DNJ treated MPS IIIA mouse brain (Chapter 2.3.3.1). Very little GFAP staining was observed on normal brain sections (Figure 5.6). Untreated, early- and late- treated MPS

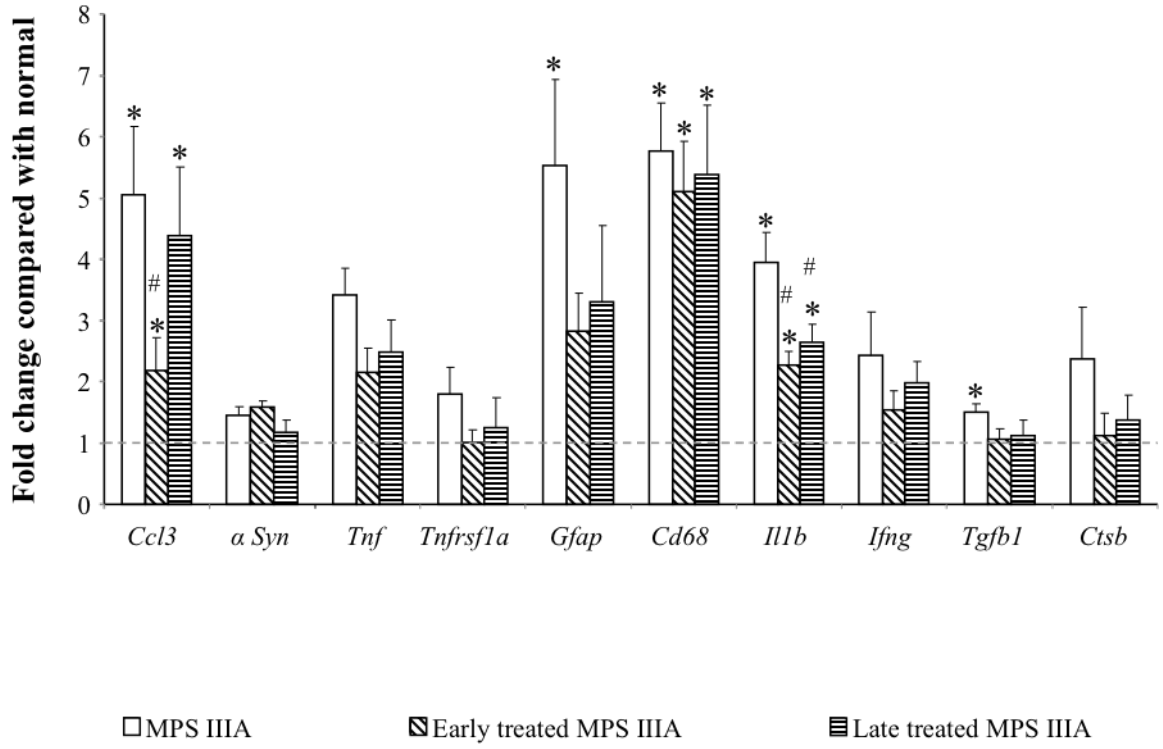

Figure 5.5: Inflammatory gene expression with *N*B-DNJ treatment.
Total RNA was extracted from normal, MPS IIIA and both early and late treated MPS IIIA mouse brain tissue and used to make cDNA. Real time PCR was used to measure *Ccl3*, *a Syn*, *Tnf*, *Tnfrsf1α*, *Gfap*, *Cd68*, *Il1β*, *Ifnγ*, *Tgfβ1* and *Ctsb* expression, which was normalised to *Cypα* expression levels. The fold change as compared to expression in normal brain was calculated and expressed as mean ± SEM of n=6. Significant differences from normal (*) or untreated MPS IIIA ($^{\#}$) are indicated, $p<0.05$ (two-way ANOVA, Tukey's HSD).

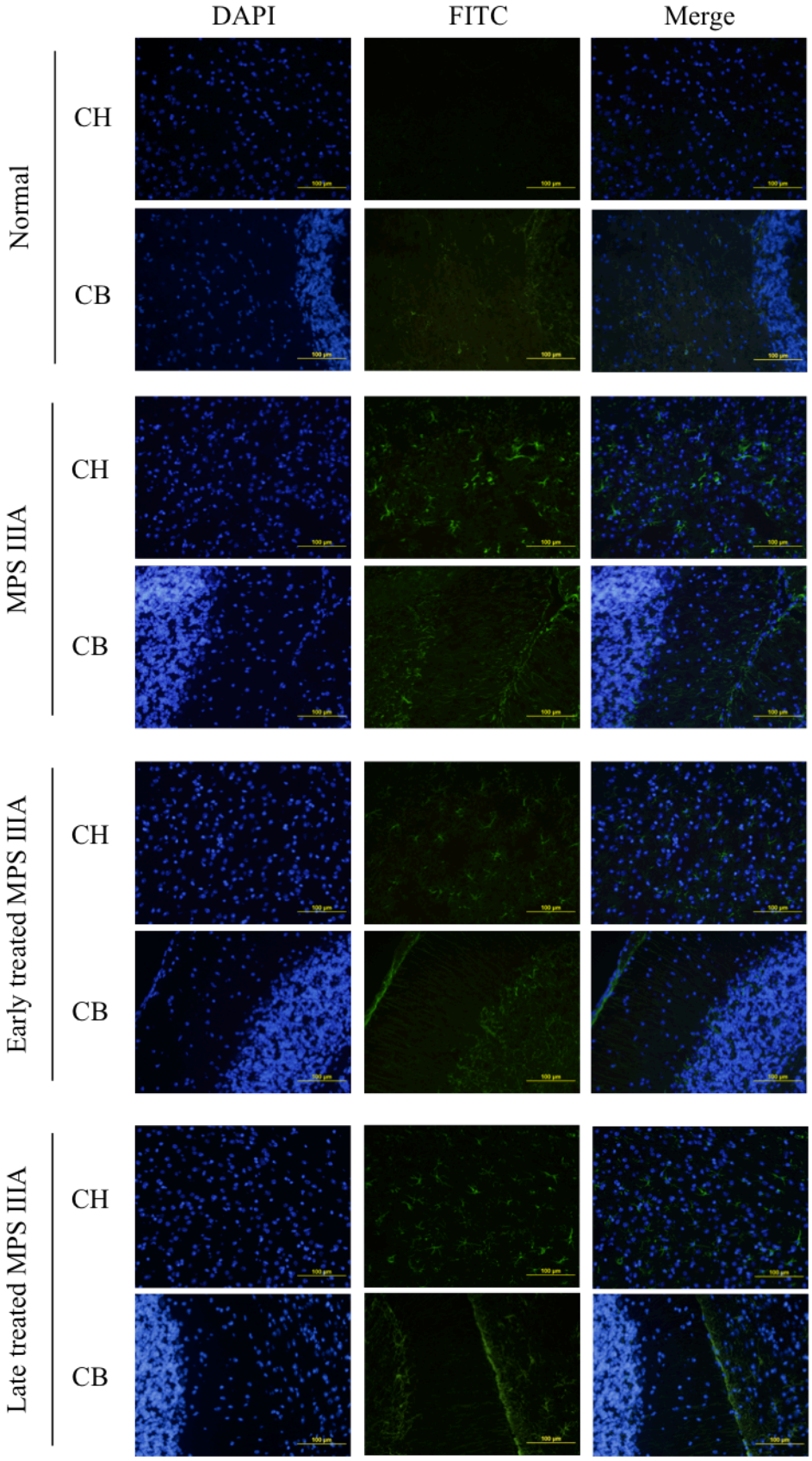

Figure 5.6: GFAP localisation with *N*B-DNJ treatment.
GFAP localisation was determined by immunohistochemistry on formalin fixed frozen sections of normal, MPS IIIA and both early and late treated MPS IIIA mouse brain using a primary antibody specific to GFAP and a FITC conjugated secondary antibody. Nuclei were stained with DAPI. Images of the cerebellum (CB) and the cerebral hemisphere (CH) are shown, at a magnification of 40x.

IIIA brains all stained positively for GFAP in both the cerebellum and cerebral hemisphere (Figure 5.6). There appeared to be a greater amount of GFAP staining in the cerebral hemisphere of untreated MPS IIIA brain, compared with both early- and late- treatment groups, which was consistent with *Gfap* expression levels. GFAP staining of the cerebellum appeared relatively similar between MPS IIIA mice with and without treatment (Figure 5.6).

5.4 Discussion

An investigation into murine MPS IIIA and MPS VII brain membrane lipids and inflammatory mediators was conducted to determine whether any alterations in these were associated with MPS neurodegeneration. This is important for the development of an understanding of progressive MPS brain disease, to provide a baseline against which treatments can be assessed and to suggest new therapeutic options.

TLC profiles of the major lipid classes: neutral, phospho- and glyco- lipids, were determined in brain samples from six month old mice, at which time alterations in GAG, ganglioside and behaviour in both the MPS IIIA and MPS VII mouse models were significant (Chapter Three). Gangliosides are closely associated with other lipids in membrane rafts and a dramatic change in one species in these structures can have a significant effect on other components (Ohmi *et al.* 2009b; Sanchez-Wandelmer *et al.* 2009; Singh *et al.* 2010; Ohmi *et al.* 2011). However, this study has demonstrated that no other global changes in brain lipid levels occur in these MPSs. This is consistent with a recent report demonstrating that MPS I mouse brain neutral, phospho- and glyco- lipid levels do not differ from normal (Heinecke *et al.* 2011).

Cholesterol is a simple lipid present in high levels in lipid rafts and an additional secondary storage product in the MPS brain (McGlynn *et al.* 2004; Sanchez-Wandelmer *et al.* 2009; Ohmi *et al.* 2011). Histological studies have demonstrated the abnormal staining of

cholesterol in the perikarya of murine MPS I, IIIA, IIIB and VII neurons (McGlynn *et al.* 2004). Importantly, this study demonstrates that there is no change in overall brain cholesterol levels in the six month old MPS IIIA and MPS VII mouse brain and supports the contention that it is an alteration in cholesterol distribution that accounts for the histological changes in cholesterol staining observed in other studies (McGlynn *et al.* 2004). This is consistent with the findings in the neurodegenerative cholesterol trafficking disorder NPC where overall brain cholesterol levels have also been shown to remain normal, despite increased histological staining of cholesterol in neuronal cell bodies (Vanier 1999; Karten *et al.* 2002; Walkley and Vanier 2009). It is possible that in the MPS brain cholesterol becomes 'trapped' within the cell as gangliosides are internalised, due to the close association of these two lipid types in lipid rafts (Glaros *et al.* 2005; Sanchez-Wandelmer *et al.* 2009; Singh *et al.* 2010). This is supported by the observation that neuronal cholesterol storage co-localises with that of G_{M2} and G_{M3} in the MPSs (McGlynn *et al.* 2004; Glaros *et al.* 2005; Sanchez-Wandelmer *et al.* 2009; Singh *et al.* 2010).

Profiles of phospholipid and glycolipid membrane components were also observed using TLC. Again, no changes were observed between groups. This included SM, which is a secondary storage product in the cholesterol trafficking disorder, NPC (Lloyd-Evans *et al.* 2008). NPC is otherwise similar to the MPSs, in that they both have an altered distribution of cholesterol and secondary storage of gangliosides (Zervas *et al.* 2001a; McGlynn *et al.* 2004).

Brain membrane lipid TLC profiles from early- and late- *N*B-DNJ treated MPS IIIA mice were also unchanged. *N*B-DNJ treatment decreases ganglioside levels in the short term (Chapter Four); however, decreasing the synthesis of gangliosides did not affect levels of other glycolipids. Nor did decreasing MPS IIIA ganglioside synthesis have a flow on effect on other membrane lipids. This is a positive outcome, given that the knock out of G_{M2}/ G_{D2} synthase and G_{D3} synthase in mice can disrupt lipid rafts and decrease phospholipid and

cholesterol components (Ohmi *et al.* 2009b; Ohmi *et al.* 2011). It is likely that these effects were not observed as *N*B-DNJ treatment does not completely suppress ganglioside production.

In addition to the analysis of membrane lipids, inflammatory lipid levels were also assessed in MPS VII, IIIA and both early- and late- *N*B-DNJ treated MPS IIIA mouse brains. Inflammation is a significant component of MPS brain disease and has been demonstrated to contribute to behavioural deficits (Richard *et al.* 2008; DiRosario *et al.* 2009; Arfi *et al.* 2011). The involvement of inflammatory lipids in the neurodegenerative process has been assessed for the first time in this thesis and could provide insight into the mechanisms behind brain inflammation in the MPSs. This is important for the development of a model for understanding the processes leading to brain dysfunction, required for the assessment of therapeutic outcomes at the cellular level and to provide new therapeutic options.

Mass spectrometry was used to measure brain PUFAs, and their derivatives (listed in Table 5.1). There is indirect evidence from the treatment of MPS IIIA mice with aspirin, which acts by preventing the production of pro-inflammatory lipids from AA, that pro-inflammatory metabolites are raised in the MPS brain (Arfi *et al.* 2011). In addition, inflammatory molecules such as the prostoglandins (PGs) are associated with brain disease in other neurodegenerative disorders such as Alzheimer's disease and multiple sclerosis (Greco *et al.* 1999; Kotilinek *et al.* 2008; Schulte *et al.* 2009). However, PUFA metabolites quantified in brains from MPS IIIA and MPS VII mice in this chapter demonstrated few diversions from normal levels.

No change in the AA/DHA and AA/EPA ratios was demonstrated in MPS IIIA or MPS VII brains compared with normal at any time point, indicating that the immune response is neither being directed towards inflammation nor its resolution. However, the measurement of AA and

DHA derivatives revealed one significant difference between groups; the pro-inflammatory AA derivative 15(s)-HETE (Table 5.1), which has been implicated in monocyte cytokine production, was significantly raised over normal in the MPS IIIA brain at 12 months of age (Prato *et al.* 2008). However, this is not correlated with increased brain inflammatory gene expression and microglial activation (Ohmi *et al.* 2003; Richard *et al.* 2008; Arfi *et al.* 2011) or behavioural deficits (Chapter Three), which occur much earlier. Thus, inflammation in the MPS brain is not likely to be PUFA- mediated. AA oxidation may not be the reason for the effect of aspirin on MPS IIIA inflammatory gene expression described by Arfi *et al*. (2011).

While few differences in lipid metabolite levels were seen between normal and MPS IIIA brain, *iv N*B-DNJ treatment of MPS IIIA mice generated significant changes. Changes in PUFAs and their derivatives appeared to be similar in early-treated and late-treated brains, but were generally greater with early treatment. This suggests that longer treatment with *N*B-DNJ has a bigger impact on fatty acid oxidation. However, it is not clear whether *N*B-DNJ directs lipid metabolites towards inflammation or its resolution, as inflammatory AA derivatives are both increased (TXB2 and 6-keto-PGF2α) and decreased (12(s)-HETE) and anti-inflammatory DHA derivatives are increased (RVD1α). Little is known about the role of 12(s)-HETE, however, TXB2 and 6-keto-PGF2α have previously been reported as present during inflammatory events such as after the infusion of bacterial lipopolysaccharide (Basselin *et al.* 2011). RVD1α has been shown to prevent TNFα-induced IL-β production and leukocyte infiltration (Serhan *et al.* 2002; Hong *et al.* 2003; Marcheselli *et al.* 2003). Thus an increase in RVD1α with *N*B-DNJ treatment could suppress MPS brain inflammation (Villani *et al.* 2007; Ausseil *et al.* 2008; DiRosario *et al.* 2009).

It is important to note that not all metabolites generated from AA have inflammatory properties: PGE2 for example can act either to promote or resolve inflammation and has been observed to improve inflammation through the suppression of migroglial activation *in vitro* in

Sandhoff disease (Kawashita *et al.* 2011). In contrast, both AA and PGE2 are raised in NPC cells and are associated with cytotoxicity (Nakamura *et al.* 2011). Data presented in this chapter did demonstrate an increase in PGD2/PGE2 with *N*B-DNJ treatment, however this increase was not significant.

Further study into the effect of *N*B-DNJ on the oxidation of PUFAs and the role of PUFA metabolites on MPS brain degeneration is required in order to better understand this process. The investigation of inflammatory gene expression and astroglial activation supports the contention that brain inflammation is reduced with *N*B-DNJ treatment. Both early and late treatment gave similar results, with early treatment producing some greater changes than late treatment. This demonstrates a difference in the anti-inflammatory effects of short and long term *N*B-DNJ treatment, as was observed in the PUFA analysis. *Cd68*, expressed by monocytes, granulocytes and activated T-cells, was the only gene to be raised in the MPS IIIA brain and to be unchanged by either early or late *N*B-DNJ treatment, although *N*B-DNJ treatment has been demonstrated previously to decrease CD68 staining in the NPC mouse thalamus and Sandhoff mouse cerebellum and brainstem (Ashe *et al.* 2011; Nietupski *et al.* 2012). The reason for these differences may have been that the analysis of gene expression in this chapter was of a central, sagittal piece of brain tissue and did not differentiate between regions.

Given the significant increase in MPS IIIA brain *Gfap* expression and its reduction with both early and late treatment, GFAP staining of sagittal brain sections was also conducted. This was consistent with gene expression, demonstrating reduced GFAP staining in the cerebral hemisphere in brains from treated mice. Reduced brain GFAP staining with *N*B-DNJ treatment has also been shown previously in Sandhoff mice (Ashe *et al.* 2011). This again supports an anti-inflammatory role for *N*B-DNJ, in addition to its inhibition of ceramide glucosyltransferase (Chapter Four).

Together, the analysis of membrane lipids and inflammatory mediators has demonstrated that these are largely unchanged in the MPS brain, compared with normal brains. This does not rule out a redistribution of membrane lipids, as is believed to occur in the case of cholesterol. Furthermore, inflammatory lipids may be involved in later stage brain pathology in response to a threshold of brain damage, given the observed increase in 15(s)-HETE in 12 month old MPS IIIA mice. However, with *N*B-DNJ treatment, levels of a number of inflammatory lipids were altered and inflammatory gene expression and astroglial activation were reduced. This supports the assertion that *N*B-DNJ treatment reduces brain inflammation. Thus, the anti-inflammatory role of *N*B-DNJ may have contributed to the behavioural improvements observed with treatment of MPS IIIA mice in Chapter Four.

Chapter Six: Discussion

6.1 MPS brain biochemistry and behaviour

The biochemistry of the MPS brain and its relationship with behaviour is not yet fully understood, however, the study of MPS animal models continues to provide insight into the processes leading to CNS degeneration. Through the characterisation of murine models of MPS IIIA and MPS VII, and the manipulation of MPS IIIA GSL metabolism, this thesis has contributed to our understanding of the sequence of storage events that precede MPS brain dysfunction.

6.1.1 HS accumulation leads to secondary ganglioside accumulation and a redistribution of cholesterol in the MPS brain

The build-up of storage material in the MPS brain occurs in three stages: (1) HS levels increase due to defective lysosomal degradation; (2) G_{M2} accumulation commences; (3) G_{M3} accumulation is initiated (Chapter Three; Figure 6.1). The greater the level of HS storage in the MPS brain, the greater the level of G_{M2} and G_{M3} accumulation (Chapter Three). Differences in the rate and time-line of accumulation (Chapter Three), as well as the localisation (McGlynn *et al.* 2004; Dawson *et al.* 2012) of the three storage products, suggests that undegraded HS fragments may not be directly responsible for G_{M2} and G_{M3} storage. Furthermore, secondary brain ganglioside accumulation is also present in LSDs that do not store HS, including NPC, and in other neurodegenerative disorders, such as Alzheimer's disease (Kracun *et al.* 1992; Zervas *et al.* 2001a; Molander-Melin *et al.* 2005). Rather than having a direct effect on secondary storage, HS storage is likely to disrupt the normal function of the endosomal-lysosomal system, contributing to the accumulation of G_{M2} and G_{M3} in endosomal structures as well as exacerbating the storage of HS itself (Figure 6.1) (Kiselyov *et al.* 2007; Settembre *et al.* 2007; Settembre *et al.* 2008b).

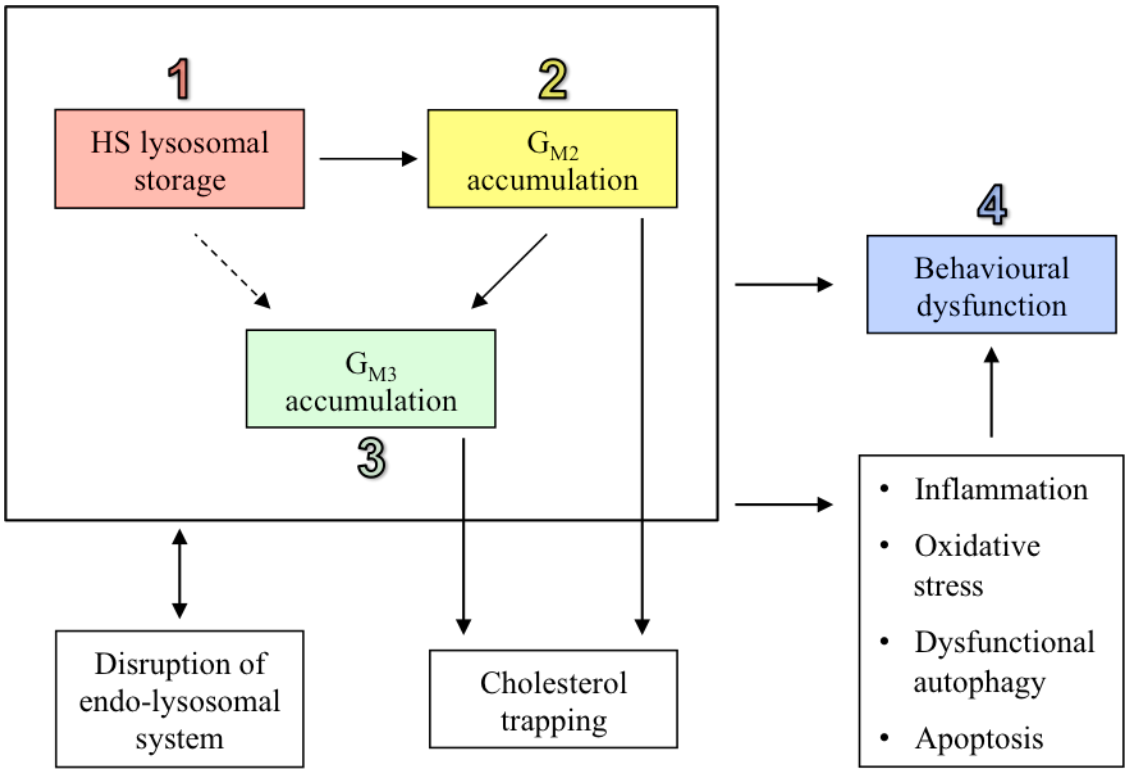

Figure 6.1: The sequence of events that lead to MPS behavioural deficits.
This study has used mouse models of MPS IIIA and MPS VII to generate a time-line of storage and behavioural dysfunction. (1) HS is stored within the lysosomes due to a deficiency in its degradation. (2) G_{M2} accumulation closely follows HS storage. (3) G_{M3} begins to accumulate after HS and G_{M2}, thus either HS or G_{M2} may trigger G_{M3} storage. (4) Behavioural dysfunction occurs after the storage of HS, G_{M2} and G_{M3}. It is not known which storage materials, either alone or in combination, contribute to a loss of brain function. Other studies have implicated many other processes in the exacerbation of storage and the development of behavioural deficits, including disruption of the endo-lysosomal system, cholesterol trapping, oxidative stress, dysfunctional autophagy, apoptosis and inflammation (Di Domenico *et al.* 2005; Glaros *et al.* 2005; Villani *et al.* 2007; Richard *et al.* 2008; Settembre *et al.* 2008b; DiRosario *et al.* 2009; Arfi *et al.* 2011).

It is likely that G_{M2} storage influences G_{M3} levels given that a rise in G_{M3} levels is also observed in the G_{M2} gangliosidoses (Rosengren *et al.* 1987; Kolter *et al.* 2002); however, it is not known how this occurs or whether HS also plays a role in G_{M3} accumulation (Figure 6.1). G_{M2} accumulates early in MPS neuro-degeneration, however, G_{M3} accumulates later and to greater levels (Chapter Three; Figure 6.1). This suggests that the triggers for G_{M2} and G_{M3} storage are separate, which is consistent with a previous study demonstrating that the two ganglioside species do not co-localise (McGlynn *et al.* 2004).

G_{M2} and G_{M3} are normally found in lipid rafts, where they are closely associated with a heterogeneous mix of other membrane lipids. The majority of membrane lipids, including cholesterol, do not change in their overall levels in the MPS brain (Chapter Five); however levels of both G_{M2} and G_{M3} increase significantly (Chapters Three and Five). Not only are overall brain G_{M2} and G_{M3} levels raised in the MPS brain (Chapter Three), but they have also been demonstrated to be significantly increased in lipid rafts in the seven month old MPS IIIA mouse brain (Dawson *et al.* 2012). The initial change in G_{M2} levels in lipid rafts can affect levels of other raft components, such as G_{M3}, and may be the mechanism through which G_{M3} accumulates in the MPS brain (Ohmi *et al.* 2009a; Ohmi *et al.* 2009b; Sanchez-Wandelmer *et al.* 2009; Singh *et al.* 2010).

The increase in overall levels of the two ganglioside species (Chapter Three) also suggests a shift in ganglioside synthesis and/or degradation in MPS neurodegenerative disease resulting in the accumulation of G_{M2} and G_{M3}. As well as being associated in lipid rafts, G_{M2} and G_{M3} are closely related in their positions in the GSL metabolic pathway (Figure 1.1). Thus, the observation in Chapter Three that a build up of G_{M2} precedes a build up of G_{M3} may indicate a reduction in synthesis of G_{M2} from G_{M3}, or alternatively, an increase in G_{M2} degradation to G_{M3}.

Overall brain cholesterol levels on the other hand do not increase in MPS (Chapter Five), although there is an increase in intracellular cholesterol staining (Constantopoulos and Dekaban 1978; Constantopoulos *et al.* 1980; McGlynn *et al.* 2004). GSL accumulation can prevent cholesterol efflux, causing it to become 'trapped' within the cell (Glaros *et al.* 2005). This phenomenon may be involved in the MPS brain given that neuronal cholesterol storage co-localises with that of G_{M2} and G_{M3} in the MPSs (McGlynn *et al.* 2004).

In addition to cholesterol trapping, the storage of HS, G_{M2} and G_{M3} leads to a number of inter-related cell-damaging processes, including dysfunctional autophagy, inflammation, oxidative stress and apoptosis (Figure 6.1) (Di Domenico *et al.* 2005; Villani *et al.* 2007; Richard *et al.* 2008; Settembre *et al.* 2008b; DiRosario *et al.* 2009; Arfi *et al.* 2011). All of these factors are likely to contribute to the behavioural dysfunction typical of degenerative MPS brain disease (Figure 6.1).

6.1.2 Ganglioside accumulation is associated with MPS behavioural deficits

Maximal neuronal storage of HS, G_{M2} and G_{M3} associated with CNS degeneration precedes changes in behaviour (Chapter Three; Figure 6.1). Given the similarities in neuronal morphology and CNS degeneration between the MPSs and G_{M2} gangliosidoses, it has been hypothesised that gangliosides are the pathological culprits in MPS brain deterioration (Constantopoulos *et al.* 1976; Constantopoulos and Dekaban 1978; Constantopoulos *et al.* 1980; McGlynn *et al.* 2004). However, until now, there has been no way to separate ganglioside accumulation from GAG accumulation for the characterisation of their individual roles in MPS brain disease. Previously, all therapeutic trials for the MPSs including BMT, ERT, GT and SDT have targeted GAG storage and resulted in a decrease in both GAG and ganglioside storage (Frisella *et al.* 2001; Ellinwood *et al.* 2007; Malinowska *et al.* 2010; Vite *et al.* 2011; Wolf *et al.* 2011). For the first time, *N*B-DNJ treatment has been used to target gangliosides without affecting GAG levels (Chapter Four), allowing for the separation of

disease outcomes from these two storage materials. *N*B-DNJ treatment was trialled in the MPS IIIA mouse model, as brain G_{M2} and G_{M3} were significantly elevated and behavioural deficits could be attributed to brain dysfunction given the absence of skeletal disease in this model (Chapter Three).

With both early and late *N*B-DNJ treatment of MPS IIIA mice, the fear response was restored while GAG levels remained unchanged, indicating that GAG accumulation is not responsible for this behaviour. Ganglioside levels were initially decreased with treatment, as demonstrated in both the late *N*B-DNJ treatment group and the initial short term *iv N*B-DNJ trial (Chapter Four), suggesting that an early reduction in ganglioside levels could be responsible for improvements in the fear response. However, as both G_{M2} and G_{M3} were affected by *N*B-DNJ, this did not distinguish between the effects of the two ganglioside species.

This thesis has demonstrated that NB-DNJ treatment can improve MPS IIIA behavioural disease; however, it is not clear whether this is due to a reduction in ganglioside synthesis or modulation of the immune system. *N*B-DNJ treatment results in changes in levels of lipid metabolites involved in inflammation and its resolution, decreases inflammatory gene expression and reduces cerebellar astroglial activation in the MPS IIIA brain (Chapter Five). It is likely that the anti-inflammatory role of *N*B-DNJ contributes to the improvement in brain function observed in MPS IIIA treated mice in Chapter Four, given that the suppression of MPS brain inflammation by prednisolone alleviates behavioural deficits (DiRosario *et al.* 2009). These changes in inflammation with *N*B-DNJ treatment are not likely to be due to the drug's inhibition of GSL synthesis as the iminosugar *N*B-DGJ decreases GSL synthesis but does not have an immune-modulatory effect (Andersson *et al.* 2000; Elliot-Smith *et al.* 2008).

6.2 *N*B-DNJ for the treatment of MPS brain disease

*N*B-DNJ crosses the BBB, decreases GSL levels and has been demonstrated to be safe for human use in SDT trials for systemic (Gaucher disease type 1) and neurological disease (Gaucher disease type 3, Tay-Sachs disease, Sandhoff disease and NPC) in LSDs (Cox *et al.* 2003; Bembi *et al.* 2006; Patterson *et al.* 2007; Schiffmann *et al.* 2008; Maegawa *et al.* 2009; Shapiro *et al.* 2009). Moreover, *N*B-DNJ appears to be most effective for the treatment of NPC, which like MPSs has secondary G_{M2} storage (Patterson *et al.* 2007; Santos *et al.* 2008). These characteristics are important for a study aimed at improving MPS brain function, with a possibility for future human clinical use.

Since starting this study, a human trial of *N*B-DNJ was published by Guffon *et al.* (2011), in which 13 patients with MPS IIIA, B, C or D of two to ten years of age were treated with *N*B-DNJ over a 12-month period. All patients were symptomatic when treatment was initiated. *N*B-DNJ was found to be present in the CSF, although, no decrease in ganglioside levels was observed after six months of treatment, similar to findings in Chapter Four. However, unlike the findings from the treatment of MPS IIIA mice, no significant stabilisation or improvement of neurological symptoms was observed in the human trial (Guffon *et al.* 2011). A major factor that may have contributed to this finding was that all MPS III patients displayed motor trouble, speech impairment and behavioural disturbances at baseline, which may have been too far progressed for *N*B-DNJ treatment to be effective. In contrast, the positive behavioural outcomes with *N*B-DNJ treatment of MPS IIIA mice displayed in this thesis resulted from treatment initiated both prior to (early treatment) and after (late treatment) the appearance of the majority of behavioural deficits (Chapters Three and Four).

Furthermore, the inability to predict the course of human MPS III disease, coupled with the treatment of MPS III patients of varying ages, disease stages, and enzyme deficiencies would have made the assessment of changes in behaviour and cognitive function difficult (Young

and Harper 1983; Valstar *et al.* 2010b; Valstar *et al.* 2010c; Valstar *et al.* 2011). An extensive study in Holland characterising MPS III cognitive development also cited hyperactivity, distractibility, aggression, anxiety and visual impairment as factors that complicated accurate assessment (Valstar *et al.* 2011). In contrast, NPC patients who's disease progression respond positively to *N*B-DNJ have far fewer behavioural problems to complicate the assessment of treatment (Patterson *et al.* 2012).

The clinical trial of *N*B-DNJ for the treatment of MPS III was able to bypass animal trials, as the drug is known to be safe and was already in clinical use for Gaucher disease type 1; however, animal data is useful for the determination of the effect of *N*B-DNJ on MPS IIIA behaviour, where patient assessment is difficult (Cox *et al.* 2003; Valstar *et al.* 2011). In addition, a more extensive analysis of the GSL synthetic/ degradative pathway is possible and will be useful in future to determine why decreases in ganglioside accumulation with *N*B-DNJ treatment only occur in the short term.

Overall, it has been demonstrated that whether through the inhibition of GSL synthesis, modulation of the immune system or both, *N*B-DNJ is effective at improving the innate fear response in the MPS IIIA murine model. This suggests that it is worth revisiting *N*B-DNJ treatment of MPS patients with CNS involvement, despite poor treatment outcomes in the first clinical trail of this kind by Guffon *et al.* (2011). However, questions have arisen from this thesis, which require further investigation using the MPS IIIA animal model. The optimum time frame for treatment with *N*B-DNJ in maintaining decreased levels of brain gangliosides is yet to be determined. Further investigation into the effect of different treatment regimens in the MPS IIIA mouse model, including an 'on-again off-again' cycle, could potentially lead to better treatment outcomes for MPS patients.

Appendix 1: Materials list

Genotyping reagents

agarose	Progen Biosciences, Australia
bromophenol blue	BDH Chemicals Ltd., England
dNTPs	Roche, Australia
EDTA	Sigma-Aldrich, USA
ethidium bromide	Sigma-Aldrich, USA
Ficoll 400	Sigma-Aldrich, USA
lysis buffer	Viagen Biotech Inc., USA
magnesium chloride	Qiagen, Germany
MspA1 restriction enzyme	New England Biolabs Inc., USA
NEB4 buffer	New England Biolabs Inc., USA
NciI restriction enzyme	New England Biolabs Inc., USA
PCR buffer	Roche, Australia
primers	Geneworks, Australia
proteinase K	Viagen Biotech Inc., USA
Puc19/HpaII molecular weight marker	Geneworks, Australia
Q solution	Qiagen, Germany
SDS	Sigma-Aldrich, USA
Taq polymerase	Roche, Australia
tris-acetate	Sigma-Aldrich, USA

*N*B-DNJ treatment reagents

*N*B-DNJ (intravenously administered)	Sigma-Aldrich, USA
*N*B-DNJ (orally administered)	Actellion Pharmaceuticals Ltd., Switzerland

sodium chloride	Ajax Finechem Pty Ltd., Australia
powdered chow	Specialty Feeds Pty Ltd., Australia

Reagents for brain lipid extraction and analysis

12(s)-HETE-d8	Cayman Chemical Company, USA
6-keto-PGF1α-d4	Cayman Chemical Company, USA
AA-d8	Cayman Chemical Company, USA
acetic acid	Ajax Finechem Pty Ltd., Australia
acetonitrile	Ajax Finechem Pty Ltd., Australia
ammonium formate	Sigma-Aldrich, USA
Bond Elut C18 column	Varian Inc., USA
calcium chloride	Sigma-Aldrich, USA
ceramide trihexoside	Matreya LLC, USA
chloroform	Burdick and Jackson, USA
cholesterol	Matreya LLC, USA
cholesterol ester	Avanti Polar Lipids Inc., USA
DHA-d5	Cayman Chemical Company, USA
diethylether	Sigma-Aldrich, USA
EPA-d5	Cayman Chemical Company, USA
formic acid	Sigma-Aldrich, USA
free fatty acid	Sigma-Aldrich, USA
galactocerebroside	Avanti Polar Lipids Inc., USA
G_{M1}	Matreya LLC, USA
G_{M2}	Matreya LLC, USA
G_{M3}	Matreya LLC, USA
hexane	Sigma-Aldrich, USA
high performance TLC pre-coated silica	

gel plates	Merck, Germany
iso-PGF2α-d4	Cayman Chemical Company, USA
methanol	Burdick and Jackson, USA
N-octadecanoyl-d_3-monosialoganglioside 1	Matreya LLC, USA
N-palmitoyl-DL-dihydro	Avanti Polar Lipids Inc., USA
orcinol	Sigma-Aldrich, USA
PGD2-d4	Cayman Chemical Company, USA
PGE2-d4	Cayman Chemical Company, USA
PGF2α-d4	Cayman Chemical Company, USA
phosphatidylcholine	Matreya LLC, USA
phosphatidylethanolamine	Matreya LLC, USA
phosphomolybdic acid	Sigma-Aldrich, USA
potassium chloride	Ajax Finechem Pty Ltd., Australia
sphingomyelin	Matreya LLC, USA
sulphamide	ChemFine International Co. Ltd., China
sulphuric acid	Ajax Finechem Pty Ltd., Australia
tetrahydrofuran	Merck, Germany
TXB2-d4	Cayman Chemical Company, USA
triglyceride	Sigma-Aldrich, USA

Reagents for brain GAG extraction and analysis

3-phenylphenol	Sigma- Aldrich, USA
alcian blue	Sigma- Aldrich, USA
ammonium hydroxide	Sigma- Aldrich, USA
barium acetate	Sigma- Aldrich, USA
C6-NBD-ceramide fluorescent substrate	Invitrogen, USA
cellulose acetate sheets	Helena Laboratories, USA

cetylpyridinium chloride	Sigma- Aldrich, USA
chondroitinase ABC	Sigma- Aldrich, USA
citrate	Sigma-Aldrich, USA
CS	Sigma-Aldrich, USA
DEAE Sephacel	Amersham Biosciences, Sweden
Dowex 1 (X8; acetate form)	Biorad, USA
Dowex 50 (X8; H^+ form)	Sigma-Aldrich, USA
DS	Sigma-Aldrich, USA
ethanol	Chem Supply, Australia
glucuronic acid	Sigma-Aldrich, USA
HS	Sigma-Aldrich, USA
iduronic acid	Carbosynth Ltd., UK
L-α-phosphatidylcholine	Sigma-Aldrich, USA
lithium chloride	Sigma-Aldrich, USA
PD-10 column	GE healthcare, UK
silver nitrate	Calbiochem-Novabiochem Corporation, USA
sodium acetate	Merck, Germany
sodium hydroxide	Ajax Finechem Pty Ltd., Australia
sodium thiosulphate	Ajax Finechem Pty Ltd., Australia
tetraborate	Sigma-Aldrich, USA
trifluoroacetic acid	Sigma-Aldrich, USA
tris-HCl	Fisher Scientific, USA
Triton X-100	Sigma-Aldrich, USA
UDP-Glucose	Sigma-Aldrich, USA
zinc acetate	Sigma-Aldrich, USA

RNA extraction and real time PCR reagents

CYBR green real-time PCR master mix	Applied Biosystems
Qiagen QuantiTec reverse transcription kit	Qiagen, Germany
TRIzol	Invitrogen, USA

Immunohistochemistry reagents

anti-rabbit FITC conjugated	Silenus Labs, Australia
bovine serum albumen	Sigma-Aldrich, USA
neutral buffered formalin	ACE Chemical Company, Australia
OCT	Sakura Finetek USA Inc., USA
phosphate buffered saline	Sigma-Aldrich, USA
ProLong Gold antifade reagent with DAPI	Invitrogen, USA
rabbit anti-GFAP primary antibody	Dako, Denmark
superfrost plus microscope slides	Menzel-Glaser, Germany

References

Abramow-Newerly, W., Lipina, T., Abramow-Newerly, M., Kim, D., Bechard, A.R., Xie, G., Clapcote, S.J. and Roder, J.C. (2006). "Methods to rapidly and accurately screen a large number of ENU mutagenized mice for abnormal motor phenotypes." Amyotroph Lateral Scler **7**(2): 112-118.

Accardo, A., Pensiero, S., Ciana, G., Parentin, F. and Bembi, B. (2010). "Eye movement impairment recovery in a Gaucher patient treated with miglustat." Neurol Res Int **2010**: 358534.

Allen, J.A., Halverson-Tamboli, R.A. and Rasenick, M.M. (2007). "Lipid raft microdomains and neurotransmitter signalling." Nat Rev Neurosci **8**(2): 128-140.

Alvaro, F., Toogood, I., Fletcher, J.M., Clements, P., Rawling, T. and To, B. (1998). "Allogeneic CD34 selected peripheral stem cell transplant for Maroteaux-Lamy syndrome (mucopolysaccharidosis type VI): rapid haemopoietic and biochemical reconstitution." Bone marrow transplantation **21**(4): 419-421.

Amiri, M. and Naim, H.Y. (2012). "Miglustat-induced intestinal carbohydrate malabsorption is due to the inhibition of alpha-glucosidases, but not beta-galactosidases." Journal of inherited metabolic disease **35**(6): 949-954.

Andersson, U., Butters, T.D., Dwek, R.A. and Platt, F.M. (2000). "N-butyldeoxygalactonojirimycin: a more selective inhibitor of glycosphingolipid biosynthesis than N-butyldeoxynojirimycin, in vitro and in vivo." Biochem Pharmacol **59**(7): 821-829.

Arfi, A., Richard, M., Gandolphe, C., Bonnefont-Rousselot, D., Therond, P. and Scherman, D. (2011). "Neuroinflammatory and oxidative stress phenomena in MPS IIIA mouse model: The positive effect of long-term aspirin treatment." Mol Genet Metab.

Ashe, K.M., Bangari, D., Li, L., Cabrera-Salazar, M.A., Bercury, S.D., Nietupski, J.B., Cooper, C.G., Aerts, J.M., Lee, E.R., Copeland, D.P., Cheng, S.H., Scheule, R.K. and Marshall, J. (2011). "Iminosugar-based inhibitors of glucosylceramide synthase increase brain glycosphingolipids and survival in a mouse model of sandhoff disease." PloS one **6**(6): e21758.

Auclair, D., Hopwood, J.J., Lemontt, J.F., Chen, L. and Byers, S. (2007). "Long-term intra-articular administration of recombinant human N-acetylgalactosamine-4-sulfatase in feline mucopolysaccharidosis VI." Molecular genetics and metabolism **91**(4): 352-361.

Ausseil, J., Desmaris, N., Bigou, S., Attali, R., Corbineau, S., Vitry, S., Parent, M., Cheillan, D., Fuller, M., Maire, I., Vanier, M.T. and Heard, J.M. (2008). "Early neurodegeneration progresses independently of microglial activation by heparan sulfate in the brain of mucopolysaccharidosis IIIB mice." PLoS ONE **3**(5): e2296.

Avila, J.L. and Convit, J. (1975). "Inhibition of leucocytic lysosomal enzymes by glycosaminoglycans in vitro." Biochem J **152**(1): 57-64.

Baldo, G., Wozniak, D.F., Ohlemiller, K.K., Zhang, Y., Giugliani, R. and Ponder, K.P. (2013). "Retroviral-vector-mediated gene therapy to mucopolysaccharidosis I mice improves sensorimotor impairments and other behavioral deficits." Journal of inherited metabolic disease **36**(3): 499-512.

Bame, K.J. and Robson, K. (1997). "Heparanases produce distinct populations of heparan sulfate glycosaminoglycans in Chinese hamster ovary cells." J Biol Chem **272**(4): 2245-2251.

Barbier, A.J., Bielefeld, B., Whiteman, D.A., Natarajan, M., Pano, A. and Amato, D.A. (2013). "The relationship between anti-idursulfase antibody status and safety and efficacy outcomes in attenuated mucopolysaccharidosis II patients aged 5years and older treated with intravenous idursulfase." Molecular genetics and metabolism **110**(3): 303-310.

Bartholomew, W.R. and Rattazzi, M.C. (1974). "Immunochemical characterization of human beta-D-N-acetyl hexosaminidase from normal individuals and patients with Tay-Sachs disease. I. Antigenic differences between hexosaminidase A and hexosaminidase B." Int Arch Allergy Appl Immunol **46**(4): 512-524.

Barton, N.W., Furbish, F.S., Murray, G.J., Garfield, M. and Brady, R.O. (1990). "Therapeutic response to intravenous infusions of glucocerebrosidase in a patient with Gaucher disease." Proc Natl Acad Sci U S A **87**(5): 1913-1916.

Basselin, M., Ramadan, E., Chen, M. and Rapoport, S.I. (2011). "Anti-inflammatory effects of chronic aspirin on brain arachidonic acid metabolites." Neurochemical research **36**(1): 139-145.

Bastedo, L., Sands, M.S., Lambert, D.T., Pisa, M.A., Birkenmeier, E. and Chang, P.L. (1994). "Behavioral consequences of bone marrow transplantation in the treatment of murine mucopolysaccharidosis type VII." The Journal of clinical investigation **94**(3): 1180-1186.

Baudry, M., Yao, Y., Simmons, D., Liu, J. and Bi, X. (2003). "Postnatal development of inflammation in a murine model of Niemann-Pick type C disease: immunohistochemical observations of microglia and astroglia." Exp Neurol **184**(2): 887-903.

Bembi, B., Marchetti, F., Guerci, V.I., Ciana, G., Addobbati, R., Grasso, D., Barone, R., Cariati, R., Fernandez-Guillen, L., Butters, T. and Pittis, M.G. (2006). "Substrate reduction therapy in the infantile form of Tay-Sachs disease." Neurology **66**(2): 278-280.

Beutler, E., Kay, A., Saven, A., Garver, P., Thurston, D., Dawson, A. and Rosenbloom, B. (1991). "Enzyme replacement therapy for Gaucher disease." Blood **78**(5): 1183-1189.
Bhattacharyya, R., Gliddon, B., Beccari, T., Hopwood, J.J. and Stanley, P. (2001). "A novel missense mutation in lysosomal sulfamidase is the basis of MPS III A in a spontaneous mouse mutant." Glycobiology **11**(1): 99-103.

Bhaumik, M., Muller, V.J., Rozaklis, T., Johnson, L., Dobrenis, K., Bhattacharyya, R., Wurzelmann, S., Finamore, P., Hopwood, J.J., Walkley, S.U. and Stanley, P. (1999). "A mouse model for mucopolysaccharidosis type III A (Sanfilippo syndrome)." Glycobiology **9**(12): 1389-1396.

Bielicki, J., McIntyre, C. and Anson, D.S. (2010). "Comparison of ventricular and intravenous lentiviral-mediated gene therapy for murine MPS VII." Mol Genet Metab **101**(4): 370-382.

Birkenmeier, E.H., Davisson, M.T., Beamer, W.G., Ganschow, R.E., Vogler, C.A., Gwynn, B., Lyford, K.A., Maltais, L.M. and Wawrzyniak, C.J. (1989). "Murine mucopolysaccharidosis type VII. Characterization of a mouse with beta-glucuronidase deficiency." J Clin Invest **83**(4): 1258-1266.

Blumenkrantz, N. and Asboe-Hansen, G. (1973). "New method for quantitative determination of uronic acids." Anal Biochem **54**(2): 484-489.

Boelens, J.J., Aldenhoven, M., Purtill, D., Ruggeri, A., Defor, T., Wynn, R., Wraith, E., Cavazzana-Calvo, M., Rovelli, A., Fischer, A., Tolar, J., Prasad, V.K., Escolar, M., Gluckman, E., O'Meara, A., Orchard, P.J., Veys, P., Eapen, M., Kurtzberg, J. and Rocha, V. (2013). "Outcomes of transplantation using various hematopoietic cell sources in children with Hurler syndrome after myeloablative conditioning." Blood **121**(19): 3981-3987.

Boland, B., Smith, D.A., Mooney, D., Jung, S.S., Walsh, D.M. and Platt, F.M. (2010). "Macroautophagy is not directly involved in the metabolism of amyloid precursor protein." The Journal of biological chemistry **285**(48): 37415-37426.

Boomkamp, S.D., Rountree, J.S., Neville, D.C., Dwek, R.A., Fleet, G.W. and Butters, T.D. (2010). "Lysosomal storage of oligosaccharide and glycosphingolipid in imino sugar treated cells." Glycoconj J **27**(3): 297-308.

Brady, R.O., Kanfer, J.N., Bradley, R.M. and Shapiro, D. (1966). "Demonstration of a deficiency of glucocerebroside-cleaving enzyme in Gaucher's disease." J Clin Invest **45**(7): 1112-1115.

Brands, M.M., Hoogeveen-Westerveld, M., Kroos, M.A., Nobel, W., Ruijter, G.J., Ozkan, L., Plug, I., Grinberg, D., Vilageliu, L., Halley, D.J., Ploeg, A.T. and Reuser, A.J. (2013). "Mucopolysaccharidosis type VI phenotypes-genotypes and antibody response to galsulfase." Orphanet journal of rare diseases **8**(1): 51.

Brooks, A.I., Cory-Slechta, D.A., Murg, S.L. and Federoff, H.J. (2000). "Repeated acquisition and performance chamber for mice: a paradigm for assessment of spatial learning and memory." Neurobiology of learning and memory **74**(3): 241-258.

Brooks, A.I., Stein, C.S., Hughes, S.M., Heth, J., McCray, P.M., Jr., Sauter, S.L., Johnston, J.C., Cory-Slechta, D.A., Federoff, H.J. and Davidson, B.L. (2002). "Functional correction of established central nervous system deficits in an animal model of lysosomal storage disease with feline immunodeficiency virus-based vectors." Proc Natl Acad Sci U S A **99**(9): 6216-6221.

Bunge, S., Clements, P.R., Byers, S., Kleijer, W.J., Brooks, D.A. and Hopwood, J.J. (1998). "Genotype-phenotype correlations in mucopolysaccharidosis type I using enzyme kinetics, immunoquantification and in vitro turnover studies." Biochim Biophys Acta **1407**(3): 249-256.

Capablo, J.L., Franco, R., de Cabezon, A.S., Alfonso, P., Pocovi, M. and Giraldo, P. (2007). "Neurologic improvement in a type 3 Gaucher disease patient treated with imiglucerase/miglustat combination." Epilepsia **48**(7): 1406-1408.

Cardone, M., Polito, V.A., Pepe, S., Mann, L., D'Azzo, A., Auricchio, A., Ballabio, A. and Cosma, M.P. (2006). "Correction of Hunter syndrome in the MPSII mouse model by AAV2/8-mediated gene delivery." Hum Mol Genet **15**(7): 1225-1236.

Carter, N.M., Ali, S. and Kirby, J.A. (2003). "Endothelial inflammation: the role of differential expression of N-deacetylase/N-sulphotransferase enzymes in alteration of the immunological properties of heparan sulphate." Journal of cell science **116**(Pt 17): 3591-3600.

Chan, R.B., Oliveira, T.G., Cortes, E.P., Honig, L.S., Duff, K.E., Small, S.A., Wenk, M.R., Shui, G. and Di Paolo, G. (2012). "Comparative lipidomic analysis of mouse and human brain with Alzheimer disease." The Journal of biological chemistry **287**(4): 2678-2688.

Cheng, D., Jenner, A.M., Shui, G., Cheong, W.F., Mitchell, T.W., Nealon, J.R., Kim, W.S., McCann, H., Wenk, M.R., Halliday, G.M. and Garner, B. (2011). "Lipid pathway alterations in Parkinson's disease primary visual cortex." PloS one **6**(2): e17299.

Chien, Y.H., Lee, N.C., Tsai, L.K., Huang, A.C., Peng, S.F., Chen, S.J. and Hwu, W.L. (2007). "Treatment of Niemann-Pick disease type C in two children with miglustat: initial responses and maintenance of effects over 1 year." J Inherit Metab Dis **30**(5): 826.

Ciron, C., Desmaris, N., Colle, M.A., Raoul, S., Joussemet, B., Verot, L., Ausseil, J., Froissart, R., Roux, F., Cherel, Y., Ferry, N., Lajat, Y., Schwartz, B., Vanier, M.T., Maire, I., Tardieu, M., Moullier, P. and Heard, J.M. (2006). "Gene therapy of the brain in the dog model of Hurler's syndrome." Ann Neurol **60**(2): 204-213.

Clarke, L.A., Wraith, J.E., Beck, M., Kolodny, E.H., Pastores, G.M., Muenzer, J., Rapoport, D.M., Berger, K.I., Sidman, M., Kakkis, E.D. and Cox, G.F. (2009). "Long-term efficacy and safety of laronidase in the treatment of mucopolysaccharidosis I." Pediatrics **123**(1): 229-240.

Colville, G.A., Watters, J.P., Yule, W. and Bax, M. (1996). "Sleep problems in children with Sanfilippo syndrome." Dev Med Child Neurol **38**(6): 538-544.

Constantopoulos, G. and Dekaban, A.S. (1978). "Neurochemistry of the mucopolysaccharidoses: brain lipids and lysosomal enzymes in patients with four types of mucopolysaccharidosis and in normal controls." J Neurochem **30**(5): 965-973.

Constantopoulos, G., Iqbal, K. and Dekaban, A.S. (1980). "Mucopolysaccharidosis types IH, IS, II, and IIIA: glycosaminoglycans and lipids of isolated brain cells and other fractions from autopsied tissues." J Neurochem **34**(6): 1399-1411.

Constantopoulos, G., McComb, R.D. and Dekaban, A.S. (1976). "Neurochemistry of the mucopolysaccharidoses: brain glycosaminoglycans in normals and four types of mucopolysaccharidoses." J Neurochem **26**(5): 901-908.

Conzelmann, E. and Sandhoff, K. (1978). "AB variant of infantile GM2 gangliosidosis: deficiency of a factor necessary for stimulation of hexosaminidase A-catalyzed degradation of ganglioside GM2 and glycolipid GA2." Proceedings of the National Academy of Sciences of the United States of America **75**(8): 3979-3983.

Cox, T., Lachmann, R., Hollak, C., Aerts, J., van Weely, S., Hrebicek, M., Platt, F., Butters, T., Dwek, R., Moyses, C., Gow, I., Elstein, D. and Zimran, A. (2000). "Novel oral treatment of Gaucher's disease with N-butyldeoxynojirimycin (OGT 918) to decrease substrate biosynthesis." Lancet **355**(9214): 1481-1485.

Cox, T.M., Aerts, J.M., Andria, G., Beck, M., Belmatoug, N., Bembi, B., Chertkoff, R., Vom Dahl, S., Elstein, D., Erikson, A., Giralt, M., Heitner, R., Hollak, C., Hrebicek, M., Lewis, S., Mehta, A., Pastores, G.M., Rolfs, A., Miranda, M.C. and Zimran, A. (2003). "The role of the

iminosugar N-butyldeoxynojirimycin (miglustat) in the management of type I (non-neuronopathic) Gaucher disease: a position statement." J Inherit Metab Dis **26**(6): 513-526.
Crawley, A.C., Gliddon, B.L., Auclair, D., Brodie, S.L., Hirte, C., King, B.M., Fuller, M., Hemsley, K.M. and Hopwood, J.J. (2006). "Characterization of a C57BL/6 congenic mouse strain of mucopolysaccharidosis type IIIA." Brain Res **1104**(1): 1-17.

Cressant, A., Desmaris, N., Verot, L., Brejot, T., Froissart, R., Vanier, M.T., Maire, I. and Heard, J.M. (2004). "Improved behavior and neuropathology in the mouse model of Sanfilippo type IIIB disease after adeno-associated virus-mediated gene transfer in the striatum." J Neurosci **24**(45): 10229-10239.

Dawson, G., Fuller, M., Helmsley, K.M. and Hopwood, J.J. (2012). "Abnormal Gangliosides are Localized in Lipid Rafts in Sanfilippo (MPS3a) Mouse Brain." Neurochemical research **37**(6): 1372-1380.

de Duve, C. (1983). "Lysosomes revisited." Eur J Biochem **137**(3): 391-397.

de Pablo-Latorre, R., Saide, A., Polishhuck, E.V., Nusco, E., Fraldi, A. and Ballabio, A. (2012). "Impaired parkin-mediated mitochondrial targeting to autophagosomes differentially contributes to tissue pathology in lysosomal storage diseases." Human molecular genetics.

Dekaban, A.S. and Constantopoulos, G. (1977). "Mucopolysaccharidosis type I, II, IIIA and V. Pathological and biochemical abnormalities in the neural and mesenchymal elements of the brain." Acta Neuropathol **39**(1): 1-7.

Di Domenico, C., Villani, G.R., Di Napoli, D., Nusco, E., Cali, G., Nitsch, L. and Di Natale, P. (2009). "Intracranial gene delivery of LV-NAGLU vector corrects neuropathology in murine MPS IIIB." American journal of medical genetics. Part A **149A**(6): 1209-1218.

Di Domenico, C., Villani, G.R., Di Napoli, D., Reyero, E.G., Lombardo, A., Naldini, L. and Di Natale, P. (2005). "Gene therapy for a mucopolysaccharidosis type I murine model with lentiviral-IDUA vector." Hum Gene Ther **16**(1): 81-90.

Di Rocco, M., Dardis, A., Madeo, A., Barone, R. and Fiumara, A. (2012). "Early miglustat therapy in infantile Niemann-Pick disease type C." Pediatric neurology **47**(1): 40-43.

Dickson, P.I., Hanson, S., McEntee, M.F., Vite, C.H., Vogler, C.A., Mlikotic, A., Chen, A.H., Ponder, K.P., Haskins, M.E., Tippin, B.L., Le, S.Q., Passage, M.B., Guerra, C., Dierenfeld, A., Jens, J., Snella, E., Kan, S.H. and Ellinwood, N.M. (2010). "Early versus late treatment of spinal cord compression with long-term intrathecal enzyme replacement therapy in canine mucopolysaccharidosis type I." Molecular genetics and metabolism **101**(2-3): 115-122.

DiRosario, J., Divers, E., Wang, C., Etter, J., Charrier, A., Jukkola, P., Auer, H., Best, V., Newsom, D.L., McCarty, D.M. and Fu, H. (2009). "Innate and adaptive immune activation in the brain of MPS IIIB mouse model." J Neurosci Res **87**(4): 978-990.

Donsante, A., Levy, B., Vogler, C. and Sands, M.S. (2007a). "Clinical response to persistent, low-level beta-glucuronidase expression in the murine model of mucopolysaccharidosis type VII." J Inherit Metab Dis **30**(2): 227-238.

Donsante, A., Miller, D.G., Li, Y., Vogler, C., Brunt, E.M., Russell, D.W. and Sands, M.S. (2007b). "AAV vector integration sites in mouse hepatocellular carcinoma." Science **317**(5837): 477.

Donsante, A., Vogler, C., Muzyczka, N., Crawford, J.M., Barker, J., Flotte, T., Campbell-Thompson, M., Daly, T. and Sands, M.S. (2001). "Observed incidence of tumorigenesis in long-term rodent studies of rAAV vectors." Gene Ther **8**(17): 1343-1346.

Downs-Kelly, E., Jones, M.Z., Alroy, J., Cavanagh, K.T., King, B., Lucas, R.E., Baker, J.C., Kraemer, S.A. and Hopwood, J.J. (2000). "Caprine mucopolysaccharidosis IIID: a preliminary trial of enzyme replacement therapy." J Mol Neurosci **15**(3): 251-262.

Duda, M.K., O'Shea, K.M., Tintinu, A., Xu, W., Khairallah, R.J., Barrows, B.R., Chess, D.J., Azimzadeh, A.M., Harris, W.S., Sharov, V.G., Sabbah, H.N. and Stanley, W.C. (2009). "Fish oil, but not flaxseed oil, decreases inflammation and prevents pressure overload-induced cardiac dysfunction." Cardiovasc Res **81**(2): 319-327.

Dunham, N.W. and Miya, T.S. (1957). "A note on a simple apparatus for detecting neurological deficit in rats and mice." J Am Pharm Assoc Am Pharm Assoc (Baltim) **46**(3): 208-209.

Ellinwood, N.M., Colle, M.A., Weil, M.A., Casal, M.L., Vite, C.H., Wiemelt, S., Hasson, C.W., O'Malley, T.M., He, X., Prociuk, U., Verot, L., Melniczek, J.R., Lannon, A., Aguirre, G.D., Knox, V.W., Evans, S.M., Vanier, M.T., Schuchman, E.H., Walkley, S.U. and Haskins, M.E. (2007). "Bone marrow transplantation for feline mucopolysaccharidosis I." Molecular genetics and metabolism **91**(3): 239-250.

Elliot-Smith, E., Speak, A.O., Lloyd-Evans, E., Smith, D.A., van der Spoel, A.C., Jeyakumar, M., Butters, T.D., Dwek, R.A., d'Azzo, A. and Platt, F.M. (2008). "Beneficial effects of substrate reduction therapy in a mouse model of GM1 gangliosidosis." Mol Genet Metab **94**(2): 204-211.

Elstein, D., Dweck, A., Attias, D., Hadas-Halpern, I., Zevin, S., Altarescu, G., Aerts, J.F., van Weely, S. and Zimran, A. (2007). "Oral maintenance clinical trial with miglustat for type I Gaucher disease: switch from or combination with intravenous enzyme replacement." Blood **110**(7): 2296-2301.

Elstein, D., Hollak, C., Aerts, J.M., van Weely, S., Maas, M., Cox, T.M., Lachmann, R.H., Hrebicek, M., Platt, F.M., Butters, T.D., Dwek, R.A. and Zimran, A. (2004). "Sustained therapeutic effects of oral miglustat (Zavesca, N-butyldeoxynojirimycin, OGT 918) in type I Gaucher disease." J Inherit Metab Dis **27**(6): 757-766.

Esposito, G., Giovacchini, G., Liow, J.S., Bhattacharjee, A.K., Greenstein, D., Schapiro, M., Hallett, M., Herscovitch, P., Eckelman, W.C., Carson, R.E. and Rapoport, S.I. (2008). "Imaging neuroinflammation in Alzheimer's disease with radiolabeled arachidonic acid and PET." J Nucl Med **49**(9): 1414-1421.

Fabelo, N., Martin, V., Santpere, G., Marin, R., Torrent, L., Ferrer, I. and Diaz, M. (2011). "Severe alterations in lipid composition of frontal cortex lipid rafts from Parkinson's disease and incidental Parkinson's disease." Mol Med **17**(9-10): 1107-1118.

Fecarotta, S., Amitrano, M., Romano, A., Della Casa, R., Bruschini, D., Astarita, L., Parenti, G. and Andria, G. (2011). "The videofluoroscopic swallowing study shows a sustained improvement of dysphagia in children with Niemann-Pick disease type C after therapy with miglustat." Am J Med Genet A.

Fischl, M.A., Resnick, L., Coombs, R., Kremer, A.B., Pottage, J.C., Jr., Fass, R.J., Fife, K.H., Powderly, W.G., Collier, A.C., Aspinall, R.L. and et al. (1994). "The safety and efficacy of

combination N-butyl-deoxynojirimycin (SC-48334) and zidovudine in patients with HIV-1 infection and 200-500 CD4 cells/mm3." J Acquir Immune Defic Syndr **7**(2): 139-147.

Folch, J., Lees, M. and Sloane Stanley, G.H. (1957). "A simple method for the isolation and purification of total lipides from animal tissues." The Journal of biological chemistry **226**(1): 497-509.

Frisella, W.A., O'Connor, L.H., Vogler, C.A., Roberts, M., Walkley, S., Levy, B., Daly, T.M. and Sands, M.S. (2001). "Intracranial injection of recombinant adeno-associated virus improves cognitive function in a murine model of mucopolysaccharidosis type VII." Mol Ther **3**(3): 351-358.

Friso, A., Tomanin, R., Salvalaio, M. and Scarpa, M. (2010). "Genistein reduces glycosaminoglycan levels in a mouse model of mucopolysaccharidosis type II." Br J Pharmacol **159**(5): 1082-1091.

Fyfe, J.C., Kurzhals, R.L., Lassaline, M.E., Henthorn, P.S., Alur, P.R., Wang, P., Wolfe, J.H., Giger, U., Haskins, M.E., Patterson, D.F., Sun, H., Jain, S. and Yuhki, N. (1999). "Molecular basis of feline beta-glucuronidase deficiency: an animal model of mucopolysaccharidosis VII." Genomics **58**(2): 121-128.

Gabrielli, O., Salvolini, U., Maricotti, M., Mariani, M.G., Coppa, G.V. and Giorgi, P.L. (1992). "Cerebral MRI in two brothers with mucopolysaccharidosis type I and different clinical phenotypes." Neuroradiology **34**(4): 313-315.

Galanaud, D., Tourbah, A., Lehericy, S., Leveque, N., Heron, B., Billette de Villemeur, T., Guffon, N., Feillet, F., Baumann, N., Vanier, M.T. and Sedel, F. (2009). "24 month-treatment with miglustat of three patients with Niemann-Pick disease type C: follow up using brain spectroscopy." Mol Genet Metab **96**(2): 55-58.

Garcia-Rivera, M.F., Colvin-Wanshura, L.E., Nelson, M.S., Nan, Z., Khan, S.A., Rogers, T.B., Maitra, I., Low, W.C. and Gupta, P. (2007). "Characterization of an immunodeficient mouse model of mucopolysaccharidosis type I suitable for preclinical testing of human stem cell and gene therapy." Brain Res Bull **74**(6): 429-438.

Giraldo, P., Alfonso, P., Atutxa, K., Fernandez-Galan, M.A., Barez, A., Franco, R., Alonso, D., Martin, A., Latre, P. and Pocovi, M. (2009). "Real-world clinical experience with long-term miglustat maintenance therapy in type 1 Gaucher disease: the ZAGAL project." Haematologica **94**(12): 1771-1775.

Glaros, E.N., Kim, W.S., Quinn, C.M., Wong, J., Gelissen, I., Jessup, W. and Garner, B. (2005). "Glycosphingolipid accumulation inhibits cholesterol efflux via the ABCA1/apolipoprotein A-I pathway: 1-phenyl-2-decanoylamino-3-morpholino-1-propanol is a novel cholesterol efflux accelerator." The Journal of biological chemistry **280**(26): 24515-24523.

Gliddon, B.L. and Hopwood, J.J. (2004). "Enzyme-replacement therapy from birth delays the development of behavior and learning problems in mucopolysaccharidosis type IIIA mice." Pediatric research **56**(1): 65-72.

Grabowski, G.A., Barton, N.W., Pastores, G., Dambrosia, J.M., Banerjee, T.K., McKee, M.A., Parker, C., Schiffmann, R., Hill, S.C. and Brady, R.O. (1995). "Enzyme therapy in type 1 Gaucher disease: comparative efficacy of mannose-terminated glucocerebrosidase from natural and recombinant sources." Ann Intern Med **122**(1): 33-39.

Grabowski, G.A. and Hopkin, R.J. (2003). "Enzyme therapy for lysosomal storage disease: principles, practice, and prospects." Annu Rev Genomics Hum Genet **4**: 403-436.

Gravel, R.A., Kaback, M.M., Proia, R.L., Sandhoff, K., Suzuki, K. and Suzuki, K. (2001). The G_{M2} gangliosidoses. The Metabolic and Molecular Bases of Inherited Disease. Scriver, C.R., Beaudet, A.L., Sly, W.S. and Valle, D. New York, McGraw-Hill Companies Inc. **2:** 3827-3865.

Greco, A., Minghetti, L., Sette, G., Fieschi, C. and Levi, G. (1999). "Cerebrospinal fluid isoprostane shows oxidative stress in patients with multiple sclerosis." Neurology **53**(8): 1876-1879.

Guffon, N., Bin-Dorel, S., Decullier, E., Paillet, C., Guitton, J. and Fouilhoux, A. (2011). "Evaluation of Miglustat Treatment in Patients with Type III Mucopolysaccharidosis: A Randomized, Double-Blind, Placebo-Controlled Study." The Journal of pediatrics **159**(5): 838-844 e831.

Hakomori, S.I. and Siddiqui, B. (1974). "Isolation and characterization of glycosphingolipid from animal cells and their membranes." Methods in enzymology **32**(Part B): 345-367.

Hamano, K., Hayashi, M., Shioda, K., Fukatsu, R. and Mizutani, S. (2008). "Mechanisms of neurodegeneration in mucopolysaccharidoses II and IIIB: analysis of human brain tissue." Acta neuropathologica **115**(5): 547-559.

Harmatz, P., Giugliani, R., Schwartz, I., Guffon, N., Teles, E.L., Miranda, M.C., Wraith, J.E., Beck, M., Arash, L., Scarpa, M., Yu, Z.F., Wittes, J., Berger, K.I., Newman, M.S., Lowe, A.M., Kakkis, E. and Swiedler, S.J. (2006). "Enzyme replacement therapy for mucopolysaccharidosis VI: a phase 3, randomized, double-blind, placebo-controlled, multinational study of recombinant human N-acetylgalactosamine 4-sulfatase (recombinant human arylsulfatase B or rhASB) and follow-on, open-label extension study." J Pediatr **148**(4): 533-539.

Harmatz, P., Giugliani, R., Schwartz, I.V., Guffon, N., Teles, E.L., Miranda, M.C., Wraith, J.E., Beck, M., Arash, L., Scarpa, M., Ketteridge, D., Hopwood, J.J., Plecko, B., Steiner, R., Whitley, C.B., Kaplan, P., Yu, Z.F., Swiedler, S.J. and Decker, C. (2008). "Long-term follow-up of endurance and safety outcomes during enzyme replacement therapy for mucopolysaccharidosis VI: Final results of three clinical studies of recombinant human N-acetylgalactosamine 4-sulfatase." Mol Genet Metab **94**(4): 469-475.

Harmatz, P., Ketteridge, D., Giugliani, R., Guffon, N., Teles, E.L., Miranda, M.C., Yu, Z.F., Swiedler, S.J. and Hopwood, J.J. (2005). "Direct comparison of measures of endurance, mobility, and joint function during enzyme-replacement therapy of mucopolysaccharidosis VI (Maroteaux-Lamy syndrome): results after 48 weeks in a phase 2 open-label clinical study of recombinant human N-acetylgalactosamine 4-sulfatase." Pediatrics **115**(6): e681-689.

Harmatz, P., Yu, Z.F., Giugliani, R., Schwartz, I.V., Guffon, N., Teles, E.L., Miranda, M.C., Wraith, J.E., Beck, M., Arash, L., Scarpa, M., Ketteridge, D., Hopwood, J.J., Plecko, B., Steiner, R., Whitley, C.B., Kaplan, P., Swiedler, S.J., Hardy, K., Berger, K.I. and Decker, C. (2010). "Enzyme replacement therapy for mucopolysaccharidosis VI: evaluation of long-term pulmonary function in patients treated with recombinant human N-acetylgalactosamine 4-sulfatase." J Inherit Metab Dis **33**(1): 51-60.

Haskins, M.E., Desnick, R.J., DiFerrante, N., Jezyk, P.F. and Patterson, D.F. (1984). "Beta-glucuronidase deficiency in a dog: a model of human mucopolysaccharidosis VII." Pediatr Res **18**(10): 980-984.

Haurigot, V., Marco, S., Ribera, A., Garcia, M., Ruzo, A., Villacampa, P., Ayuso, E., Anor, S., Andaluz, A., Pineda, M., Garcia-Fructuoso, G., Molas, M., Maggioni, L., Munoz, S., Motas, S., Ruberte, J., Mingozzi, F., Pumarola, M. and Bosch, F. (2013). "Whole body correction of mucopolysaccharidosis IIIA by intracerebrospinal fluid gene therapy." The Journal of clinical investigation.

Heinecke, K.A., Peacock, B.N., Blazar, B.R., Tolar, J. and Seyfried, T.N. (2011). "Lipid composition of whole brain and cerebellum in Hurler syndrome (MPS IH) mice." Neurochemical research **36**(9): 1669-1676.

Heldermon, C.D., Hennig, A.K., Ohlemiller, K.K., Ogilvie, J.M., Herzog, E.D., Breidenbach, A., Vogler, C., Wozniak, D.F. and Sands, M.S. (2007). "Development of sensory, motor and behavioral deficits in the murine model of Sanfilippo syndrome type B." PLoS ONE **2**(1): e772.

Heldermon, C.D., Qin, E.Y., Ohlemiller, K.K., Herzog, E.D., Brown, J.R., Vogler, C., Hou, W., Orrock, J.L., Crawford, B.E. and Sands, M.S. (2013). "Disease correction by combined neonatal intracranial AAV and systemic lentiviral gene therapy in Sanfilippo Syndrome type B mice." Gene therapy **20**(9): 913-921.

Hemsley, K.M. and Hopwood, J.J. (2005). "Development of motor deficits in a murine model of mucopolysaccharidosis type IIIA (MPS-IIIA)." Behav Brain Res **158**(2): 191-199.

Heron, B., Valayannopoulos, V., Baruteau, J., Chabrol, B., Ogier, H., Latour, P., Dobbelaere, D., Eyer, D., Labarthe, F., Maurey, H., Cuisset, J.M., de Villemeur, T.B., Sedel, F. and Vanier, M.T. (2012). "Miglustat therapy in the French cohort of paediatric patients with Niemann-Pick disease type C." Orphanet journal of rare diseases **7**: 36.

Herskhovitz, E., Young, E., Rainer, J., Hall, C.M., Lidchi, V., Chong, K. and Vellodi, A. (1999). "Bone marrow transplantation for Maroteaux-Lamy syndrome (MPS VI): long-term follow-up." J Inherit Metab Dis **22**(1): 50-62.

Hobbs, J.R., Hugh-Jones, K., Barrett, A.J., Byrom, N., Chambers, D., Henry, K., James, D.C., Lucas, C.F., Rogers, T.R., Benson, P.F., Tansley, L.R., Patrick, A.D., Mossman, J. and Young, E.P. (1981). "Reversal of clinical features of Hurler's disease and biochemical improvement after treatment by bone-marrow transplantation." Lancet **2**(8249): 709-712.

Hoff, J. (2000). Methods of blood collection in the mouse. Lab animal. **29:** 47-53.

Hogan, M.V., Saito, M. and Rosenberg, A. (1988). "Influence of monensin on ganglioside anabolism and neurite stability in cultured chick neurons." J Neurosci Res **20**(3): 390-394.

Hong, S., Gronert, K., Devchand, P.R., Moussignac, R.L. and Serhan, C.N. (2003). "Novel docosatrienes and 17S-resolvins generated from docosahexaenoic acid in murine brain, human blood, and glial cells. Autacoids in anti-inflammation." The Journal of biological chemistry **278**(17): 14677-14687.

Hook, M., Lindahl, U. and Iverius, P.H. (1974). "Distribution of sulphate and iduronic acid residues in heparin and heparan sulphate." Biochem J **137**(1): 33-43.

Horovitz, D.D., Magalhaes, T.S., Acosta, A., Ribeiro, E.M., Giuliani, L.R., Palhares, D.B., Kim, C.A., de Paula, A.C., Kerstenestzy, M., Pianovski, M.A., Costa, M.I., Santos, F.C., Martins, A.M., Aranda, C.S., Correa Neto, J., Holanda, G.B., Cardoso, L., Jr., da Silva, C.A., Bonatti, R.C., Ribeiro, B.F., Rodrigues Mdo, C. and Llerena, J.C., Jr. (2013). "Enzyme replacement therapy with galsulfase in 34 children younger than five years of age with MPS VI." Molecular genetics and metabolism **109**(1): 62-69.

Huang, J.Q., Trasler, J.M., Igdoura, S., Michaud, J., Hanal, N. and Gravel, R.A. (1997). "Apoptotic cell death in mouse models of GM2 gangliosidosis and observations on human Tay-Sachs and Sandhoff diseases." Hum Mol Genet **6**(11): 1879-1885.

Ichikawa, S., Sakiyama, H., Suzuki, G., Hidari, K.I. and Hirabayashi, Y. (1996). "Expression cloning of a cDNA for human ceramide glucosyltransferase that catalyzes the first glycosylation step of glycosphingolipid synthesis." Proc Natl Acad Sci U S A **93**(10): 4638-4643.

Inokuchi, J. and Radin, N.S. (1987). "Preparation of the active isomer of 1-phenyl-2-decanoylamino-3-morpholino-1-propanol, inhibitor of murine glucocerebroside synthetase." J Lipid Res **28**(5): 565-571.

Ishibashi, S., Yamazaki, T. and Okamoto, K. (2009). "Association of autophagy with cholesterol-accumulated compartments in Niemann-Pick disease type C cells." J Clin Neurosci **16**(7): 954-959.

Jacobs, J.F., Willemsen, M.A., Groot-Loonen, J.J., Wevers, R.A. and Hoogerbrugge, P.M. (2005). "Allogeneic BMT followed by substrate reduction therapy in a child with subacute Tay-Sachs disease." Bone Marrow Transplant **36**(10): 925-926.

Jesus, S., Caceres-Redondo, M.T., Carrillo, F., Cordones, I., Escudero, M., Macias-Vidal, J., Coll, M.J., Bautista, J. and Mir, P. (2013). "Adult form of Niemann-Pick type C with the variant biochemical phenotype on treatment with Miglustat." Parkinsonism & related disorders **19**(10): 916-917.

Jeyakumar, M., Butters, T.D., Cortina-Borja, M., Hunnam, V., Proia, R.L., Perry, V.H., Dwek, R.A. and Platt, F.M. (1999). "Delayed symptom onset and increased life expectancy in Sandhoff disease mice treated with N-butyldeoxynojirimycin." Proc Natl Acad Sci U S A **96**(11): 6388-6393.

Jeyakumar, M., Norflus, F., Tifft, C.J., Cortina-Borja, M., Butters, T.D., Proia, R.L., Perry, V.H., Dwek, R.A. and Platt, F.M. (2001). "Enhanced survival in Sandhoff disease mice receiving a combination of substrate deprivation therapy and bone marrow transplantation." Blood **97**(1): 327-329.

Jeyakumar, M., Smith, D.A., Williams, I.M., Borja, M.C., Neville, D.C., Butters, T.D., Dwek, R.A. and Platt, F.M. (2004). "NSAIDs increase survival in the Sandhoff disease mouse: synergy with N-butyldeoxynojirimycin." Ann Neurol **56**(5): 642-649.

Jeyakumar, M., Thomas, R., Elliot-Smith, E., Smith, D.A., van der Spoel, A.C., d'Azzo, A., Perry, V.H., Butters, T.D., Dwek, R.A. and Platt, F.M. (2003). "Central nervous system inflammation is a hallmark of pathogenesis in mouse models of GM1 and GM2 gangliosidosis." Brain **126**(Pt 4): 974-987.

Jones, B.J. and Roberts, D.J. (1968). "The quantiative measurement of motor inco-ordination in naive mice using an acelerating rotarod." J Pharm Pharmacol **20**(4): 302-304.

Jones, M.Z., Brumfield, L.K., King, B.M., Hopwood, J.J. and Byers, S. (1998). "Recombinant caprine 3H-[N-acetylglucosamine-6-sulfatase] and human 3H-[N-acetylgalactosamine-4-sulfatase]: plasma clearance, tissue distribution, and cellular uptake in the rat." J Mol Neurosci **11**(3): 223-232.

Kakkis, E., McEntee, M., Vogler, C., Le, S., Levy, B., Belichenko, P., Mobley, W., Dickson, P., Hanson, S. and Passage, M. (2004). "Intrathecal enzyme replacement therapy reduces lysosomal storage in the brain and meninges of the canine model of MPS I." Mol Genet Metab **83**(1-2): 163-174.

Kakkis, E.D., Muenzer, J., Tiller, G.E., Waber, L., Belmont, J., Passage, M., Izykowski, B., Phillips, J., Doroshow, R., Walot, I., Hoft, R. and Neufeld, E.F. (2001). "Enzyme-replacement therapy in mucopolysaccharidosis I." N Engl J Med **344**(3): 182-188.

Kara, S., Sherr, E.H. and Barkovich, A.J. (2008). "Dilated perivascular spaces: an informative radiologic finding in Sanfilippo syndrome type A." Pediatr Neurol **38**(5): 363-366.

Karimzadeh, P., Tonekaboni, S.H., Ashrafi, M.R., Shafeghati, Y., Rezayi, A., Salehpour, S., Ghofrani, M., Taghdiri, M.M., Rahmanifar, A., Zaman, T., Aryani, O., Shoar, B.N., Shiva, F., Tavasoli, A. and Houshmand, M. (2012). "Effects of Miglustat on Stabilization of Neurological Disorder in Niemann-Pick Disease Type C: Iranian Pediatric Case Series." Journal of child neurology.

Karimzadeh, P., Tonekaboni, S.H., Ashrafi, M.R., Shafeghati, Y., Rezayi, A., Salehpour, S., Ghofrani, M., Taghdiri, M.M., Rahmanifar, A., Zaman, T., Aryani, O., Shoar, B.N., Shiva, F., Tavasoli, A. and Houshmand, M. (2013). "Effects of miglustat on stabilization of neurological disorder in niemann-pick disease type C: Iranian pediatric case series." Journal of child neurology **28**(12): 1599-1606.

Karten, B., Vance, D.E., Campenot, R.B. and Vance, J.E. (2002). "Cholesterol accumulates in cell bodies, but is decreased in distal axons, of Niemann-Pick C1-deficient neurons." Journal of neurochemistry **83**(5): 1154-1163.

Kawashita, E., Tsuji, D., Toyoshima, M., Kanno, Y., Matsuno, H. and Itoh, K. (2011). "Prostaglandin E2 reverses aberrant production of an inflammatory chemokine by microglia from Sandhoff disease model mice through the cAMP-PKA pathway." PloS one **6**(1): e16269.

Kim, J., Park, M.R., Kim, D.S., Lee, J.O., Maeng, S.H., Cho, S.Y., Han, Y., Ahn, K. and Jin, D.K. (2013). "IgE-mediated anaphylaxis and allergic reactions to idursulfase in patients with Hunter syndrome." Allergy **68**(6): 796-802.

Kiselyov, K., Jennigs, J.J., Jr., Rbaibi, Y. and Chu, C.T. (2007). "Autophagy, mitochondria and cell death in lysosomal storage diseases." Autophagy **3**(3): 259-262.

Kobayashi, H., Carbonaro, D., Pepper, K., Petersen, D., Ge, S., Jackson, H., Shimada, H., Moats, R. and Kohn, D.B. (2005). "Neonatal gene therapy of MPS I mice by intravenous injection of a lentiviral vector." Mol Ther **11**(5): 776-789.

Kolodny, E.H., Brady, R.O. and Volk, B.W. (1969). "Demonstration of an alteration of ganglioside metabolism in Tay-Sachs disease." Biochem Biophys Res Commun **37**(3): 526-531.

Kolter, T., Proia, R.L. and Sandhoff, K. (2002). "Combinatorial ganglioside biosynthesis." J Biol Chem **277**(29): 25859-25862.
Kornguth, S., Wannamaker, B., Kolodny, E., Geison, R., Scott, G. and O'Brien, J.F. (1974). "Subcellular fractions from Tay-Sachs brains: ganglioside, lipid, and protein composition and hexosaminidase activities." Journal of the neurological sciences **22**(3): 383-406.

Koseoglu, S.T., Harmatz, P., Turbeville, S. and Nicely, H. (2009). "Reversed papilledema in an MPS VI patient with galsulfase (Naglazyme) therapy." Int Ophthalmol **29**(4): 267-269.

Kotani, M., Kawashima, I., Ozawa, H., Ogura, K., Ishizuka, I., Terashima, T. and Tai, T. (1994). "Immunohistochemical localization of minor gangliosides in the rat central nervous system." Glycobiology **4**(6): 855-865.

Kotani, M., Kawashima, I., Ozawa, H., Terashima, T. and Tai, T. (1993). "Differential distribution of major gangliosides in rat central nervous system detected by specific monoclonal antibodies." Glycobiology **3**(2): 137-146.

Kotani, M., Terashima, T. and Tai, T. (1995). "Developmental changes of ganglioside expressions in postnatal rat cerebellar cortex." Brain Res **700**(1-2): 40-58.

Kotilinek, L.A., Westerman, M.A., Wang, Q., Panizzon, K., Lim, G.P., Simonyi, A., Lesne, S., Falinska, A., Younkin, L.H., Younkin, S.G., Rowan, M., Cleary, J., Wallis, R.A., Sun, G.Y., Cole, G., Frautschy, S., Anwyl, R. and Ashe, K.H. (2008). "Cyclooxygenase-2 inhibition improves amyloid-beta-mediated suppression of memory and synaptic plasticity." Brain **131**(Pt 3): 651-664.

Kowalewski, B., Lamanna, W.C., Lawrence, R., Damme, M., Stroobants, S., Padva, M., Kalus, I., Frese, M.A., Lubke, T., Lullmann-Rauch, R., D'Hooge, R., Esko, J.D. and Dierks, T. (2012). "Arylsulfatase G inactivation causes loss of heparan sulfate 3-O-sulfatase activity and mucopolysaccharidosis in mice." Proceedings of the National Academy of Sciences of the United States of America **109**(26): 10310-10315.

Kracun, I., Kalanj, S., Talan-Hranilovic, J. and Cosovic, C. (1992). "Cortical distribution of gangliosides in Alzheimer's disease." Neurochemistry international **20**(3): 433-438.

Kracun, I., Rosner, H., Cosovic, C. and Stavljenic, A. (1984). "Topographical atlas of the gangliosides of the adult human brain." J Neurochem **43**(4): 979-989.

Krivit, W., Lockman, L.A., Watkins, P.A., Hirsch, J. and Shapiro, E.G. (1995). "The future for treatment by bone marrow transplantation for adrenoleukodystrophy, metachromatic leukodystrophy, globoid cell leukodystrophy and Hurler syndrome." J Inherit Metab Dis **18**(4): 398-412.

Krivit, W., Pierpont, M.E., Ayaz, K., Tsai, M., Ramsay, N.K., Kersey, J.H., Weisdorf, S., Sibley, R., Snover, D., McGovern, M.M. and et al. (1984). "Bone-marrow transplantation in the Maroteaux-Lamy syndrome (mucopolysaccharidosis type VI). Biochemical and clinical status 24 months after transplantation." N Engl J Med **311**(25): 1606-1611.

Kurihara, T. (2006). "Abducens nerve palsy and ipsilateral incomplete Horner syndrome: a significant sign of locating the lesion in the posterior cavernous sinus." Intern Med **45**(17): 993-994.

Kytzia, H.J. and Sandhoff, K. (1985). "Evidence for two different active sites on human beta-hexosaminidase A. Interaction of GM2 activator protein with beta-hexosaminidase A." J Biol Chem **260**(12): 7568-7572.
Langford-Smith, A., Langford-Smith, K.J., Jones, S.A., Wynn, R.F., Wraith, J.E., Wilkinson, F.L. and Bigger, B.W. (2011a). "Female Mucopolysaccharidosis IIIA Mice Exhibit Hyperactivity and a Reduced Sense of Danger in the Open Field Test." PloS one **6**(10): e25717.

Langford-Smith, A., Malinowska, M., Langford-Smith, K.J., Wegrzyn, G., Jones, S., Wynn, R., Wraith, J.E., Wilkinson, F.L. and Bigger, B.W. (2011b). "Hyperactive behaviour in the mouse model of mucopolysaccharidosis IIIB in the open field and home cage environments." Genes, brain, and behavior **10**(6): 673-682.

Laraway, S., Breen, C., Mercer, J., Jones, S. and Wraith, J.E. (2013). "Does early use of enzyme replacement therapy alter the natural history of mucopolysaccharidosis I? Experience in three siblings." Molecular genetics and metabolism **109**(3): 315-316.

Lau, A.A., Crawley, A.C., Hopwood, J.J. and Hemsley, K.M. (2008). "Open field locomotor activity and anxiety-related behaviors in mucopolysaccharidosis type IIIA mice." Behav Brain Res **191**(1): 130-136.

Levy, B., Galvin, N., Vogler, C., Birkenmeier, E.H. and Sly, W.S. (1996). "Neuropathology of murine mucopolysaccharidosis type VII." Acta Neuropathol **92**(6): 562-568.

Li, H.H., Zhao, H.Z., Neufeld, E.F., Cai, Y. and Gomez-Pinilla, F. (2002). "Attenuated plasticity in neurons and astrocytes in the mouse model of Sanfilippo syndrome type B." J Neurosci Res **69**(1): 30-38.

Liu, G., Martins, I., Wemmie, J.A., Chiorini, J.A. and Davidson, B.L. (2005a). "Functional correction of CNS phenotypes in a lysosomal storage disease model using adeno-associated virus type 4 vectors." J Neurosci **25**(41): 9321-9327.

Liu, Y., Xu, L., Hennig, A.K., Kovacs, A., Fu, A., Chung, S., Lee, D., Wang, B., Herati, R.S., Mosinger Ogilvie, J., Cai, S.R. and Parker Ponder, K. (2005b). "Liver-directed neonatal gene therapy prevents cardiac, bone, ear, and eye disease in mucopolysaccharidosis I mice." Mol Ther **11**(1): 35-47.

Livak, K.J. and Schmittgen, T.D. (2001). "Analysis of relative gene expression data using real-time quantitative PCR and the 2(-Delta Delta C(T)) Method." Methods **25**(4): 402-408.

Llano Lopez, L., Hauser, J., Feldon, J., Gargiulo, P.A. and Yee, B.K. (2010). "Evaluating spatial memory function in mice: a within-subjects comparison between the water maze test and its adaptation to dry land." Behavioural brain research **209**(1): 85-92.

Lloyd-Evans, E., Morgan, A.J., He, X., Smith, D.A., Elliot-Smith, E., Sillence, D.J., Churchill, G.C., Schuchman, E.H., Galione, A. and Platt, F.M. (2008). "Niemann-Pick disease type C1 is a sphingosine storage disease that causes deregulation of lysosomal calcium." Nature medicine **14**(11): 1247-1255.

Ma, X., Liu, Y., Tittiger, M., Hennig, A., Kovacs, A., Popelka, S., Wang, B., Herati, R., Bigg, M. and Ponder, K.P. (2007). "Improvements in mucopolysaccharidosis I mice after adult retroviral vector-mediated gene therapy with immunomodulation." Mol Ther **15**(5): 889-902.

Macsai, C.E., Derrick-Roberts, A.L., Ding, X., Zarrinkalam, K.H., McIntyre, C., Anderson, P.H., Anson, D.S. and Byers, S. (2012). "Skeletal response to lentiviral mediated gene therapy in a mouse model of MPS VII." Molecular genetics and metabolism **106**(2): 202-213.
Maegawa, G.H., Banwell, B.L., Blaser, S., Sorge, G., Toplak, M., Ackerley, C., Hawkins, C., Hayes, J. and Clarke, J.T. (2009). "Substrate reduction therapy in juvenile GM2 gangliosidosis." Mol Genet Metab **98**(1-2): 215-224.

Malinowska, M., Wilkinson, F.L., Langford-Smith, K.J., Langford-Smith, A., Brown, J.R., Crawford, B.E., Vanier, M.T., Grynkiewicz, G., Wynn, R.F., Wraith, J.E., Wegrzyn, G. and Bigger, B.W. (2010). "Genistein improves neuropathology and corrects behaviour in a mouse model of neurodegenerative metabolic disease." PloS one **5**(12): e14192.

Mango, R.L., Xu, L., Sands, M.S., Vogler, C., Seiler, G., Schwarz, T., Haskins, M.E. and Ponder, K.P. (2004). "Neonatal retroviral vector-mediated hepatic gene therapy reduces bone, joint, and cartilage disease in mucopolysaccharidosis VII mice and dogs." Mol Genet Metab **82**(1): 4-19.

Marcheselli, V.L., Hong, S., Lukiw, W.J., Tian, X.H., Gronert, K., Musto, A., Hardy, M., Gimenez, J.M., Chiang, N., Serhan, C.N. and Bazan, N.G. (2003). "Novel docosanoids inhibit brain ischemia-reperfusion-mediated leukocyte infiltration and pro-inflammatory gene expression." The Journal of biological chemistry **278**(44): 43807-43817.

Martin, V., Fabelo, N., Santpere, G., Puig, B., Marin, R., Ferrer, I. and Diaz, M. (2010). "Lipid alterations in lipid rafts from Alzheimer's disease human brain cortex." J Alzheimers Dis **19**(2): 489-502.

Masciullo, M., Santoro, M., Modoni, A., Ricci, E., Guitton, J., Tonali, P. and Silvestri, G. (2010). "Substrate reduction therapy with miglustat in chronic GM2 gangliosidosis type Sandhoff: results of a 3-year follow-up." J Inherit Metab Dis.

McCarty, D.M., DiRosario, J., Gulaid, K., Killedar, S., Oosterhof, A., van Kuppevelt, T.H., Martin, P.T. and Fu, H. (2011). "Differential distribution of heparan sulfate glycoforms and elevated expression of heparan sulfate biosynthetic enzyme genes in the brain of mucopolysaccharidosis IIIB mice." Metabolic brain disease **26**(1): 9-19.

McDowell, G.A., Cowan, T.M., Blitzer, M.G. and Greene, C.L. (1993). "Intrafamilial variability in Hurler syndrome and Sanfilippo syndrome type A: implications for evaluation of new therapies." Am J Med Genet **47**(7): 1092-1095.

McGlynn, R., Dobrenis, K. and Walkley, S.U. (2004). "Differential subcellular localization of cholesterol, gangliosides, and glycosaminoglycans in murine models of mucopolysaccharide storage disorders." J Comp Neurol **480**(4): 415-426.

McIntyre, C., Byers, S. and Anson, D.S. (2010). "Correction of mucopolysaccharidosis type IIIA somatic and central nervous system pathology by lentiviral-mediated gene transfer." J Gene Med **12**(9): 717-728.

McIntyre, C., Derrick Roberts, A.L., Ranieri, E., Clements, P.R., Byers, S. and Anson, D.S. (2008). "Lentiviral-mediated gene therapy for murine mucopolysaccharidosis type IIIA." Molecular genetics and metabolism **93**(4): 411-418.

McKinnis, E.J., Sulzbacher, S., Rutledge, J.C., Sanders, J. and Scott, C.R. (1996). "Bone marrow transplantation in Hunter syndrome." J Pediatr **129**(1): 145-148.

Meier, E.M., Schwarzmann, G., Furst, W. and Sandhoff, K. (1991). "The human GM2 activator protein. A substrate specific cofactor of beta-hexosaminidase A." J Biol Chem **266**(3): 1879-1887.
Meikle, P.J., Hopwood, J.J., Clague, A.E. and Carey, W.F. (1999). "Prevalence of lysosomal storage disorders." JAMA **281**(3): 249-254.

Miyamoto, I. and Nagase, S. (1981). "A simple and rapid electrophoretic method for the separation of glucuronic acid and iduronic acid." Anal Biochem **115**(2): 308-310.

Molander-Melin, M., Blennow, K., Bogdanovic, N., Dellheden, B., Mansson, J.E. and Fredman, P. (2005). "Structural membrane alterations in Alzheimer brains found to be associated with regional disease development; increased density of gangliosides GM1 and GM2 and loss of cholesterol in detergent-resistant membrane domains." Journal of neurochemistry **92**(1): 171-182.

Morris, R. (1984). "Developments of a water-maze procedure for studying spatial learning in the rat." Journal of neuroscience methods **11**(1): 47-60.

Muenzer, J., Gucsavas-Calikoglu, M., McCandless, S.E., Schuetz, T.J. and Kimura, A. (2007). "A phase I/II clinical trial of enzyme replacement therapy in mucopolysaccharidosis II (Hunter syndrome)." Mol Genet Metab **90**(3): 329-337.

Myerowitz, R., Lawson, D., Mizukami, H., Mi, Y., Tifft, C.J. and Proia, R.L. (2002). "Molecular pathophysiology in Tay-Sachs and Sandhoff diseases as revealed by gene expression profiling." Hum Mol Genet **11**(11): 1343-1350.

Nakamura, H., Yasufuku, K., Makiyama, T., Matsumoto, I., Fujino, H. and Murayama, T. (2011). "Arachidonic acid metabolism via cytosolic phospholipase A(2) alpha induces cytotoxicity in Niemann-Pick disease type C cells." Journal of cellular physiology.

Nakatsuji, Y. and Miller, R.H. (2001). "Selective cell-cycle arrest and induction of apoptosis in proliferating neural cells by ganglioside GM3." Exp Neurol **168**(2): 290-299.

Neufield, E.F. and Muenzer, J. (2001). The Mucopolysaccharidoses. The Metabolic and Molecular Bases of Inherited Disease. Scriver, C.R., Beaudet, A.L., Sly, W.S. and Valle, D. New York, McGraw-Hill Companies Inc. **3:** 3421-3452.

Nietupski, J.B., Pacheco, J.J., Chuang, W.L., Maratea, K., Li, L., Foley, J., Ashe, K.M., Cooper, C.G., Aerts, J.M., Copeland, D.P., Scheule, R.K., Cheng, S.H. and Marshall, J. (2012). "Iminosugar-based inhibitors of glucosylceramide synthase prolong survival but paradoxically increase brain glucosylceramide levels in Niemann-Pick C mice." Molecular genetics and metabolism **105**(4): 621-628.

Noll, E.N., Lin, J., Nakatsuji, Y., Miller, R.H. and Black, P.M. (2001). "GM3 as a novel growth regulator for human gliomas." Exp Neurol **168**(2): 300-309.

Ohkuma, S. and Poole, B. (1978). "Fluorescence probe measurement of the intralysosomal pH in living cells and the perturbation of pH by various agents." Proc Natl Acad Sci U S A **75**(7): 3327-3331.

Ohmi, K., Greenberg, D.S., Rajavel, K.S., Ryazantsev, S., Li, H.H. and Neufeld, E.F. (2003). "Activated microglia in cortex of mouse models of mucopolysaccharidoses I and IIIB." Proc Natl Acad Sci U S A **100**(4): 1902-1907.

Ohmi, K., Kudo, L.C., Ryazantsev, S., Zhao, H.Z., Karsten, S.L. and Neufeld, E.F. (2009a). "Sanfilippo syndrome type B, a lysosomal storage disease, is also a tauopathy." Proc Natl Acad Sci U S A **106**(20): 8332-8337.
Ohmi, Y., Ohkawa, Y., Yamauchi, Y., Tajima, O. and Furukawa, K. (2012). "Essential roles of gangliosides in the formation and maintenance of membrane microdomains in brain tissues." Neurochemical research **37**(6): 1185-1191.

Ohmi, Y., Tajima, O., Ohkawa, Y., Mori, A., Sugiura, Y. and Furukawa, K. (2009b). "Gangliosides play pivotal roles in the regulation of complement systems and in the maintenance of integrity in nerve tissues." Proceedings of the National Academy of Sciences of the United States of America **106**(52): 22405-22410.

Ohmi, Y., Tajima, O., Ohkawa, Y., Yamauchi, Y., Sugiura, Y. and Furukawa, K. (2011). "Gangliosides are essential in the protection of inflammation and neurodegeneration via maintenance of lipid rafts: elucidation by a series of ganglioside-deficient mutant mice." Journal of neurochemistry **116**(5): 926-935.

Pacheco, C.D., Kunkel, R. and Lieberman, A.P. (2007). "Autophagy in Niemann-Pick C disease is dependent upon Beclin-1 and responsive to lipid trafficking defects." Human molecular genetics **16**(12): 1495-1503.

Paciorkowski, A.R., Westwell, M., Ounpuu, S., Bell, K., Kagan, J., Mazzarella, C. and Greenstein, R.M. (2008). "Motion analysis of a child with Niemann-Pick disease type C treated with miglustat." Mov Disord **23**(1): 124-128.

Pan, D., Sciascia, A., 2nd, Vorhees, C.V. and Williams, M.T. (2008). "Progression of multiple behavioral deficits with various ages of onset in a murine model of Hurler syndrome." Brain Res **1188**: 241-253.

Papadia, F., Lozupone, M.S., Gaeta, A., Capodiferro, D. and Lacalendola, G. (2011). "Long-term enzyme replacement therapy in a severe case of mucopolysaccharidosis type II (Hunter syndrome)." Eur Rev Med Pharmacol Sci **15**(3): 253-258.

Park, Y., Yu, G., Gunay, N.S. and Linhardt, R.J. (1999). "Purification and characterization of heparan sulphate proteoglycan from bovine brain." The Biochemical journal **344 Pt 3**: 723-730.

Pastores, G.M., Barnett, N.L. and Kolodny, E.H. (2005). "An open-label, noncomparative study of miglustat in type I Gaucher disease: efficacy and tolerability over 24 months of treatment." Clinical Therapeutics **27**(8): 1215-1227.

Pastores, G.M., Elstein, D., Hrebicek, M. and Zimran, A. (2007). "Effect of miglustat on bone disease in adults with type 1 Gaucher disease: a pooled analysis of three multinational, open-label studies." Clinical Therapeutics **29**(8): 1645-1654.

Patterson, M.C., Hendriksz, C.J., Walterfang, M., Sedel, F., Vanier, M.T. and Wijburg, F. (2012). "Recommendations for the diagnosis and management of Niemann-Pick disease type C: an update." Molecular genetics and metabolism **106**(3): 330-344.

Patterson, M.C., Vecchio, D., Jacklin, E., Abel, L., Chadha-Boreham, H., Luzy, C., Giorgino, R. and Wraith, J.E. (2010). "Long-term miglustat therapy in children with Niemann-Pick disease type C." Journal of child neurology **25**(3): 300-305.

Patterson, M.C., Vecchio, D., Prady, H., Abel, L. and Wraith, J.E. (2007). "Miglustat for treatment of Niemann-Pick C disease: a randomised controlled study." Lancet Neurol **6**(9): 765-772.
Perkins, K.J., Muller, V., Weber, B. and Hopwood, J.J. (2001). "Prediction of Sanfilippo phenotype severity from immunoquantification of heparan-N-sulfamidase in cultured fibroblasts from mucopolysaccharidosis type IIIA patients." Mol Genet Metab **73**(4): 306-312.

Peters, C. and Steward, C.G. (2003). "Hematopoietic cell transplantation for inherited metabolic diseases: an overview of outcomes and practice guidelines." Bone Marrow Transplant **31**(4): 229-239.

Peterson, L.D., Jeffery, N.M., Thies, F., Sanderson, P., Newsholme, E.A. and Calder, P.C. (1998). "Eicosapentaenoic and docosahexaenoic acids alter rat spleen leukocyte fatty acid composition and prostaglandin E2 production but have different effects on lymphocyte functions and cell-mediated immunity." Lipids **33**(2): 171-180.

Pettegrew, J.W., Panchalingam, K., Hamilton, R.L. and McClure, R.J. (2001). "Brain membrane phospholipid alterations in Alzheimer's disease." Neurochem Res **26**(7): 771-782.

Pineda, M., Perez-Poyato, M.S., O'Callaghan, M., Vilaseca, M.A., Pocovi, M., Domingo, R., Portal, L.R., Perez, A.V., Temudo, T., Gaspar, A., Penas, J.J., Roldan, S., Fumero, L.M., de la Barca, O.B., Silva, M.T., Macias-Vidal, J. and Coll, M.J. (2010). "Clinical experience with miglustat therapy in pediatric patients with Niemann-Pick disease type C: a case series." Molecular genetics and metabolism **99**(4): 358-366.

Pineda, M., Wraith, J.E., Mengel, E., Sedel, F., Hwu, W.L., Rohrbach, M., Bembi, B., Walterfang, M., Korenke, G.C., Marquardt, T., Luzy, C., Giorgino, R. and Patterson, M.C. (2009). "Miglustat in patients with Niemann-Pick disease Type C (NP-C): a multicenter observational retrospective cohort study." Molecular genetics and metabolism **98**(3): 243-249.

Piotrowska, E., Jakobkiewicz-Banecka, J., Maryniak, A., Tylki-Szymanska, A., Puk, E., Liberek, A., Wegrzyn, A., Czartoryska, B., Slominska-Wojewodzka, M. and Wegrzyn, G. (2011). "Two-year follow-up of Sanfilippo Disease patients treated with a genistein-rich isoflavone extract: Assessment of effects on cognitive functions and general status of patients." Med Sci Monit **17**(4): CR196-202.

Piotrowska, E., Jakobkiewicz-Banecka, J., Tylki-Szymanska, A., Czartoryska, B., Wegrzyn, A. and Wegrzyn, G. (2009). "Correlation between severity of mucopolysaccharidoses and combination of the residual enzyme activity and efficiency of glycosaminoglycan synthesis." Acta Paediatr **98**(4): 743-749.

Piotrowska, E., Jakobkiewicz-Banecka, J., Tylki-Szymanska, A., Liberek, A., Maryniak, A., Malinowska, M., Czartoryska, B., Puk, E., Kloska, A., Liberek, T., Baranska, S., Wegrzyn, A. and Wegrzyn, G. (2008). "Genistin-rich soy isoflavone extract in substrate reduction therapy for Sanfilippo syndrome: An open-label, pilot study in 10 pediatric patients." Current Therapeutic Research-Clinical and Experimental **69**(2): 166-179.

Platt, F.M., Neises, G.R., Dwek, R.A. and Butters, T.D. (1994). "N-butyldeoxynojirimycin is a novel inhibitor of glycolipid biosynthesis." J Biol Chem **269**(11): 8362-8365.

Platt, F.M., Neises, G.R., Reinkensmeier, G., Townsend, M.J., Perry, V.H., Proia, R.L., Winchester, B., Dwek, R.A. and Butters, T.D. (1997a). "Prevention of lysosomal storage in Tay-Sachs mice treated with N-butyldeoxynojirimycin." Science **276**(5311): 428-431.

Platt, F.M., Reinkensmeier, G., Dwek, R.A. and Butters, T.D. (1997b). "Extensive glycosphingolipid depletion in the liver and lymphoid organs of mice treated with N-butyldeoxynojirimycin." J Biol Chem **272**(31): 19365-19372.

Polito, V.A., Abbondante, S., Polishchuk, R.S., Nusco, E., Salvia, R. and Cosma, M.P. (2010). "Correction of CNS defects in the MPSII mouse model via systemic enzyme replacement therapy." Human molecular genetics **19**(24): 4871-4885.

Ponder, K.P. and Haskins, M.E. (2007). "Gene therapy for mucopolysaccharidosis." Expert Opin Biol Ther **7**(9): 1333-1345.

Ponder, K.P., Melniczek, J.R., Xu, L., Weil, M.A., O'Malley, T.M., O'Donnell, P.A., Knox, V.W., Aguirre, G.D., Mazrier, H., Ellinwood, N.M., Sleeper, M., Maguire, A.M., Volk, S.W., Mango, R.L., Zweigle, J., Wolfe, J.H. and Haskins, M.E. (2002). "Therapeutic neonatal hepatic gene therapy in mucopolysaccharidosis VII dogs." Proc Natl Acad Sci U S A **99**(20): 13102-13107.

Ponder, K.P., Wang, B., Wang, P., Ma, X., Herati, R., Cullen, K., O'Donnell, P., Ellinwood, N.M., Traas, A., Primeau, T.M. and Haskins, M.E. (2006). "Mucopolysaccharidosis I cats mount a cytotoxic T lymphocyte response after neonatal gene therapy that can be blocked with CTLA4-Ig." Mol Ther **14**(1): 5-13.

Prato, M., Gallo, V., Giribaldi, G. and Arese, P. (2008). "Phagocytosis of haemozoin (malarial pigment) enhances metalloproteinase-9 activity in human adherent monocytes: role of IL-1beta and 15-HETE." Malar J **7**: 157.

Prows, C.A., Sanchez, N., Daugherty, C. and Grabowski, G.A. (1997). "Gaucher disease: enzyme therapy in the acute neuronopathic variant." Am J Med Genet **71**(1): 16-21.

Purpura, D.P. and Suzuki, K. (1976). "Distortion of neuronal geometry and formation of aberrant synapses in neuronal storage disease." Brain Res **116**(1): 1-21.

Reolon, G.K., Braga, L.M., Camassola, M., Luft, T., Henriques, J.A., Nardi, N.B. and Roesler, R. (2006). "Long-term memory for aversive training is impaired in Idua(-/-) mice, a genetic model of mucopolysaccharidosis type I." Brain research **1076**(1): 225-230.

Reolon, G.K., Reinke, A., de Oliveira, M.R., Braga, L.M., Camassola, M., Andrades, M.E., Moreira, J.C., Nardi, N.B., Roesler, R. and Dal-Pizzol, F. (2009). "Alterations in oxidative markers in the cerebellum and peripheral organs in MPS I mice." Cellular and molecular neurobiology **29**(4): 443-448.

Richard, M., Arfi, A., Rhinn, H., Gandolphe, C. and Scherman, D. (2008). "Identification of new markers for neurodegeneration process in the mouse model of Sly disease as revealed by expression profiling of selected genes." J Neurosci Res **86**(15): 3285-3294.

Roberts, A.L., Howarth, G.S., Liaw, W.C., Moretta, S., Kritas, S., Lymn, K.A., Yazbeck, R., Tran, C., Fletcher, J.M., Butler, R.N. and Byers, S. (2009). "Gastrointestinal pathology in a mouse model of mucopolysaccharidosis type IIIA." J Cell Physiol.

Roberts, A.L., Rees, M.H., Klebe, S., Fletcher, J.M. and Byers, S. (2007). "Improvement in behaviour after substrate deprivation therapy with rhodamine B in a mouse model of MPS IIIA." Mol Genet Metab **92**(1-2): 115-121.
Roberts, A.L., Thomas, B.J., Wilkinson, A.S., Fletcher, J.M. and Byers, S. (2006). "Inhibition of glycosaminoglycan synthesis using rhodamine B in a mouse model of mucopolysaccharidosis type IIIA." Pediatr Res **60**(3): 309-314.

Rogers, D.C., Fisher, E.M., Brown, S.D., Peters, J., Hunter, A.J. and Martin, J.E. (1997). "Behavioral and functional analysis of mouse phenotype: SHIRPA, a proposed protocol for comprehensive phenotype assessment." Mamm Genome **8**(10): 711-713.

Rogers, D.C., Peters, J., Martin, J.E., Ball, S., Nicholson, S.J., Witherden, A.S., Hafezparast, M., Latcham, J., Robinson, T.L., Quilter, C.A. and Fisher, E.M. (2001). "SHIRPA, a protocol for behavioral assessment: validation for longitudinal study of neurological dysfunction in mice." Neurosci Lett **306**(1-2): 89-92.

Rosenberg, A. and Stern, N. (1966). "Changes in sphingosine and fatty acid components of the gangliosides in developing rat and human brain." J Lipid Res **7**(1): 122-131.

Rosengren, B., Mansson, J.E. and Svennerholm, L. (1987). "Composition of gangliosides and neutral glycosphingolipids of brain in classical Tay-Sachs and Sandhoff disease: more lyso-GM2 in Sandhoff disease?" J Neurochem **49**(3): 834-840.

Ruijter, G.J., Valstar, M.J., van de Kamp, J.M., van der Helm, R.M., Durand, S., van Diggelen, O.P., Wevers, R.A., Poorthuis, B.J., Pshezhetsky, A.V. and Wijburg, F.A. (2008). "Clinical and genetic spectrum of Sanfilippo type C (MPS IIIC) disease in The Netherlands." Mol Genet Metab **93**(2): 104-111.

Saif, M.A., Bigger, B.W., Brookes, K.E., Mercer, J., Tylee, K.L., Church, H.J., Bonney, D.K., Jones, S., Wraith, J.E. and Wynn, R.F. (2012). "Hematopoietic stem cell transplantation improves the high incidence of neutralizing allo-antibodies observed in Hurler's syndrome after pharmacological enzyme replacement therapy." Haematologica **97**(9): 1320-1328.

Sakurai, K., Iizuka, S., Shen, J.S., Meng, X.L., Mori, T., Umezawa, A., Ohashi, T. and Eto, Y. (2004). "Brain transplantation of genetically modified bone marrow stromal cells corrects CNS pathology and cognitive function in MPS VII mice." Gene therapy **11**(19): 1475-1481.

Samuels, S., Korey, S.R., Gonatas, J., Terry, R.D. and Weiss, M. (1963). "Studies in Tay-Sachs disease. IV. Membranous cytoplasmic bodies." J Neuropathol Exp Neurol **22**: 81-97.

Sanchez-Wandelmer, J., Davalos, A., Herrera, E., Giera, M., Cano, S., de la Pena, G., Lasuncion, M.A. and Busto, R. (2009). "Inhibition of cholesterol biosynthesis disrupts lipid raft/caveolae and affects insulin receptor activation in 3T3-L1 preadipocytes." Biochimica et biophysica acta **1788**(9): 1731-1739.

Sandhoff, K. (1969). "Variation of beta-N-acetylhexosaminidase-pattern in Tay-Sachs disease." FEBS Lett **4**(4): 351-354.

Sandhoff, K., Harzer, K., Wassle, W. and Jatzkewitz, H. (1971). "Enzyme alterations and lipid storage in three variants of Tay-Sachs disease." J Neurochem **18**(12): 2469-2489.

Sands, M.S. and Birkenmeier, E.H. (1993). "A single-base-pair deletion in the beta-glucuronidase gene accounts for the phenotype of murine mucopolysaccharidosis type VII." Proc Natl Acad Sci U S A **90**(14): 6567-6571.

Santos, M.L., Raskin, S., Telles, D.S., Lohr Junior, A., Liberalesso, P.B., Vieira, S.C. and Cordeiro, M.L. (2008). "Treatment of a child diagnosed with Niemann-Pick disease type C with miglustat: A case report in Brazil." J Inherit Metab Dis.

Schiffmann, R., Fitzgibbon, E.J., Harris, C., DeVile, C., Davies, E.H., Abel, L., van Schaik, I.N., Benko, W., Timmons, M., Ries, M. and Vellodi, A. (2008). "Randomized, controlled trial of miglustat in Gaucher's disease type 3." Ann Neurol **64**(5): 514-522.

Schiffmann, R., Heyes, M.P., Aerts, J.M., Dambrosia, J.M., Patterson, M.C., DeGraba, T., Parker, C.C., Zirzow, G.C., Oliver, K., Tedeschi, G., Brady, R.O. and Barton, N.W. (1997). "Prospective study of neurological responses to treatment with macrophage-targeted glucocerebrosidase in patients with type 3 Gaucher's disease." Ann Neurol **42**(4): 613-621.

Schulte, E.C., Slawik, H., Schule, R., Gunther, T. and Hull, M. (2009). "Alterations in excitotoxicity and prostaglandin metabolism in a transgenic mouse model of Alzheimer's disease." Neurochem Int **55**(7): 689-696.

Serhan, C.N., Hong, S., Gronert, K., Colgan, S.P., Devchand, P.R., Mirick, G. and Moussignac, R.L. (2002). "Resolvins: a family of bioactive products of omega-3 fatty acid transformation circuits initiated by aspirin treatment that counter proinflammation signals." The Journal of experimental medicine **196**(8): 1025-1037.

Seto, T., Kono, K., Morimoto, K., Inoue, Y., Shintaku, H., Hattori, H., Matsuoka, O., Yamano, T. and Tanaka, A. (2001). "Brain magnetic resonance imaging in 23 patients with mucopolysaccharidoses and the effect of bone marrow transplantation." Annals of neurology **50**(1): 79-92.

Settembre, C., Annunziata, I., Spampanato, C., Zarcone, D., Cobellis, G., Nusco, E., Zito, E., Tacchetti, C., Cosma, M.P. and Ballabio, A. (2007). "Systemic inflammation and neurodegeneration in a mouse model of multiple sulfatase deficiency." Proc Natl Acad Sci U S A **104**(11): 4506-4511.

Settembre, C., Fraldi, A., Jahreiss, L., Spampanato, C., Venturi, C., Medina, D., de Pablo, R., Tacchetti, C., Rubinsztein, D.C. and Ballabio, A. (2008a). "A block of autophagy in lysosomal storage disorders." Hum Mol Genet **17**(1): 119-129.

Settembre, C., Fraldi, A., Rubinsztein, D.C. and Ballabio, A. (2008b). "Lysosomal storage diseases as disorders of autophagy." Autophagy **4**(1): 113-114.

Shapiro, B.E., Pastores, G.M., Gianutsos, J., Luzy, C. and Kolodny, E.H. (2009). "Miglustat in late-onset Tay-Sachs disease: a 12-month, randomized, controlled clinical study with 24 months of extended treatment." Genet Med **11**(6): 425-433.

Shapiro, E.G., Lockman, L.A., Balthazor, M. and Krivit, W. (1995). "Neuropsychological outcomes of several storage diseases with and without bone marrow transplantation." J Inherit Metab Dis **18**(4): 413-429.

Shi, X. and Zaia, J. (2009). "Organ-specific heparan sulfate structural phenotypes." J Biol Chem **284**(18): 11806-11814.

Sifuentes, M., Doroshow, R., Hoft, R., Mason, G., Walot, I., Diament, M., Okazaki, S., Huff, K., Cox, G.F., Swiedler, S.J. and Kakkis, E.D. (2007). "A follow-up study of MPS I patients

treated with laronidase enzyme replacement therapy for 6 years." Mol Genet Metab **90**(2): 171-180.
Simon, P., Dupuis, R. and Costentin, J. (1994). "Thigmotaxis as an index of anxiety in mice. Influence of dopaminergic transmissions." Behavioural brain research **61**(1): 59-64.

Singh, R.D., Marks, D.L., Holicky, E.L., Wheatley, C.L., Kaptzan, T., Sato, S.B., Kobayashi, T., Ling, K. and Pagano, R.E. (2010). "Gangliosides and beta1-integrin are required for caveolae and membrane domains." Traffic **11**(3): 348-360.

Sivakumur, P. and Wraith, J.E. (1999). "Bone marrow transplantation in mucopolysaccharidosis type IIIA: a comparison of an early treated patient with his untreated sibling." J Inherit Metab Dis **22**(7): 849-850.

Skorpen, J., Helland, I.B. and Tennoe, B. (2012). "Use of miglustat in a child with late-infantile-onset Niemann-Pick disease type C and frequent seizures: a case report." Journal of medical case reports **6**(1): 383.

Smith, D., Wallom, K.L., Williams, I.M., Jeyakumar, M. and Platt, F.M. (2009). "Beneficial effects of anti-inflammatory therapy in a mouse model of Niemann-Pick disease type C1." Neurobiol Dis **36**(2): 242-251.

Sohn, H., Kim, Y.S., Kim, H.T., Kim, C.H., Cho, E.W., Kang, H.Y., Kim, N.S., Ryu, S.E., Lee, J.H. and Ko, J.H. (2006). "Ganglioside GM3 is involved in neuronal cell death." FASEB J **20**(8): 1248-1250.

Sohn, Y.B., Cho, S.Y., Park, S.W., Kim, S.J., Ko, A.R., Kwon, E.K., Han, S.J. and Jin, D.K. (2013). "Phase I/II clinical trial of enzyme replacement therapy with idursulfase beta in patients with mucopolysaccharidosis II (Hunter syndrome)." Orphanet journal of rare diseases **8**: 42.

Srivastava, S.K. and Beutler, E. (1974). "Studies on human beta-D-N-acetylhexosaminidases. 3. Biochemical genetics of Tay-Sachs and Sandhoff's diseases." J Biol Chem **249**(7): 2054-2057.

Summers, B.L., Rofe, A.M. and Coyle, P. (2006). "Prenatal zinc treatment at the time of acute ethanol exposure limits spatial memory impairments in mouse offspring." Pediatric research **59**(1): 66-71.

Svennerholm, L. (1962). "The chemical structure of normal human brain and Tay-Sachs gangliosides." Biochem Biophys Res Commun **9**: 436-441.

Tajima, G., Sakura, N., Kosuga, M., Okuyama, T. and Kobayashi, M. (2013). "Effects of idursulfase enzyme replacement therapy for Mucopolysaccharidosis type II when started in early infancy: comparison in two siblings." Molecular genetics and metabolism **108**(3): 172-177.

Tallaksen, C.M. and Berg, J.E. (2009). "Miglustat therapy in juvenile Sandhoff disease." J Inherit Metab Dis.

Tierney, M., Pottage, J., Kessler, H., Fischl, M., Richman, D., Merigan, T., Powderly, W., Smith, S., Karim, A., Sherman, J. and et al. (1995). "The tolerability and pharmacokinetics of N-butyl-deoxynojirimycin in patients with advanced HIV disease (ACTG 100). The AIDS Clinical Trials Group (ACTG) of the National Institute of Allergy and Infectious Diseases." J Acquir Immune Defic Syndr Hum Retrovirol **10**(5): 549-553.

Toida, T., Yoshida, H., Toyoda, H., Koshiishi, I., Imanari, T., Hileman, R.E., Fromm, J.R. and Linhardt, R.J. (1997). "Structural differences and the presence of unsubstituted amino groups in heparan sulphates from different tissues and species." The Biochemical journal **322 (Pt 2)**: 499-506.

Tomatsu, S., Montano, A.M., Dung, V.C., Grubb, J.H. and Sly, W.S. (2009). "Mutations and polymorphisms in GUSB gene in mucopolysaccharidosis VII (Sly Syndrome)." Hum Mutat **30**(4): 511-519.

Traas, A.M., Wang, P., Ma, X., Tittiger, M., Schaller, L., O'Donnell, P., Sleeper, M.M., Vite, C., Herati, R., Aguirre, G.D., Haskins, M. and Ponder, K.P. (2007). "Correction of clinical manifestations of canine mucopolysaccharidosis I with neonatal retroviral vector gene therapy." Mol Ther **15**(8): 1423-1431.

Treiber, A., Morand, O. and Clozel, M. (2007). "The pharmacokinetics and tissue distribution of the glucosylceramide synthase inhibitor miglustat in the rat." Xenobiotica; the fate of foreign compounds in biological systems **37**(3): 298-314.

Unterwurzacher, I., Koal, T., Bonn, G.K., Weinberger, K.M. and Ramsay, S.L. (2008). "Rapid sample preparation and simultaneous quantitation of prostaglandins and lipoxygenase derived fatty acid metabolites by liquid chromatography-mass spectrometry from small sample volumes." Clinical chemistry and laboratory medicine : CCLM / FESCC **46**(11): 1589-1597.

Valstar, M.J., Bertoli-Avella, A.M., Wessels, M.W., Ruijter, G.J., de Graaf, B., Olmer, R., Elfferich, P., Neijs, S., Kariminejad, R., Suheyl Ezgu, F., Tokatli, A., Czartoryska, B., Bosschaart, A.N., van den Bos-Terpstra, F., Puissant, H., Burger, F., Omran, H., Eckert, D., Filocamo, M., Simeonov, E., Willems, P.J., Wevers, R.A., Niermeijer, M.F., Halley, D.J., Poorthuis, B.J. and van Diggelen, O.P. (2010a). "Mucopolysaccharidosis type IIID: 12 new patients and 15 novel mutations." Hum Mutat **31**(5): E1348-1360.

Valstar, M.J., Bruggenwirth, H.T., Olmer, R., Wevers, R.A., Verheijen, F.W., Poorthuis, B.J., Halley, D.J. and Wijburg, F.A. (2010b). "Mucopolysaccharidosis type IIIB may predominantly present with an attenuated clinical phenotype." J Inherit Metab Dis **33**(6): 759-767.

Valstar, M.J., Marchal, J.P., Grootenhuis, M., Colland, V. and Wijburg, F.A. (2011). "Cognitive development in patients with Mucopolysaccharidosis type III (Sanfilippo syndrome)." Orphanet journal of rare diseases **6**: 43.

Valstar, M.J., Neijs, S., Bruggenwirth, H.T., Olmer, R., Ruijter, G.J., Wevers, R.A., van Diggelen, O.P., Poorthuis, B.J., Halley, D.J. and Wijburg, F.A. (2010c). "Mucopolysaccharidosis type IIIA: clinical spectrum and genotype-phenotype correlations." Ann Neurol **68**(6): 876-887.

van de Kamp, J.J., Niermeijer, M.F., von Figura, K. and Giesberts, M.A. (1981). "Genetic heterogeneity and clinical variability in the Sanfilippo syndrome (types A, B, and C)." Clin Genet **20**(2): 152-160.

Vanier, M.T. (1999). "Lipid changes in Niemann-Pick disease type C brain: personal experience and review of the literature." Neurochem Res **24**(4): 481-489.

Vellodi, A., Young, E., Cooper, A., Lidchi, V., Winchester, B. and Wraith, J.E. (1999). "Long-term follow-up following bone marrow transplantation for Hunter disease." J Inherit Metab Dis **22**(5): 638-648.

Vellodi, A., Young, E., New, M., Pot-Mees, C. and Hugh-Jones, K. (1992). "Bone marrow transplantation for Sanfilippo disease type B." J Inherit Metab Dis **15**(6): 911-918.

Vera, M., Le, S., Kan, S.H., Garban, H., Naylor, D., Mlikotic, A., Kaitila, I., Harmatz, P., Chen, A. and Dickson, P. (2013). "Immune response to intrathecal enzyme replacement therapy in mucopolysaccharidosis I patients." Pediatric research.

Villani, G.R., Di Domenico, C., Musella, A., Cecere, F., Di Napoli, D. and Di Natale, P. (2009). "Mucopolysaccharidosis IIIB: oxidative damage and cytotoxic cell involvement in the neuronal pathogenesis." Brain Res **1279**: 99-108.

Villani, G.R., Gargiulo, N., Faraonio, R., Castaldo, S., Gonzalez, Y.R.E. and Di Natale, P. (2007). "Cytokines, neurotrophins, and oxidative stress in brain disease from mucopolysaccharidosis IIIB." J Neurosci Res **85**(3): 612-622.

Vite, C.H., Wang, P., Patel, R.T., Walton, R.M., Walkley, S.U., Sellers, R.S., Ellinwood, N.M., Cheng, A.S., White, J.T., O'Neill, C.A. and Haskins, M. (2011). "Biodistribution and pharmacodynamics of recombinant human alpha-L-iduronidase (rhIDU) in mucopolysaccharidosis type I-affected cats following multiple intrathecal administrations." Mol Genet Metab **103**(3): 268-274.

Vogler, C., Birkenmeier, E.H., Sly, W.S., Levy, B., Pegors, C., Kyle, J.W. and Beamer, W.G. (1990). "A murine model of mucopolysaccharidosis VII. Gross and microscopic findings in beta-glucuronidase-deficient mice." Am J Pathol **136**(1): 207-217.

Vogler, C., Levy, B., Galvin, N., Lessard, M., Soper, B. and Barker, J. (2005a). "Early onset of lysosomal storage disease in a murine model of mucopolysaccharidosis type VII: undegraded substrate accumulates in many tissues in the fetus and very young MPS VII mouse." Pediatr Dev Pathol **8**(4): 453-462.

Vogler, C., Levy, B., Grubb, J.H., Galvin, N., Tan, Y., Kakkis, E., Pavloff, N. and Sly, W.S. (2005b). "Overcoming the blood-brain barrier with high-dose enzyme replacement therapy in murine mucopolysaccharidosis VII." Proc Natl Acad Sci U S A **102**(41): 14777-14782.

Wada, R., Tifft, C.J. and Proia, R.L. (2000). "Microglial activation precedes acute neurodegeneration in Sandhoff disease and is suppressed by bone marrow transplantation." Proceedings of the National Academy of Sciences of the United States of America **97**(20): 10954-10959.

Walkley, S.U., Baker, H.J., Rattazzi, M.C., Haskins, M.E. and Wu, J.Y. (1991). "Neuroaxonal dystrophy in neuronal storage disorders: evidence for major GABAergic neuron involvement." J Neurol Sci **104**(1): 1-8.

Walkley, S.U., Thrall, M.A., Haskins, M.E., Mitchell, T.W., Wenger, D.A., Brown, D.E., Dial, S. and Seim, H. (2005). "Abnormal neuronal metabolism and storage in mucopolysaccharidosis type VI (Maroteaux-Lamy) disease." Neuropathol Appl Neurobiol **31**(5): 536-544.

Walkley, S.U. and Vanier, M.T. (2009). "Secondary lipid accumulation in lysosomal disease." Biochim Biophys Acta **1793**(4): 726-736.

Walkley, S.U., Zervas, M. and Wiseman, S. (2000). "Gangliosides as modulators of dendritogenesis in normal and storage disease-affected pyramidal neurons." Cereb Cortex **10**(10): 1028-1037.

Wei, H., Kim, S.J., Zhang, Z., Tsai, P.C., Wisniewski, K.E. and Mukherjee, A.B. (2008). "ER and oxidative stresses are common mediators of apoptosis in both neurodegenerative and non-neurodegenerative lysosomal storage disorders and are alleviated by chemical chaperones." Hum Mol Genet **17**(4): 469-477.

Weinreb, N.J., Charrow, J., Andersson, H.C., Kaplan, P., Kolodny, E.H., Mistry, P., Pastores, G., Rosenbloom, B.E., Scott, C.R., Wappner, R.S. and Zimran, A. (2002). "Effectiveness of enzyme replacement therapy in 1028 patients with type 1 Gaucher disease after 2 to 5 years of treatment: a report from the Gaucher Registry." Am J Med **113**(2): 112-119.

Werth, N., Schuette, C.G., Wilkening, G., Lemm, T. and Sandhoff, K. (2001). "Degradation of membrane-bound ganglioside GM2 by beta -hexosaminidase A. Stimulation by GM2 activator protein and lysosomal lipids." J Biol Chem **276**(16): 12685-12690.

Wheeler, D., Bandaru, V.V., Calabresi, P.A., Nath, A. and Haughey, N.J. (2008). "A defect of sphingolipid metabolism modifies the properties of normal appearing white matter in multiple sclerosis." Brain : a journal of neurology **131**(Pt 11): 3092-3102.

Whishaw, I.Q. and Tomie, J. (1996). "Of mice and mazes: similarities between mice and rats on dry land but not water mazes." Physiology & behavior **60**(5): 1191-1197.

Whitley, C.B., Belani, K.G., Chang, P.N., Summers, C.G., Blazar, B.R., Tsai, M.Y., Latchaw, R.E., Ramsay, N.K. and Kersey, J.H. (1993). "Long-term outcome of Hurler syndrome following bone marrow transplantation." Am J Med Genet **46**(2): 209-218.

Wilkinson, F.L., Holley, R.J., Langford-Smith, K.J., Badrinath, S., Liao, A., Langford-Smith, A., Cooper, J.D., Jones, S.A., Wraith, J.E., Wynn, R.F., Merry, C.L. and Bigger, B.W. (2012). "Neuropathology in mouse models of mucopolysaccharidosis type I, IIIA and IIIB." PloS one **7**(4): e35787.

Wolf, D.A., Lenander, A.W., Nan, Z., Belur, L.R., Whitley, C.B., Gupta, P., Low, W.C. and McIvor, R.S. (2011). "Direct gene transfer to the CNS prevents emergence of neurologic disease in a murine model of mucopolysaccharidosis type I." Neurobiol Dis **43**(1): 123-133.

Wolfe, J.H. and Sands, M.S. (1996). Murine mucopolysaccharidosis type VII: a model system for somatic gene therapy of the central nervous system. Protocols for Gene Transfer in Neuroscience: Towards Gene Therapy of Neurologic Disorders. Enquist, P.R. and Enquist, L.W. Essex, Wiley**:** 263-274.

Wooten, W.I., 3rd, Muenzer, J., Vaughn, B.V. and Muhlebach, M.S. (2013). "Relationship of sleep to pulmonary function in mucopolysaccharidosis II." The Journal of pediatrics **162**(6): 1210-1215.

Wortmann, S.B., Lefeber, D.J., Dekomien, G., Willemsen, M.A., Wevers, R.A. and Morava, E. (2009). "Substrate deprivation therapy in juvenile Sandhoff disease." J Inherit Metab Dis.

Wraith, J.E. (2006). "Limitations of enzyme replacement therapy: current and future." J Inherit Metab Dis **29**(2-3): 442-447.

Wraith, J.E., Baumgartner, M.R., Bembi, B., Covanis, A., Levade, T., Mengel, E., Pineda, M., Sedel, F., Topcu, M., Vanier, M.T., Widner, H., Wijburg, F.A. and Patterson, M.C. (2009). "Recommendations on the diagnosis and management of Niemann-Pick disease type C." Molecular genetics and metabolism **98**(1-2): 152-165.

Wraith, J.E., Clarke, L.A., Beck, M., Kolodny, E.H., Pastores, G.M., Muenzer, J., Rapoport, D.M., Berger, K.I., Swiedler, S.J., Kakkis, E.D., Braakman, T., Chadbourne, E., Walton-Bowen, K. and Cox, G.F. (2004). "Enzyme replacement therapy for mucopolysaccharidosis I: a randomized, double-blinded, placebo-controlled, multinational study of recombinant human alpha-L-iduronidase (laronidase)." The Journal of pediatrics **144**(5): 581-588.

Wraith, J.E. and Imrie, J. (2009). "New therapies in the management of Niemann-Pick type C disease: clinical utility of miglustat." Therapeutics and clinical risk management **5**: 877-887.

Wraith, J.E., Vecchio, D., Jacklin, E., Abel, L., Chadha-Boreham, H., Luzy, C., Giorgino, R. and Patterson, M.C. (2010). "Miglustat in adult and juvenile patients with Niemann-Pick disease type C: long-term data from a clinical trial." Mol Genet Metab **99**(4): 351-357.

Wu, Y.P., Mizukami, H., Matsuda, J., Saito, Y., Proia, R.L. and Suzuki, K. (2005). "Apoptosis accompanied by up-regulation of TNF-alpha death pathway genes in the brain of Niemann-Pick type C disease." Molecular genetics and metabolism **84**(1): 9-17.

Wu, Y.P. and Proia, R.L. (2004). "Deletion of macrophage-inflammatory protein 1 alpha retards neurodegeneration in Sandhoff disease mice." Proceedings of the National Academy of Sciences of the United States of America **101**(22): 8425-8430.

Yamada, Y., Kato, K., Sukegawa, K., Tomatsu, S., Fukuda, S., Emura, S., Kojima, S., Matsuyama, T., Sly, W.S., Kondo, N. and Orii, T. (1998). "Treatment of MPS VII (Sly disease) by allogeneic BMT in a female with homozygous A619V mutation." Bone marrow transplantation **21**(6): 629-634.

Young, I.D. and Harper, P.S. (1983). "The natural history of the severe form of Hunter's syndrome: a study based on 52 cases." Dev Med Child Neurol **25**(4): 481-489.

Zarowski, M., Steinborn, B., Gurda, B., Dvorakova, L., Vlaskova, H. and Kothare, S.V. (2011). "Treatment of cataplexy in Niemann-Pick disease type C with the use of miglustat." Eur J Paediatr Neurol **15**(1): 84-87.

Zervas, M., Dobrenis, K. and Walkley, S.U. (2001a). "Neurons in Niemann-Pick disease type C accumulate gangliosides as well as unesterified cholesterol and undergo dendritic and axonal alterations." J Neuropathol Exp Neurol **60**(1): 49-64.

Zervas, M., Somers, K.L., Thrall, M.A. and Walkley, S.U. (2001b). "Critical role for glycosphingolipids in Niemann-Pick disease type C." Curr Biol **11**(16): 1283-1287.

Zhou, S., Davidson, C., McGlynn, R., Stephney, G., Dobrenis, K., Vanier, M.T. and Walkley, S.U. (2011). "Endosomal/lysosomal processing of gangliosides affects neuronal cholesterol sequestration in Niemann-Pick disease type C." The American journal of pathology **179**(2): 890-902.